Modeling of Permafrost Distribution in the Semi-arid Chilean Andes

by

Guillermo Azócar

A thesis
presented to the University of Waterloo
in fulfillment of the
thesis requirement for the degree of
Master of Science
in
Geography

Waterloo, Ontario, Canada, 2013

AUTHOR'S DECLARATION

I hereby declare that I am the sole author of this thesis. This is a true copy of the thesis, including any required final revisions, as accepted by my examiners.

I understand that my thesis may be made electronically available to the public.

Abstract

The distribution of mountain permafrost is generally modeled using a combination of statistical techniques and empirical variables. Such models, based on topographic, climatic and geomorphological predictors of permafrost, have been widely used to estimate the spatial distribution of mountain permafrost in North America and Europe. However at present, little knowledge about the distribution and characteristics of mountain permafrost is available for the Andes. In addition, the effects of climate change on slope stability and the hydrological system, and the pressure of mining activities have increased concerns about the knowledge of mountain permafrost in the Andes.

In order to model permafrost distribution in the semi-arid Chilean Andes between ~29°S and 32°S, an inventory of rock glaciers is carried out to obtain a variable indicative of the presence and absence of permafrost conditions. Then a Linear Mixed-Effects Model (LMEM) is used to determine the spatial distribution of Mean Annual Air Temperature (MAATs), which is then used as one of the predictors of permafrost occurrence. Later, a Generalized Additive Model (GAM) with a logistic link function is used to predict permafrost occurrence in debris surfaces within the study area.

Within the study area, 3575 rock glaciers were inventoried. Of these, 1075 were classified as active, 493 as inactive, 343 as intact and 1664 as relict forms, based on visual interpretation of satellite imagery. Many of the rock glaciers (~60-80%) are situated at positive MAAT, and the number of rock glaciers at negative MAAT greatly decreases from north to south.

The results of spatial temperature distribution modeling indicated that the temperature changes by -0.71°C per each 100 m increase in altitude, and that there is a 4°C temperature difference between the northern and southern part of the study area. The altitudinal position of the 0°C MAAT isotherm is situated at ~4250 m a.s.l. in the northern (29°S) section and drops latitudinally to ~4000 m a.s.l. in the southern section (32°S) of the study area.

For permafrost modeling purposes, 1911 rock glaciers (active, inactive and intact forms) were categorized into the class indicative of permafrost presence and 1664 (relict forms) as non-permafrost. The predictors MAAT and Potential Incoming Solar Radiation (PISR) and their nonlinear interaction were modeled by the GAM using LOESS smoothing function. A temperature offset term was applied to reduce the overestimation of permafrost occurrence in debris surface areas due to the use of rock glaciers as permafrost proxies.

The dependency between the predictor variables shows that a high amount of PISR has a greater effect at positive MAAT levels than in negative ones. The GAM for permafrost distribution achieved an acceptable discrimination capability between permafrost classes (area under the ROC curve ~0.76). Considering a permafrost probability score (PPS) ≥ 0.5 and excluding steep bedrock and glacier surfaces, mountain permafrost can be potentially present in up to about 6.8% (2636 km^2) of the study area, whereas with a PPS ≥ 0.75, the potential permafrost area decreases to 2.7% (1051 km^2). Areas with the highest PPS are spatially concentrated in the north section of the study area where altitude rises considerably (the Huasco and Elqui watersheds), while permafrost is almost absent in the southern section where the topography is considerably lower (Limarí and Choapa watersheds).

This research shows that the potential mountain permafrost distribution can be spatially modeled using topoclimatic information and rock glacier inventories. Furthermore, the results have provided the first local estimation of permafrost distribution in the semi-arid Chilean Andes. The results obtained can be used for local environmental planning and to aid future research in periglacial topics.

Resumen

La distribución del permafrost de montaña es modelada generalmente usando una combinación de técnicas estadísticas y variables empíricas. Estos modelos, basados en datos topográficos, climáticos e indicadores geomorfológicos de permafrost han sido usados ampliamente para estimar la distribución espacial del permafrost de montaña en Norteamérica y Europa. Sin embargo, a la fecha, muy poco se sabe acerca de la distribución y las características del permafrost de montaña en los Andes. Asimismo, los efectos del cambio climático sobre la estabilidad de pendientes y el sistema hidrológico, y la presión de la actividad minera han aumentado la preocupación acerca del conocimiento del permafrost de montaña en los Andes.

Con el fin de modelar la distribución de permafrost en los Andes de Chile semiárido entre los ~29°S y 32°S, un inventario de glaciares rocosos se llevó a cabo para obtener una variable indicativa de la presencia y ausencia de condiciones de permafrost. Posteriormente, un modelo lineal de efectos mixtos (LMEM) fue usado para determinar la distribución espacial de la temperatura media anual del aire (MAAT), el cual posteriormente es usado como una de las variables predictoras de la ocurrencia de permafrost. A continuación, un modelo aditivo generalizado (GAM) con función de enlace logística es utilizado para predecir la ocurrencia de permafrost en superficies de detritos en el área de estudio.

En el área de estudio se inventariaron 3575 glaciares rocosos. De este total, 1075 fueron clasificados como activos, 493 como inactivos, 343 como intactos y 1664 como relictos, basado en la fotointerpretación de imágenes satelitales. La mayoría de los glaciares rocosos (~60-80%) está localizada en niveles positivos de MAAT, y el número de glaciares rocosos localizados en niveles negativos de MAAT disminuye considerablemente desde el norte al sur.

Los resultados del modelo de distribución espacial de las temperaturas indican que la temperatura disminuye -0.71°C por cada 100 m de aumento en la altitud, y que hay una diferencia en temperatura de 4°C entre el norte y el sur del área de estudio. La posición altitudinal de la isoterma de 0°C MAAT está situada a los ~4250 m s.n.m. en la sección norte (~29°S) y cae altitudinalmente hasta los ~4000 m s.n.m. en la sección sur (~32°S) del área de estudio.

Para propósitos de modelamiento del permafrost, 1911 glaciares rocosos (formas activas, inactivas e intactas) fueron categorizados dentro de la clase indicativa de la presencia de permafrost y 1664 (formas relictas) como non-permafrost. Las variables predictoras MAAT y radiación solar potencial entrante (PISR) y su interacción no-lineal fueron transformadas por el GAM usando una función de suavizado bivariado LOESS. Un offset de temperatura fue aplicado para reducir la sobreestimación de la ocurrencia de permafrost en superficies de detritos, debido al uso de glaciares rocosos como indicadores de permafrost.

La dependencia entre las variables predictoras muestra que una PISR alta tiene un mayor efecto en niveles MAAT positivos que en niveles MAAT negativos. El GAM para la distribución del permafrost logra una capacidad aceptable discriminación entre las clases de permafrost (área bajo la curva ROC $\sim$ 0.76). Teniendo en cuenta un puntaje de probabilidad de permafrost (PPS) $\geq$ 0.5 y excluyendo superficies rocosas escarpadas y glaciares, permafrost de montaña podría cubrir un 6.8% (2636 km^2) del área de estudio, mientras que con un PPS $\geq$ 0.75, el área potencial de permafrost disminuye a 2.7% (1051 km^2). Las áreas con el PPS más alto, se concentran espacialmente en la parte norte del área de estudio donde la altitud aumenta considerablemente (cuencas del Huasco y Elqui), mientras que el permafrost es casi ausente en la sección meridional donde la altitud desciende considerablemente (cuencas del Limarí y Choapa).

Esta investigación muestra que la distribución potencial del permafrost de montaña puede ser modelada espacialmente utilizando información topoclimática e inventarios de glaciares rocosos. Por otro lado, los resultados han proporcionado la primera estimación local de distribución del permafrost en los Andes de Chile semiárido. Los resultados obtenidos pueden ser utilizados para la planificación del medio ambiente local y para ayudar a futuras investigaciones en temas periglaciares.

Acknowledgements

I would like to thank and acknowledge the help and support that I received from many individuals and organization in completion of my M.Sc. research.

I am especially grateful to my supervisor Dr. Alexander Brenning for his support and guidance that he showed during all these years. I appreciate particularly his constant enthusiasm for sharing his knowledge. Without his guidance, I could not have accomplished alone. I am eternally grateful.

I would like to thanks to my funding agency, the National Commission for Scientific and Technological Research (CONICYT) from the Chilean government and its scholarship program “Becas Chile” for the financial supports. Thanks are also due to Barbara, Francisco, Carolina, Oliver, Cristian, Lorena, Pedro and Pastor for their support during the Becas Chile protests 2009, without your help, would not have this opportunity to study abroad. I also wish to acknowledge to the Chilean Water Directorate for providing access to temperature data.

A big thanks you to all the friends that I made at University of Waterloo. Thanks you to Danial, Maliha, Yue, Kiana, Hanzhe, Elena, Abdullah, Angie, Javier, Gonzalo and Juan Pablo for making my life in Waterloo more enjoyable. Without them Waterloo would not be such a great place to study and live.

To my committee members: Dr. Claude Duguay, Dr. Richard Kelly and Dr. Xavier Bodin, for their comments and suggestions during my thesis defense.

Last but not the least I would like to thank to Ms. Mary McPherson for all their help with my English writing and for sharing pleasant conversations.

Dedication

To my parents Guillermo and Veronica and my nephews Luciano and Carlitos,

and to Paulina,

thanks for your love and support.

Table of Contents

Appendices

List of Figures

List of Tables

List of Acronyms

AAT	Annual Average Temperature
AST	Apparent Satellite Temperature
AUROC	Area Under the Receiver-Operating Characteristic Curve
BTS	Basal Temperature of Snow
DEM	Digital Elevation Model
DGA	Chilean Water Directorate / Dirección General de Aguas
ELA	Modern Equilibrium Line Altitude of Glaciers
ELEV	Elevation
ENSO	El Niño–Southern Oscillation
ERT	Electrical Resistivity Tomography
GAM	Generalized Additive Model
GIS	Geographic Information System
GCM	General Circulation Model
GLM	Generalized Linear Model
GPR	Ground Penetrating Radar
GPS	Global Positioning System
GST	Ground Surface Temperature
ICC	Intraclass Correlation Coefficient
LMEM	Linear Mixed-Effects Model
MAAT	Mean Annual Air Temperature
MLE	Maximum Likelihood Estimation
NDVI	Normalized Difference Vegetation Index
PISR	Potential Incoming Solar Radiation
CPISR	Relative Potential Incoming Solar Radiation
PPS	Permafrost Probability Score
PRECIP	Precipitation
PZI	Permafrost Zonation Index model of Gruber
RSE	Residual standard error
OLS	Ordinary Least Squares Method
WS	Weather Station

Chapter 1

Introduction

Permafrost, or perennially frozen ground, is rock or sediment whose temperature remains below 0°C for two or more consecutive years (Davis, 2000). Permafrost can, but does not need to, contain water or ice. It is a zonal phenomenon, distributed geographically near to the Polar areas and the highest mountain ranges and plateaus around the Earth. Mountain permafrost (also called alpine permafrost) is the presence of frozen ground conditions in mountain areas. Mountain permafrost is invisible because it is a thermal phenomenon; however, some geomorphological indicators such as rock glaciers are commonly associated with permafrost conditions in mountain areas (Barsch, 1996; Burger *et al.*, 1999; Haeberli, 2000).

Mountain permafrost research is still a relatively young field of science and has principally emerged during the last decades (Etzelmüller, 2013). The main topics in mountain permafrost research are associated with the study of ground thermal regimes and geohazard events (i.e. slope stability and infrastructure), the handling of subsurface regimes and the design of infrastructures, the influence of permafrost thaw on hydrological systems, the study of geomorphologic permafrost features (i.e. rock glaciers) and the modeling of mountain permafrost distribution (Etzelmüller, 2013; Haeberli, 2013). In recent decades, the study of mountain permafrost has become more important due to climate change impacts associated with the permafrost thawing and its consequences for hydrological regimens and slope stability (Haeberli, 1992; Barsch, 1996; Haeberli & Burn, 2002; French, 2007; Marshall, 2012). Increased anthropogenic activities in mountain areas have raised additional concerns about mountain permafrost.

Normally, the distribution of mountain permafrost is controlled by three different environmental factors at different spatial-scales: climate, topography and ground conditions (Hoelzle *et al.*, 2001; Gruber & Haeberli, 2009).

Mountain permafrost has usually been mapped using a combination of empirical or statistical methods and a set of variables related to terrain attributes, climate data and geomorphologic indicators (Boeckli *et al.*, 2012a,b). Permafrost distribution in mountain areas has mainly been modeled in the European Alps and North American mountain ranges (Janke, 2005a,b; Boeckli *et al.*, 2012a,b). In contrast, permafrost occurrences in the Andes have barely been studied or remain unknown.

The recent availability of highly accurate Digital Elevation Models (DEMs) that cover all the land on Earth at different resolutions, the availability of new rock glacier inventories for the Chilean Andes, and the recent public and free access to climate data from weather stations along the Chilean territory have provided the basic input for an initial approach to modeling permafrost distribution in the Andes. On the other hand, the availability of powerful data analysis software such the R system now allow the application of complex statistical modelling for geospatial analysis and prediction over large geographical regions.

The objective of this research is to study permafrost distribution in the semi-arid Chilean Andes. As a first step, a new inventory of rock glaciers is carried out to obtain a variable indicative of the presence or absence of permafrost conditions. Then a Linear Mixed-Effects Model (LMEM) is used to determine the spatial temperature distribution, which is then used as a predictor variable of permafrost occurrence. Finally, a Generalized Additive Model (GAM) with a logistic function is used to predict the permafrost occurrence in debris surface areas within the study area, using as a response two classes indicative of permafrost conditions, and Potential Incoming

Solar Radiation (PISR) and Mean Annual Air Temperatures (MAATs) as predictor variables. Due to the fact that the model is based on rock glacier forms (debris surface) as evidence of permafrost conditions; a simple mask was applied to remove steep bedrock areas. Additionally, a temperature offset term was applied to moderate the overestimation of permafrost occurrence in debris surface cover reliefs.

1.1 Motivation for Research

The Andes are the longest continental mountain range in the world and include some of the highest peaks on Earth (Orme, 2007). This range is the cradle of several civilizations, a home for a rich variety of ecosystems, and a source of abundant natural resources that are driving economic growth for the Andean Community of Nations (Rundel *et al.*, 2007; Devenish & Gianella, 2012). Even though local environmental research has greatly increased in the last decades, many topics have barely been studied or remain unknown for this region, such as the significance and extension of mountain permafrost.

In the Andes, the increasing pressure of mining activities (Brenning, 2008; Brenning & Azócar, 2010b) and concerns about the consequences of climate change are increasing awareness about the importance of mountain permafrost in slope stability and its influence on the entire hydrological system (Haeberli, 2013), especially in arid and semi-arid areas of the Andes.

Although permafrost is one of the main components of the Andes periglacial environment, observing it is difficult because it is a thermal phenomenon located underneath the ground's surface, with only one distinct geomorphological expression indicative of permafrost conditions: rock glaciers (Haeberli *et al.*, 2006). Geophysical methods such as Electrical Resistivity Tomography (ERT), Ground-Penetration radar (GPR), core drilling, and surface and subsurface temperature measurements have also been used to the study the presence of permafrost conditions in mountain areas; however, these approaches are spatially limited (Hauck & Kneisel, 2008). On the other hand, mountain permafrost distribution is characterized by a high spatial heterogeneity due to the influence of topoclimatic factors such as the altitude, slope and aspect over radiation and temperature levels (Barry, 1992; Haerberli, 1975 in: Keller *et al.*, 1998). In general, attempts to model permafrost distribution in mountain areas try to address all these limitations by incorporating predictor variables that take into account the effect of the terrain on the climate.

A statistical permafrost model based on an indicator variable of permafrost occurrence, such as rock glaciers, and set of predictor variables related to temperature and solar radiation that take into account topoclimatic effects, can contribute to determining the boundaries of permafrost distribution in the Andes.

1.2 Goal and Objectives

The purpose of this research is to improve our knowledge of permafrost distribution in the semi-arid Chilean Andes. For this purpose, rock glaciers, an indicator of the permafrost conditions, along with geomatic and statistic methods are used to determine the boundaries of permafrost distribution and the influence of the main topoclimatic factors on the presence or absence of permafrost in the semi-arid Chilean Andes (~29-32°S). The specific steps to achieving the main goal for this research are to

- Compile and build a new inventory of rock glaciers based on previous and new inventories, including attributes describing the location and activity status of rock glaciers.
- Apply statistical modeling techniques to determine the spatial distribution of mean annual air temperatures along the study area using data available from weather stations.
- Apply statistical modeling techniques to analyze and predict the distribution of permafrost in the study area, using variables related to climatic and topographic conditions.

1.3 Research Significance

This research is intended to contribute to the scarce knowledge on permafrost in the semi-arid Andes through statistical and geomatic modeling. This study of rock glaciers and permafrost distribution will provide valuable information for local environmental planning, especially important with the increase of anthropogenic activities in mountain areas (i.e., mining). Moreover, it establishes a baseline of current permafrost conditions to aid future research into cryosphere topics.

1.4 Thesis Outline

The thesis is organized in seven chapters. This chapter states the scope of the study. Chapter 2 presents a literature review covering the main characteristics of mountain permafrost and the application of several techniques for permafrost mapping. In addition, characteristics of rock glaciers, mountain weather and the effects of climate change on mountain permafrost are discussed separately. Chapter 3 describes the geological, geomorphological and climate setting of the study area. Chapter 4 described the methods designed to model the spatial variability of mean annual air temperatures and permafrost occurrence. The components of the modeling process, such as sources of input data, statistical approaches and computer implementation of the model are also explained in this chapter. The findings of this research are given in Chapter 5, followed by interpretation of permafrost probability and limitations in Chapter 6. Finally, Chapter 7 states the main conclusions.

Chapter 2

Research Background

2.1 Mountain Permafrost

Permafrost refers to lithospheric material that permanently remains at or below 0°C for two or more consecutives years (French, 2007). Under this definition, permafrost can, but does not need to, contain water or ice. Permafrost that contains water in a frozen state (e.g., ground ice, frozen ground) can be considered part of the global cryosphere systems (Barry & Yew Gan, 2011). When permafrost lacks moisture or the moisture is insufficient to allow interstitial ice forms, it is commonly called dry permafrost (Embleton & King, 1975).

Most of the areas underlain by permafrost experience a seasonal thaw when near-surface ground temperatures rise over 0°C during summer and fall below 0°C in winter. The layer of the ground that is subject to seasonal temperature variation above and below 0°C is commonly called the "active layer", and its thickness depends on several environmental factors (i.e., air temperature, aspect, snow cover, rock types, vegetation, etc.; French, 2007), but it has a typical thickness of between 0.5 and 8 m (Humlum, 1997; Gruber & Haeberli, 2009). Recently, studies in the semi-arid Chilean Andes have detected thicknesses between 2.5 to near 8 m at different sites located on active rock glaciers (Brenning *et al.*, 2013).

Mountain permafrost (also called alpine permafrost) is distributed near to the polar areas and all the highest mountain ranges and plateaus of the Earth. Normally, mountain permafrost and its extreme spatial variability is dominated by three different environmental factors at different scales that influence on the ground temperatures: climate, topography and ground conditions (Hoelzle *et al.*, 2001; Gruber & Haeberli, 2009; Figure 1). Climate processes refer to the influence that latitude and global circulation have over a mountain areas (*global*-scale). Topographic conditions can modify the general climate processes (*meso*-scale). Locally, the effect of topographically altered climate conditions on ground temperatures are modified by ground properties and the role of the snow cover and their influence on heat transfer (*micro*-scale).

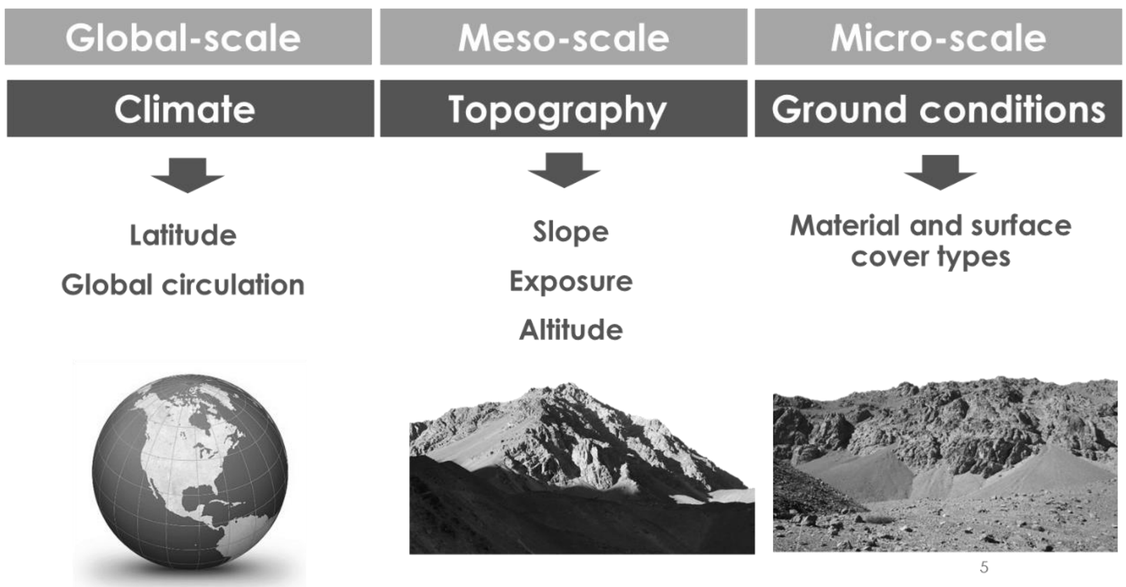

Figure 1. Idealized diagram of scales and process domains that influence ground temperature and permafrost conditions in mountain areas

2.1.1 Indicators of Permafrost Occurrence in Mountain Areas

The detection of permafrost in mountain areas can be based on direct and indirect indicators of the presence or absence of permafrost conditions. Commonly, geomorphological landforms such as rock glaciers are considered direct phenomena indicative of permafrost conditions (Haeberli, 1985; Berthling, 2011). Other indirect indicators of permafrost conditions are cryoturbation steps (terracettes), pingo protuberances, thermokarst landforms and protalus ramparts (Davis, 2000; French, 2007).

Geophysical methods such as Electrical Resistivity Tomography (ERT), Ground-Penetration radar (GPR), core drilling, and surface and subsurface temperature measurements can also give direct and indirect information about the presence of permafrost (Hauck & Kneisel, 2008). Perennial snow patches (e.g., also called penitentes) have been partially associated with permafrost conditions in different mountain ranges because they can keep the surface temperature at the negative levels (Harris & Corte, 1992; Ishikawa , 2003a); however, more research is needed on the relations between soil-atmosphere heat transfer in different climatic settings (Brenning *et al.*, 2005).

Other indicators are related to certain variables that are not directly indicative of permafrost conditions, but they do allow one to make some inferences about the presence or absence of permafrost, among these indicators are the relation between mean annual air temperatures (MAATs) and altitudes (Barsch, 1978), the measurement of the Basal Temperature of Snow (BTS) and Ground Surface Temperature (GST; Hoelzle *et al.*, 1999), and the distribution of vegetation and snow cover (Etzelmüller *et al.*, 2001).

Mountain permafrost distribution is commonly divided into different zones. According to Barsch (1978), who studied permafrost distribution in the Swiss Alps, mountain permafrost is divided into three main zones: sporadic, discontinuous and continuous. Considering the distribution of active rock glaciers and the mean annual air temperature (MAAT) as an indicator of modern permafrost zones, sporadic permafrost will be located below the zone of active rock glaciers, or where MAAT is close to positive levels (~0 to -1/-2 °C). On the other hand, above the lower altitudinal limit of active rock glaciers, where the MAAT is frequently below -2 °C, finding discontinuous mountain permafrost is likely.

Finally, continuous permafrost occurs in mountainous areas where more than 90% is underlain by permafrost (Meyer, 2009) or where the MAAT is below -3 °C (Gruber & Haeberli, 2009). However, this classification is subject to many exceptions, and its applications cannot adjust for other mountain areas. Assuming this zonation to be valid for the semi-arid Andes, Figure 2 depicts an idealized diagram of altitudinal permafrost distribution in the Chilean Andes at ~29.3°S.

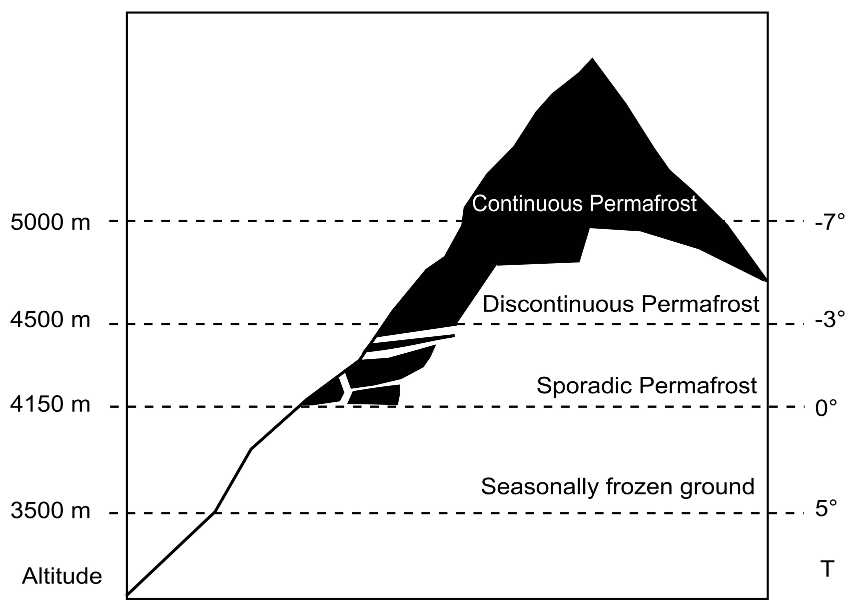

Figure 2. Idealized diagram of altitudinal permafrost distribution in semi-arid Chilean Andes at 29.3°S (In Azócar, 2013)

2.2 Mountain Permafrost and Temperature Surface Regimes

In recent years, numerous studies monitoring GSTs have determined substantial differences in temperature surface regimes between surface materials such as coarse blocks, fine grained rock-debris cover and steep bedrock slopes in mountain areas (Hoelzle *et al.*, 2003; Gubler *et al.*, 2011). Harris and Pedersen (1998) stated that GSTs of blocky materials can be 4-7°C colder than adjacent fine rock debris areas in the upper part of the Rocky Mountains. In another study, Gorbunov *et al.* (2004) determined that the GST at lower parts of blocky slopes in the Transili Alatau Range (Kazakhstan) tend to be 2.5-4 °C cooler than that in other areas. A recent study by Apaloo *et al.* (2012) observed that the cooling effect of coarse blocks (0.6-0.8°C) in the Andes near Santiago is smaller than the cooling effect observed in the Swiss Alps and Norwegian mountains (Delaloye & Lambiel, 2005; Juliussen & Humlum, 2008). Evidence of a strong cooling effect on steep bedrock slopes has been demonstrated in various studies conducted in the European Alps and in the Southern Alps of New Zealand (Gruber *et al.*,2004; Gruber & Haeberli, 2007; Allen, Gruber, & Owens, 2009). Basically, coarse block deposits tend to be cooler than other surfaces for several reasons, such as the thermal conductivity of the block layer modifying the warming influence of snow cover (Gruber & Hoezle, 2008) and the so-called *chimney* effect that produces a strong overcooling of the ground due to the ascent of warm air toward the top of the block deposit in winter, thus facilitating the aspiration of cold air deep inside of coarse block deposits (Delaloye & Lambiel, 2005). On the other hand, the absence of snow and debris cover on steep slopes of bedrock means that GST responds more quickly to atmospheric temperature (Allen *et al.*, 2009).

The majority of permafrost distribution models (See Table 1) often do not discriminate between different types of surface, even though it is very well know that near-surface material can cause differences in ground temperatures. These models often extrapolate their permafrost prediction obtained using permafrost indicators or GST measures of a particular land-surface domain to other areas.

In general, permafrost distribution models that are based on rock glacier forms as evidence of permafrost conditions (Boeckli *et al.*, 2012a,b; Deluigi & Lambiel, 2012) cannot extrapolate their permafrost prediction to other non-debris surface areas such as steep bedrock slopes because the surface and subsurface characteristics of debris and steep bedrock slopes are subject to other geographical conditions such as snow accumulation, exposure, slope and different physical material properties.

2.3 Mountain Permafrost and Climate Change

Future scenarios of climate change in mountain regions are uncertain due to the coarse resolution of the current General Circulations Models (GCMs) and the complexity of mountain environments in terms of geographical and meteorological factors (Beniston & Douglas, 1996). However, empirical evidence such as the accelerated retreat of mountain glaciers around the world has been attributed to global climate change (World Glacier Monitoring Service, 2009). Direct observation of climate change effects on mountain permafrost worldwide is still limited because most studies on this topic began only during the last few decades and mainly concentrate on the Alps and North American mountains. Temperature records from a borehole located in the Murtèl rock glacier in the Swiss Alps show that permafrost has been warming at a rate of 0.4°C per decade at a 10 m depth during the last decades, with strong seasonal increases of the active layer temperature during the summer (Haeberli & Gruber, 2009). For the Swiss Alps, Haeberli and Hohmann

(2008) project changes in temperature [precipitation] by + 2°C [+10%] in winter and + 3°C [- 20%] in summer. These temperature changes will increase the degradation of alpine permafrost in the future. Thermal conditions in ice-rich permafrost depend on snow cover thickness and duration, which are difficult to predict (Barry & Yew Gan, 2011). Recent studies have found evidence of steady acceleration in the movement of rock glaciers in the Alps during the last decade due to a general increase of ground and atmospheric temperatures (Roer *et al.*, 2005a; Kellerer-Pirklbauer & Kaufmann, 2012).

In the semi-arid Argentine Andes (32°S), changes in the active layer-thickness have been observed in two rock glaciers, indicating that the active layer depth is increasing at a rate of 15-25 cm/year (Trombotto & Borzotta, 2009). Evidence of rock glaciers in a degradation phase due to low ice content has been also found in the Bolivian Andes, in on study (Francou *et al.*, 1999). According to the authors, this change is believed to have occurred during the last century. On the other hand, recent evidence of acceleration and destabilization of rock glaciers located in the Alps and Andes have been partially associated with a rise in the temperature and precipitation in the last decades (Bodin *et al.*, 2012). In spite of the lack of studies that examine the state of mountain permafrost in other regions of the world, all permafrost regions are expected to experience an increase in the ground temperature and thickness of their active layer, and spatial changes in the distribution of mountain permafrost.

The degradation of mountain permafrost mainly has impacts on slope stability and the water cycle. Warming of perennially frozen rock walls and debris deposits increases the probability of large rock-fall events, debris flows and landslides, increasing the risk for people and infrastructure in high mountain areas (Harris *et al.*, 2001). While, the contribution of mountain permafrost to discharge has been barely studied, it is probable that thawing of ice-rich permafrost (e.g., intact rock glaciers) increases river discharge during dry seasons in arid regions (Azócar & Brenning, 2010; Caine, 2010); however, more studies on mountain permafrost runoff are needed (Brenning, 2010).

Climate change for the mainland Chile is expected to produce an increase of temperature of between 2°C and 4°C for the end of 21st century; it has been predicted that this effect will be more pronounced in the semi-arid Chilean regions than in the rest of Chilean regions (Providing Regional Climates for Impact Studies [PRECIS]; Comisión Nacional del Medio Ambiente [CONAMA], 2006). In addition, mountain areas will probably experience a temperature rise of about 5°C during the summer season and an increase in the higher minimun and maximum temperatures (Fiebig-Wittmaack *et al.*, 2012).

2.4 Geographical Controls of Mountain Weather and Climate

Mountains have different types of effects on weather and climate. First, there is a significant modification of air flows by dynamic and thermodynamic processes. Second, there is a recurrent generation of characteristic regional weather conditions. Topoclimatic factors such as slope and aspect have an effect at local scale, causing a variety of microclimate conditions (Barry, 1992).

Mountain climates are mainly controlled by three geographical factors: latitude, altitude and topography (Barry, 1992; Whiteman, 2000). The influence of latitude on climate is evident in a variety of ways. First, solar radiation and temperature decrease with increasing latitude. Second, latitude has an influence on seasonal and diurnal variation. Third, latitudinal differences in mountain climates are related to the characteristics of global atmospheric circulation patterns (i.e., regional winds). As results of these latitudinal effects, temperature and precipitation regimes are different for each mountain area around the world; moreover, snow and vegetation patterns are drastically modified as latitude changes.

Altitude is one of the geographical factors with the strongest influence on mountain climates. Temperature, atmospheric moisture, precipitation, winds, incoming solar radiation, and air density all vary with altitude (Whiteman, 2000). Typically on average temperature decrease of 6 °C/km or ~0.6°C occurs with every 100 m altitudinal change (also called the environmental lapse rate; Barry, 1992). Thus, locations at high elevation generally have cooler climates than locations at lower elevations. In general, average temperature lapse rates show considerable local as well as seasonal variability; moreover, temperature lapse rates can be affected by types of air mass (Lautensach & Bögel, 1956).

Incoming solar radiation increases with altitude because there is less depletion of solar beams through absorption and scattering than at lower elevations (Whiteman, 2000). Atmospheric moisture generally decreases with altitude; as altitude increases, the distance from the source of moisture increases, and therefore, the amount of moisture in the atmosphere decreases (Whiteman, 2000). Wind speeds increase with altitude due to peaks extending high into the atmosphere where wind speeds are greater. Moreover, mountainous areas are typically characterized by a change of wind direction twice a day (Whiteman, 2000). Winds blow up the terrain (upslope or up-valley) when surfaces are heated during daytime and blow down the terrain (downslope, down-valley) when surfaces are cooled during night time (nocturnal inversion).

According to Whiteman (2000), topographic effects of mountain ranges on the weather can be divided into two different spatial scales. A mountain range's dimension and orientation with respect to predominant winds are relevant for large-scale weather processes. An air flow approaching a mountain barrier responds differently depending on the degree of stability, the speed of air flow and the mountain's dimension (i.e., length and high of the mountain range). Terrain shapes and surface relief are particularly important for regional-scale weather processes; the roughness of the underlying surface affects wind speed and produces changes in the direction of airflow. Slope angle and aspect are important for *local-scale* weather processes. It is very well known that north-facing slopes receive more radiation than south-facing ones during the day, and that slope affects the angle of the sun's rays reflection, thus modifying the temperature conditions of each mountain site. Even though the amount of solar radiation is mainly controlled by the latitude and altitude, other factors such as day of year, time of day, cloud cover, aerosol content, shading by surrounding terrain and surface albedo can affect the amount of solar radiation received at a given mountain site.

Another geographic factor related to the other factors above mentioned is continentality. Mountain ranges located in the middle of continents experience larger diurnal and seasonal temperature changes than those located close to large bodies of water, because land surfaces heat and cool faster than oceans or large lakes (Whiteman, 2000).

2.5 The Periglacial Zone

The "Periglacial" is the term commonly used to refer to a zone peripheral to glacier areas (Barsch, 1996) in which seasonal and perennial frost and snow processes are or have been an important factor (Embleton & King, 1975; French, 2007).

The term "periglacial domain" usually refers to the global extent of the periglacial zones that mainly occur near to the Polar Regions and in high-altitude areas. In the Polar regions, the periglacial domain is mainly represented by Tundra areas, and mid-and low-latitudes, by plateaus and mountain ranges where higher elevation promotes cold conditions (French, 2007). A periglacial zone is always characterized by the presence of continuous or semi-continuous permafrost areas (Embleton & King, 1975).

In the periglacial zone, freeze-thaw actions play and important role in the weathering of rocks and landform development, producing a variety of geomorphological features (Embleton & King, 1975). Typical landforms resulting from cold weathering, sorting and transport processes are rock glaciers, solifluction lobules, pattern-grounds and blockfields (Embleton & King, 1975; Davis, 2000; Trombotto, 2000). Moreover, a variety of slope forms can be partially associated with periglacial environments such as free-face slopes (or talus slopes), rectilinear debris-mantled slopes and cryopediment slopes (French, 2007). In a mountain environment, periglacial features such as rock glaciers are the most important geomorphological expression of permafrost presence, either now or in the past (Barsch, 1996; Burger *et al.*, 1999; Haeberli, 2000).

2.6 Historical Development of Periglacial Research in the Semi-arid Chilean Andes

The first study of the periglacial environment in Chile was carried out by the glaciologist Louis Lliboutry, who describes rock glaciers as forms characteristic of the periglacial environment in the semi-arid Chilean Andes (Lliboutry, 1953). Several years later, the French geomorphologists Jean Borde and Roland Paskoff mapped, in different studies, the presence of several rock glaciers in the Andes of Santiago and in the Elqui valley (Borde, 1966; Paskoff, 1967). In the next decades, the geologist Cedomiro Marangunic (1976) conducted the first measurements of rock glacier movement on the Pedregoso rock glacier (32°S). In 1979, the Chilean Water

Directorate (*Dirección General de Aguas*, DGA) included some rock glaciers as debris-covered glaciers in the official glacier inventories for the Chilean Central Andes (e.g., Marangunic, 1979; Brenning, 2005a). An important number of rock glaciers in the northern section of the Chilean Andes between the parallels 18° and 29°S were identified by Kammer (1998), who also pointed out the strong influence of the South America Arid Diagonal over the distribution of rock glaciers between 23° and 27°S. Later studies have ratified this finding (Brenning, 2003; Brenning, 2005a,b; Azócar & Brenning, 2010).

In recent decades, several inventories of rock glaciers, obtained with different methodological approaches, have been conducted (Nicholson *et al.*, 2009; Geoestudios Ltda, 2008; UGP UC, 2010, Azócar, 2013). According to the most recent inventories for the semi-arid Chilean Andes, 1290 intact (e.g., active and inactive forms) rock glaciers can be found between ~28.5° and 32°S, covering an estimated area of 60.3 km^2, and having a water equivalent of between ~732 to 1100 million m^3 (UGP UC, 2010; Herrera *et al.*, 2011; Azócar, 2013).

The internal structure of rock glaciers in the semi-arid Andes has been studied through geophysical methods in the Tapado glacier systems near the Aguas Negras border crossing between Argentina and Chile (Milana & Güell, 2008). The authors concluded that the internal structure of glacigenic rock glaciers tend to have a less thick active layer and more ice content than cryogenic rock glaciers. Recently, Monnier and Kinnard (2013) studied the situation using core drilling and ground-penetrating radar to understand the composition of a small rock glacier located in the upper zone of the Choapa river watershed. This study pointed out that the internal structure of rock glacier is characterized by an ice-rock mixture with ice content ranging between 15-30%, indicating that the rock glacier is clearly in a degradation phase. Another recent study, focused on internal structure and ice content using ground-penetration radar, was carried out by Monnier & Kinnard (2012) in the Llano de Las Liebres rock glacier located in the Elqui river watershed. The findings of these studies have helped to clarify the structure and origin of rock glaciers; however, more research is needed for a better understanding.

Studies on the geometry, forms and classification of rock glaciers have been carried out by Ferrando (1996; 2003a), Brenning (2005) and Iribarren (2008) in some small watersheds located in the semi-arid Chilean Andes. Evidence of Late Quaternary glaciation along the Elqui valley has been studies by Caviedes & Paskoff (1975) and Kull *et al.* (2002) in the past decade.

The hydrological and geomorphological significance of rock glaciers in both the dry and semi-arid Chilean Andes have been evaluated using statistical estimation techniques to quantify rock glacier areas and their water equivalent, and to assess topographic and climate controls on rock glacier distribution (Brenning, 2003; Brenning, 2005a,b; Brenning & Azócar, 2010a; Azócar & Brenning, 2010). The studies showed that the water equivalent of rock glaciers is larger than that of the glaciers between the 29-32°S (Brenning, 2005a; Azócar & Brenning, 2010; Brenning & Azócar, 2010a). This finding may possibly explain the excess river discharge observed in the Chilean dry Andes that cannot be explained by glacier retreat (Ferrando, 2003b; Favier *et al.*, 2009; Azócar & Brenning, 2010). However, further research is needed (Brenning, 2010; Arenson & Jakob, 2010 and Gascoin *et al.*, 2011) to confirm this hypothesis.

During recent years, monitoring of rock glacier dynamics, through surface and sub-surface temperature measurements in shallow boreholes, has been carried out in periglacial zones in the Andes of Santiago and in the upper Elqui watershed (UGP UC, 2010; Bodin *et al.*, 2010; Apaloo *et al.*, 2012; Brenning *et al.*, 2010, 2013). These studies have mainly concluded that the surface thermal regimes of periglacial areas are essentially controlled by the duration of snow cover and its insulating effect on atmospheric temperatures, the relationship between topography and solar radiation, and the altitudinal changes.

New approaches for detecting local geomorphological features related to creeping mountain permafrost using texture filters, apparent thermal inertia in conjunction with statistical and machine-learning, and terrain attributes have been applied to detect rock glaciers and debris-covered glaciers in the Andes (Brenning & Azócar, 2010a; Brenning *et al.*, 2012a,b). These studies have given the first steps toward automatic detection of rock glaciers.

Over the past several decades, environmental impacts of mining operation have been noticed in periglacial zones, directly affecting debris-covered glaciers and rock glaciers mainly those located in the Aconcagua, Mapocho and Huasco watersheds in the Chilean Andes. In general, mining operations impact periglacial zones through the complete or partial removal of rock glaciers as well as through the construction of mine dump piles and infrastructure over rock glaciers that affect water resources, destroy the mountain landscape and increase the risk of landslides (Brenning, 2005a, 2008; Brenning & Azócar, 2010b).

While research in periglacial environments has significantly increased in the Chilean Andes in recent years, much of periglacial research has been conducted in Argentina through the work of Argentine and German geomorphologists in the northwestern Argentine Andes (Brenning, 2005a). Within the main studies that have been carried out in recent decades are inventories of rock glaciers realized by Corte (1978), Esper (2009) and Perucca & Esper (2011). Several studies on the significance of topographic and climatic characteristics that control the permafrost and rock glacier distributions were realized by Schrott (1991), Brenning & Trombotto (2006) and Esper (2010). The hydrological significance of rock glaciers and permafrost has been studied by Schrott (1996; 1998). Monitoring of the dynamic, ground and sub-surface temperatures over rock glaciers has been carried out in the Cordon de la Plata in the Central Andes of Mendoza (Trombotto *et al.*, 1997; Trombotto & Borzotta, 2009).

2.7 Rock Glaciers

2.7.1 General Overview

Rock Glaciers are a periglacial phenomenon widely distributed around the world. They consist of a mixture of rocks with variable or no ice content, produced during the Holocene time period (Birkeland, 1973; Haeberli *et al.*, 2003). According to Capps (1910), who established one of the first definitions that remain valid today, a rock glacier, based on its surface morphology, is "a tongue-like or lobate body, usually made up of angular boulders and resembles a small glacier" (Figure 3). Rock glaciers generally occur in high mountainous (or dry polar) terrains, and they usually have ridges, furrows and sometimes lobes on their surface, and a steep front at the angle of repose" (Potter, 1972). Their longitude can vary from hundreds of meters to several kilometers but is normally between 200 to 800 m (Barsch, 1996). Even though the morphological definition suggested by Capp (1910) is still valid today, there are many controversies about whether it is more appropriate as a definition that emphasizes process and genesis than morphology attributes (Berthling, 2011).

Several attempts to improve the definition and classification schemes for rock glaciers, based on geometric patterns, geomorphological position and sources of the debris material, have emerged in the last decades (Clark *et al.*, 1998). Within of these rock glacier classifications, the one stated by Barsch (1996) that emphasizes dynamic states has been widely accepted. By his classification, rock glaciers can be categorized into active forms (with movement and ice content), inactive forms (without movement but with the remains of ice) and fossil or relict forms (without movement and where the ice has completely melted).

Active rock glaciers are commonly recognized as the geomorphological expression of permafrost rich in ice in the current mountain environments (Barsch, 1996; Burger *et al.*, 1999; Haeberli, 2000). The internal structure of active rock glaciers is composed of ice (between 40-60% by volume) and rock fragments (Barsch, 1996; Hoelzle *et al.*, 1998; Arenson *et al.*, 2002,). They can have horizontal displacements of between ~10 cm to ~100 cm/year (Burger *et al.*, 1999; Roer *et al.*, 2005a,b; Brenning *et al.*, 2010). Due to their high percentage of ice, rock glaciers are long-term stores of frozen water that has accumulated during post-glacial times. Therefore, rock glaciers can be considered fossil groundwater bodies, or nonrenewable water resources (Azócar & Brenning, 2010). In general, rock glaciers can become inactive as well as in a relict status when there is an increase in ice thawing and growth in the unfrozen debris mantle, or when they move far away from a source of debris and ice. In addition, changes in the bedrock slope contribute to decreasing their movement (Barsch, 1996).

2.7.2 Rock Glacier Classification

Classifications of rock glaciers are normally related to the evidence of some processes or indicate certain environmental conditions (Whalley & Martin, 1992). Several classification schemes have been devised during the last decades to describe rock glaciers using criteria related to the source of the rock material, shapes, geomorphological position, dynamic status and ice type (i.e. ice-cored and interstitial ice; Janke *et al.*, 2013). However, at present, there is no commonly accepted classification, although the one by Barsch (1996) is perhaps the most widely used.

2.7.2.1 Rock Glacier Genesis

There are mainly two schools of thought about the origins of rock glaciers; the first school holds that rock glaciers are exclusively periglacial phenomena, and the other considers that some rock glaciers form through a continuum of glacial to periglacial processes (Clark *et al.*, 1998; Mahaney *et al.*, 2007; Berthling, 2011). These schools of thought argue their theories using support related to the source of ice and the geomorphologic context where rock glaciers are located. In reality, the two viewpoints are not mutually exclusive, and rock glaciers can be formed by a combination of glacial and periglacial processes (Humlum, 1996).

The periglacial school suggest that rock glaciers are exclusively phenomena of permafrost, and are inherently distinct from true glaciers or covered glaciers (Wahrhaftig & Cox, 1959; Barsch, 1996). In this model, the source of the internal ice is derived from non-glacial processes, linking the source of the ice to the freezing of rain and meltwater percolating from snow cover into the debris layers (interstitial ice; Clark *et al.*, 1998). Also included are the burial of surface snow and ice (Haeberli, 2000). However, this position recognizes that in some cases sedimentary ice can be derived from a glacial origin (e.g., Haeberli, *et al.*, 2006). This viewpoint is especially applicable to valley-wall or talus rock glaciers where it is probable that ice began to accumulate through the burial of surface snow and ice by debris (i.e., avalanches-buried snow, Clark *et al.*, 1998).

The opposing view considers that some rock glaciers form through a continuum of glacial to periglacial processes (Wahrhaftig & Cox, 1959; Clark *et al.*, 1998; Burger *et al.*, 1999). In this model, it is assumed for some rock glaciers that sedimentary ice has more likely a glacial origin (e.g., Humlum, 1996). Under this viewpoint, rock glaciers can be considered as transitional and temporal forms derived from glacial processes. Using this scheme a rock glacier is regarded as a landform located in the terminal part of a glacier system, a debris-covered glacier will be in the middle and a clean glacier will be situated in the upper zone (Clark *et al.*, 1998).

On the other hand, rock glaciers can also be produced from landslide processes such as rockfalls, debris flows, and snow avalanches over unconsolidated talus and glacier rock deposits (Johnson, 1984; Barsch, 1996). However, lack of evidence means landslides cannot yet confirmed as the third school of the source of rock glaciers.

2.7.2.2 Rock Glacier Types: Process of Formation

According to Barsch (1996) most rock glacier classifications are overloaded with complex definitions related to the source and types of internal material. Therefore, these classifications lack descriptive value and are difficult to apply. Instead he proposes two main forms of rock glacier classes, based on descriptive parameters related to topography and position that can be obtained through photointerpretation and fieldwork:

Talus rock glaciers develop at the foot of talus slopes where an accumulation of ice-supersaturated debris material can be found. The size and development of talus rock glaciers is mainly controlled by talus production, snow incorporation and the refreezing of melting water. They normally have lobate forms, but tongue-shaped forms can also present (Barsch, 1996).

Debris rock glaciers mainly occur at the end of terminal and lateral moraines of glaciers, and generally transport mainly morainic or glacier debris (till; Barsch, 1996). Usually, when moraines start to creep they are considered to be debris rock glaciers (e.g., glacier-deriver rock glaciers; Humlum, 2000).

The ice in these land forms is derived from glaciers according to some authors (Wahrhaftig & Cox, 1959; Humlum, 1996; Clark *et al.*,1998; Burger *et al.*, 1999), but melting snow water can be refrozen into the internal structure of the rock glacier

(Whalley & Martin, 1992). Tongue-shaped forms are common in this group of landforms (Humlum, 1982).

It is also possible that the material has been derived from other sources such as debris flows and mining dumps. In this situation, Barsch (1996) proposes using the term *special rock glaciers*.

This classification scheme has been widely used in inventories of rock glaciers, permafrost modeling and geomorphological studies on rock glaciers (Nyenhuis & Hoelzle, 2005; Brenning, 2005a,b; UGP UC, 2010).

2.7.2.3 Rock Glacier Dynamics

Rock glaciers are dynamic land forms. Several authors such as Warhaftig & Cox (1959), Arenson *et al.* (2002) and Haeberli *et al.* (2006) have concluded that the most characteristic movement mechanism of rock glaciers is due to the deformation of subsurface ice in different shear planes. In general, ice is the material component most susceptible to deformation processes in rock glaciers.

The deformation is in accordance with the shear stress applied, the density, the thickness, temperature, grain size and shape of rock fragments; the form, type and size of the ice crystals, the density of ice and water content (Barsch, 1996). Moreover, the topographic changes underneath the rock glacier (e.g., type of bedrock, change and length of slope) can have an influence on internal deformation processes (Arenson *et al.*, 2002).

Rock glacier movement has been measured in different sites around the world, with average movement rates of between 0.1 to 1 m/year, although displacements of over 1 m have been registered, e.g., in the Alaska Range, European Alps (Barsch, 1996; Wahrhaftig & Cox, 1959; Roer & Nyenhuis, 2007 and Delaloye *et al.*, 2008) and recently in the semi-arid Chilean Andes (UGP UC, 2010).

Rock glaciers, according to their dynamics, can be classified as active, inactive and fossil or relict forms (Vitek & Giardino, 1987; Barsch, 1996). *Active rock glaciers* are recognized as the visible expression of creeping mountain permafrost in unconsolidated materials. They are commonly described as lobate or tongue-shaped bodies of unconsolidated debris material supersaturated with interstitial ice and ice lenses that slowly move downslope or down valley as a consequence of the deformation of ice (Barsch, 1996). They normally have a front scarp and surface relief with furrows and ridges, these corrugations being the expression of compressive flow (Barsch, 1978).

A recently study (Berthling, 2011) that examined the rock glacier definition controvery, suggests that the morhpological definition of an active rock glacier should be abandoned and replaced by a common definition by which active rock glaciers are considered "the visible expression of cumulate deformation by long-term creep of ice/debris mixtures under permafrost conditions". This definition is genetically impartial about the realms (periglacial or glacial), but it is still genetic with respect to the creep process.

When rock glaciers stop moving but still contain ice, they are called *inactive rock glaciers.* According to Barsch (1996), a rock glacier can become inactive due to climatic and dynamic factors. An increase in ice thawing provokes a growth in the unfrozen debris mantle (i.e., active layer), obstructing and decreasing the flow capacity, notably in the lower part of rock glaciers (climatic inactivity). On the other hand, a rock glacier can become inactive when it moves far away from the source of debris and ice or when a reduction in the slope gradient does not allow further movement (dynamic inactivity). Inactive rock glaciers show front slopes at or below the angle of repose with a smooth front scarp.

Active and inactive rock glaciers are commonly grouped for purposes of permafrost modeling as intact rock glaciers, due to the difficulty of differentiating between active and inactive ones, especially through photointerpretation. Moreover, intact rock glaciers are used as indicators of permafrost presence in mountain areas (Barsch, 1996; Roer & Nyenhuis, 2007 and Boeckli *et al*., 2012a,b).

Rock glaciers are denominated *fossil or relict* when they do not display any horizontal and vertical movement and the ice has completely melted. Their surface relief is characterized by collapsed structures where furrows and ridges tend to look subdued and flat as a result of the complete melting of ice (Putnam & David, 2009). A relict rock glacier also has a strong decline in its frontal and sides slopes (Barsch, 1996; Ikeda & Matsuoka, 2002). The presence of vegetation cover has been used as an indicator of fossil states in the European Alps (Ikeda & Matsuoka, 2002) and the White Mountains of North America (Putnam & Putnam, 2009). However, the high mountain environment of the semi-arid Andes is often characterized by a complete absence or scarcity of vegetation due to very dry climate (Brenning, 2005a).

The first measurements of rock glacier movement in the Chilean Andes were made by Marangunic (1976) and Bodin *et al.* (2010). The results of this last study showed that a rock glacier in the Andes of Santiago (~33°S) had an average horizontal movement of 32 cm/year. Meanwhile, in the semi-arid Andes, researchers have observed horizontal displacements of between 35 to 67 cm/year on rock glaciers located in the Elqui watershed (~30°S; UGP UC, 2010). Further north, displacements of between 13 and 22 cm/year have been registered at control points located in the lower parts of three rock glaciers in the Huasco watershed (~29°S; Azócar, 2013; Rookes Serrano Ingeniería, 2011).

Figure 3. Active rock glacier “El Paso” located in the eastern side of the semi-arid Andes near the Aguas Negras border crossing between Argentina and Chile (30.2°S, 69.8°W; photographed by the author, December 12, 2009)

2.8 Modeling Process: A Brief Overview

A model can be defined as "a simplified representation of a more-complex phenomenon, process or system; an environmental model is one that pertains to a specific aspect of either the natural or the built environment" (Barnsley, 2007). According to Hardisty *et al.* (1995) and Barnsley (2007), the creation of a model involves several steps: first, a scientific question or problem must be identified. Second, a conceptual model of the problem must be developed (e.g., a flow diagram). This step involves an understanding of the relevant phenomenon, processes or systems; their respective input and output, and the relationships between the two; and the boundaries of the model. Third, the assumptions of the model should be formulated and need to reflect the limits of current knowledge about the target environmental system. Assumptions should be mentioned with the goal of clarifying the nature, purpose and limitation of the model for the modeler and future users. The intended spatial and temporal scales need to be stated to clarify the relationship and process being modeled. The following step into the modeling process describes the conceptual model using mathematical tools and concepts (i.e., function and equations); different mathematical schemes have been proposed based on several considerations, such as whether the model is derived from theory or observations, the degree of randomness, understanding of the target, characteristic static or dynamic features of the model with respect to space and time; whether the model is described in a continuous or discrete manner and the characteristics of distribution and the spatial variability of the model parameters and variables.

Wainwright & Mulligan (2007) state that the range and diversity of mathematical models are considerable; however, they can be classified as *mathematical (empirical), conceptual and physically based models*. An *empirical model* is based on observations, relationships are defined by the measurement of variables concerned, and established by a mathematical function (i.e., regression analysis is commonly used). This kind of model says nothing about the process. No physical laws or assumption about the relationships between variables are necessary. Empirical models have a valuable predictive power but a low explanatory depth. They are specific to circumstances or sets of data; thus, it is difficult to make generalizations and employ them for other spatial and temporal conditions. *Conceptual models* can be defined as models that incorporate some process understanding of target processes or are based on preconceived notions about how the target systems work (e.g., a hillslope hydrology model). Like empirical models, they typically lack generality. *Physically-based models* are derived deductively from established physical principles. Models that emphasize the implication of processes transforming input to output are commonly called *process-physic models*. Such models have the advantage of providing a better understanding of outcomes; moreover, they are more appropriate for generalizing than empirical models.

The next step in the modeling process is choosing a platform or language. Currently, several software products are available for implementing computational models ranging from simple spreadsheets to complex computer programing languages. The decision about which platform to use generally depends on the experience and preference of the user, and on the cost of model implementation (Barnsley, 2007).

As the last step in the modeling process, an evaluation of the model is necessary. Commonly, a verification process is used to check that the model is computationally running well. Validation, on the other hand, refers to the testing of the model output to confirm that the model is suitable for its intended purpose.

Normally, a common method of validation is to compare the modeled output to a set of independent field-measured data (e.g., a goodness-of-fit method). The model's accuracy (fidelity), the error (difference between observed and modeled values) and the precision (the exactness with which a measure is taken) are also considered. An additional step in the evaluation process is sensitivity analysis, which evaluates how the model is affected by changes in input parameters (Barnsley, 2007).

In modeling mountain permafrost, two main modeling approaches are commonly used*: empirical (or statistical) models and process-based models*. These two major approaches are explained in detail in the next sections.

2.9 Modeling of Mountain Permafrost

2.9.1 Empirical-statistical Models

Permafrost distribution in mountain areas has usually been modeled using combinations of empirical-statistical approaches and variables related to topographic characteristics, climate data and geomorphological indicators (i.e., rock glaciers). Most of these empirical models have been applied at different spatial-scales in the European Alps, and partially in North American, Asian and South American mountain ranges (Keller, 1992; Gruber & Hoelzle, 2001; Nyenhuis & Hoelzle, 2005; Ebohon & Schrott, 2008; Boeckli *et al.*, 2012a,b, Gruber, 2012; Bonnaventure *et al.*, 2012; Zhang *et al.*, 2012 and Azócar *et al.*, 2012). In general, most of these empirical-statistical models are more concerned with the predictiction of permafrost presence rather than the description of the actual subsurface thermal state. The first models of permafrost occurrences were expressed as "rules of thumb" that established a relationship between permafrost occurrence and topographic factors such as altitude, slope and aspect (Haerberli, 1975 in: Keller *et al.*, 1998).

In addition to the classical topographic attributes, MAAT and potential incoming solar radiation (PISR) are mainly used as predictor variables in empirical permafrost distribution models (Hoelzle *et al.*, 2001; Lewkowicz & Ednie, 2004). MAAT is commonly used as an indicator of modern permafrost zones (Hoelzle & Haeberli, 1995; Ishikawa, 2003b). In general, a MAAT below -3° C is often used as first-order classification of altitudinal belts that have a significant extent of permafrost (Gruber & Haeberli, 2009).

Remote-sensing techniques cannot be directly used to detect permafrost conditions, because sub-surface thermal conditions are hidden from sensors; however, these techniques can be used to detect landforms, to derive temperatures (radiant temperature; Jensen, 2013) and to identify land-cover or vegetation patterns related to permafrost (Leverington & Duguay, 1997; Frauenfelder *et al.*, 1998; Etzelmüller *et al.*, 2001; Duguay *et al.*, 2005). In recently permafrost modeling studies in mountain areas, Apparent Satellite Temperatures (ASTs) and the Normalized Difference Vegetation Index (NDVI) have been used as supplementary predictor variables for permafrost mapping. In general in mountain areas, a decrease of vegetation as a consequence of altitude is associated with an increase of favorable permafrost conditions (Etzelmüller *et al.*, 2001). In addition, BTS values tend to be highly correlated to altitudinal and the NDVI (Gruber & Hoelzle, 2001). On the other hand, the results of another study (Leverington & Duguay, 1996,1997; Ødegard *et al.*, 1999) have shown that AST (derived from TM6-Landsat) and NDVI are not significantly better at improving permafrost prediction than using traditional variables derived from topographic attributes (i.e., altitude aspect, solar radiation). Moreover, the NDVI is not a suitable variable for dry mountain ranges that lack vegetation (i.e., the semi-arid Andes or Kungey Alatau mountains). In addition the vegetation indexes in mountain areas tend to be high correlated with altitude, PISR and temperature values, making an NDVI in some cases a reduntant variable with respect to others (multicollinearty; Gruber & Hoelzle, 2001).

In order to improve the accuracy of permafrost prediction, several studies have used the Basal Temperature of Snow (BTS) and Ground Surface Temperature (GST) as indicators of permafrost presence or absence (Hoelzle *et al.*, 1999; Gruber & Hoelzle, 2001; Isaksen *et al.*, 2002; Ishikawa, 2003b; Lewkowicz & Ednie, 2004). In general a permafrost distribution model that use BTS values as predictor variables in regression analysis, tends also to use terrain atributes (e.g., altitude, PISR and information derived from remote sensing data (e.g., NDVI, AST) as its predictor variables.

BTS is a method introduced by Haeberli (1973) and consists of measuring the basal temperature snow cover at the end of winter but before the onset of snow melt (Gruber & Hoelzle, 2001; Permanet, 2013). It is based on two main assumptions: (1) the BTS remains constants in negative values below a thick snow cover (i.e. ≥ 0.8 m), and (2) under snow cover conditions that inhibit atmospheric temperature fluctuations, BTS values represent the heat flux from the subsurface, and thus subsurface thermal conditions (Lewkowicz & Ednie, 2004; Brenning *et al.*, 2005). In comparison to BTS measurements, GST measures the temperature slightly below ground surface (i.e., at ~5 or 10 cm) and it is typically recorded using temperature loggers buried during the whole winter or even years, thus providing a better understanding of the seasonal fluctuation of the snow cover. It is also a reliable measurement method for remote areas (Hoelzle *et al.*, 2003). Normally in the Alps, BTS measurements of values of <-3°C indicate that *permafrost is probable*, values of -2°C to -3°C that *permafrost is posible* and values >-2°C that *permafrost is improbable* (Lewkowicz & Ednie, 2004). Even though these BTS thresholds have been widely used to study permafrost in other mountain areas, there are limitations. BTS values can have great temporal and spatial variability due to changes in snow cover, vegetation and soil properties; thus, BTS values measured in the Alps cannot be direclty applied in other areas without an appropriate calibration of the context of local conditions (Lewkowicz & Ednie, 2004; Brenning *et al.*, 2005). In addition, some statistical concerns about the distribution of BTS measurements should be considered in the analysis. Consequently, Brenning *et al.* (2005) suggest that more attention must be given to the sample design in order to consider the spatial variation of BTS measurements. Finally, Brenning *et al.* (2005a) recommend that BTS values can be used as relative measurements of thermal conditions and not as direct permafrost indicators.

In recent decades, rock glacier inventories have been used to infer the occurrence and distribution of permafrost. Some studies have used the presence of active rock glaciers and their locations to identify the lower boundary of discontinuous permafrost (Barsch, 1978; Nyenhuis & Hoelzle, 2005). Other researchers have used rock glacier activity status as a response variable to model the probability of permafrost occurrence, where intact rock glaciers are indicative of the presence of permafrost and relict forms are indicative of the absence of permafrost in mountain areas (Janke, 2005a,b; Boeckli *et al.*, 2012a,b; Azócar *et al.*, 2012).

For model assessments of mountain permafrost distribution models, different sources of data have been used, such as temperature measurements from boreholes and near ground surface (Ødegard *et al.*, 1999), and geophysical survey results (i.e., resistivity soundings; In Heggem *et al.*, 2005; Etzelmüller *et al.*, 2006). In addition, some studies have utilized rock glaciers for model assessment (Imhof, 1996; Gruber & Hoelzle, 2001; Etzelmüller *et al.*, 2007; Boeckli *et al.*, 2012a; Bonnaventure *et al.*, 2012).

2.9.1.1 Statistical Approaches to Empirical Permafrost Modeling

A variety of statistical model approaches have been used to study permafrost distribution in mountain areas. Table 1 gives an overview of methods and data in use during the last decades. Empirical-statistical models based on Generalized Linear Models (GLMs) and Generalized Additive models (GAMs) are commonly used to study permafrost distribution at different spatial scales (Lewkowicz & Ednie, 2004; Heggem *et al.*, 2005; Etzelmüller *et al.*, 2006; Brenning & Azócar, 2010a; Bonnaventure *et al.*, 2012). GLMs and GAMs are used with a logistic link function where a binary response variable represents the presence (Y=1) or absence (Y=0) of permafrost. Normally, geomorphological evidence of permafrost occurrences (i.e., rock glaciers) and temperature thresholds are used to build the binary response variable indicative of a permafrost condition.

Recently, more sophisticated statistical approaches have used the Generalized Linear Mixed-effects Model (LMEM, with a probit link function) to account for random inventory effects in the permafrost model (Boeckli *et al.*, 2012a,b), and Support Vector Machines to account for the complexity of permafrost distribution at local spatial scales (Deluigi & Lambiel, 2012). Moreover, the Multivariate Adaptive Regression Spline model has been used as an alternative statistical method to traditional logistic regression models (Zhang *et al.*, 2012).

The evaluation of mountain permafrost models is typically done through the calculation of different indexes of the goodness-of-fit between the modeled and observed values, such as the coefficient of determination R^2 or measures derived from the confusion matrix, such as the overall accuracy, sensitivity, misclassification error, and Area Under the Receiver-Operating Characteristic (ROC) Curve (AUROC). Less rigorous validation methods through comparison or correlation of permafrost prediction with an independent set of observations of permafrost presence or absence are frequently carried out on the models. Sensitivity analyses are not usually performed; however, some attempts to determine the influence of change in model parameters using cross-validation and bootstrap methods have been performed by Azócar & Brenning (2010), Boeckli *et al.* (2012a), Zhang *et al.* (2012) and Deluigi & Lambiel (2012).

2.9.2 Process-based Permafrost Models

Process-based permafrost models are mainly focused on representing energy fluxes between the atmosphere and the ground surface based on principles of heat transfer. They can be categorized using temporal, thermal and spatial criteria (Riseborough *et al.*, 2008). Temporal models capture the transient evolution of permafrost conditions from initial states to future conditions. Thermal models study the presence or absence of permafrost using a transfer function between the atmosphere and ground. Spatial process-based models represent conditions at a single location along one (i.e., a vertical profile) or two dimension (i.e., a transect line or areas). They are often more complex than semi-parametric methods, but more suitable for spatial-temporal extrapolation; moreover most of them have the advantage of estimating permafrost thickness. Due to their high complexity and the lack of data they are not normally applied in mountain areas, and few researchers have used these approaches recently.

As a first step toward the application of such approaches to mountain areas, some initiatives have carried out in the Europe Mountains through the Permafrost and Climate in Europe project (PACE; Harris *et al.*, 2001a). Drilling of several boreholes and measurements of temperatures realized in different mountain sites around Europe have evidenced rising temperatures and increasingly of active layer (Harris *et al.*, 2009). Some attempts have tried to simulate Ground Surface

Temperatures (GSTs) in relation to vertical energy fluxes, where the modeled GSTs are compared with BTS measurements (Stocker-Mittaz *et al.*, 2002). Process-based permafrost model approaches are not considered and applied in this research.

Table 1. Review of predictive modeling and validation approaches used in mountain permafrost modeling

Citation	Method	Response variable	Predictor variables	Validation and Evaluation methods	Sensitivity analysis (Yes/No)
Keller (1992)	Heuristic weights of evidence"?	Bottom Temperature Snow (BTS)	Elevation (ELEV), aspect, slope	-	NO
Imhof (1996)	Heuristic weights of evidence"?	-	Slope, surface cover classification	Comparison of the probability of permafrost with presence of active and inactive rock glaciers	NO
Leverington & Duguay (1996)	Maximum Likelihood/ Reasoning Agreement/ Neural Network	Late-summer depth to frozen ground classes	TM bands (3, 4, 5), NDVI, aspect, equivalent latitude, land covers	Classification table/ Overall accuracy	NO
Leverington & Duguay (1997)	Neural Network	A binary variable indicative of permafrost presence or absence	TM band 6, equivalent latitude, aspect, land cover	Classification table/ Overall accuracy/ Misclassification error	NO
Ødegard *et al.* (1999)	Multiple linear regression	BTS measurements	ELEV, apparent satellite temperature (AST), NDVI, snow depth	Coefficient of determination R^2/ Comparison of BTS predicted with random BTS measurements	NO
Gruber & Hoelzle (2001)	Multiple linear regression	BTS measurements	ELEV, Potential incoming solar Radiation (PSR)	Coefficient of determination R^2/ Comparison with BTS measurement not used in the model	YES (Cross-validation)

Citation	Method	Response variable	Predictor variables	Validation and Evaluation methods	Sensitivity analysis (Yes/No)
Lewkowicz & Ednie (2004)	Generalized linear model (GLM)- Logistic regression / Multiple linear regression	A binary variable indicative of permafrost presence or absence (pits observations)/a continuous variable: BTS (for multiple linear regression)	BTS (for the logistic regression)/ ELEV, PISR (for the multiple linear regression)	Coefficient of determination R^2/ Comparison of permafrost probability between different logistic regression models	NO
Janke (2005b)	Generalized linear model (GLM)-Logistic regression	A binary variable: intact vs. active rock glaciers	ELEV, aspect	Comparison of permafrost probability from the logistic regression with MAATs and BTS measurement	NO
Heggem *et al.* (2005)	Generalized linear model (GLM)-Logistic regression	BTS measurements	ELEV, PISR, Wetness index	Coefficient of determination R^2/ Comparison of permafrost probability from the logistic regression with resistivity sounding data	NO
Etzelmüller *et al.* (2006)	Generalized linear model (GLM)-Logistic regression	A binary variable obtained from ground-surface-temperature data	ELEV, PISR, Curvature indexes , Wetness Index, NDVI, Slope	Coefficient of determination R^2/ Relative comparison with resistivity tomography measurements	NO

Citation	Method	Response variable	Predictor variables	Validation and Evaluation methods	Sensitivity analysis (Yes/No)
Brenning & Trombotto (2006)	Generalized linear model (GLM)- Logistic regression	A binary variable indicative of rock glacier presence (debris) vs. other types of surfaces	ELEV, contribute areas, curvature index, PISR	Overall accuracy /Area under the receiver-operating characteristic (ROC) curve (AUROC)	NO
Brenning *et al.* (2007)	Generalized additive model (GAM)-Logistic Regression	A binary variable: intact rock glaciers vs. surfaces classes	ELEV, easting, northing, north exposedness, curvature, slope	Area under the receiver-operating characteristic (ROC) curve (AUROC)	NO
Brenning & Azócar (2010a)	Generalized additive model (GAM)-Logistic Regression	A binary variable indicative of presence or absence of rock glaciers	Variables representing terrain attribute and position, climate conditions and multispectral remote-sensing data	Overall accuracy / Sensitivity/ Misclassification error/Area under the receiver-operating characteristic (ROC) curve (AUROC)	YES (Bootstrapping)
Panda *et al.* (2010)	Generalized additive model (GAM)-Logistic Regression	A binary variable indicative of permafrost presence or absence	Vegetation types, aspect, elevation	Overall accuracy	YES (Cross-validation)
Azócar *et al.* (2012)	Generalized additive model (GAM)-Logistic regression	A binary variable: intact vs. relict rock glaciers	ELEV, PISR	Area under the receiver-operating characteristic (ROC) curve (AUROC)	NO
Schrott *et al.* (2012)	Generalized linear model (GLM)-Logistic Regression	Geomorphological evidence of permafrost occurrences	Topographic parameters	Comparison with BTS -GST and geophysical measurements	NO

Citation	Method	Response variable	Predictor variables	Validation and Evaluation methods	Sensitivity analysis (Yes/No)
Boeckli *et al*. (2012a,b)	A combination between: Generalized linear mixed -effects model (GLMEM)-Probit link function (debris model) and linear model (bedrock model)	A binary variable: intact vs. active rock glaciers (*debris model*) / A continuous variable: Mean Annual Rock Surface Temperature; *bedrock model*)	Mean Annual Air Temperature (MAAT), PISR, PRECIP	Area under the receiver-operating characteristic (ROC) curve (AUROC) / Comparison of the probability of permafrost with presence of active and inactive-rock-glacier and borehole data	YES (Cross-validation)
Bonnaventure *et al*. (2012)	Generalized linear model (GLM)- Logistic regression	BTS measurements and ground-truthing points in summer reclassified as binary variable indicative of permafrost presence or absence	ELEV, PISR , Equivalent elevation (MAAT), NDVI	Comparison of the probability of permafrost with presence of active and inactive-rock-glacier and borehole data	NO
Deluigi & Lambiel (2012)	Support Vector Machines (SVMs)	Several variables indicative of permafrost presence or absence: intact rock glaciers, rock wall, talus slope, etc.	ELEV, aspect, slope, PISR, MAAT	Overall accuracy /Area under the receiver-operating characteristic (ROC) curve (AUROC)/Comparison of the probability of permafrost with a random sample not included in model	YES (Cross-validation)
Gruber (2012)	-	Global air temperature data	-	-	-

Citation	Method	Response variable	Predictor variables	Validation and Evaluation methods	Sensitivity analysis (Yes/No)
Zhang *et al.* (2012)	Multivariate adaptive regression splines (MARS) / Generalized linear model (GLM)-Logistic regression	A binary variable indicative of permafrost presence or absence / A continuous variable: Mean Annual Ground Surface Temperature	ELEV, PISR	Overall Accuracy and compared between models	YES (Cross-validation)

Chapter 3
Study Area

3.1 Location

The study area occupies a portion of the semi-arid Chilean Andes, covering from north to south, the upper sections of the Huasco, Elqui, Limarí and Choapa watersheds between ~28.5 and 32.2° S (Figure 4). In terms of political boundaries, the study area extends along the Atacama and Coquimbo regions and it is bordered on the East by the Province of San Juan, Argentina. The population is distributed in towns near to the coastal border (e.g., Coquimbo-La Serena) and in towns along the main rivers (e.g., Vallenar, Ovalle). As the altitude increases, the presence of population become scarce; most of the human settlements located over 2000 m a.s.l. are related to activities such as seasonal grazing of animals, customs services and mining operations. As in many other semi-arid regions around the world, the population relies on water resources from the high-altitude upper watershed areas (Viviroli *et al.*, 2007).

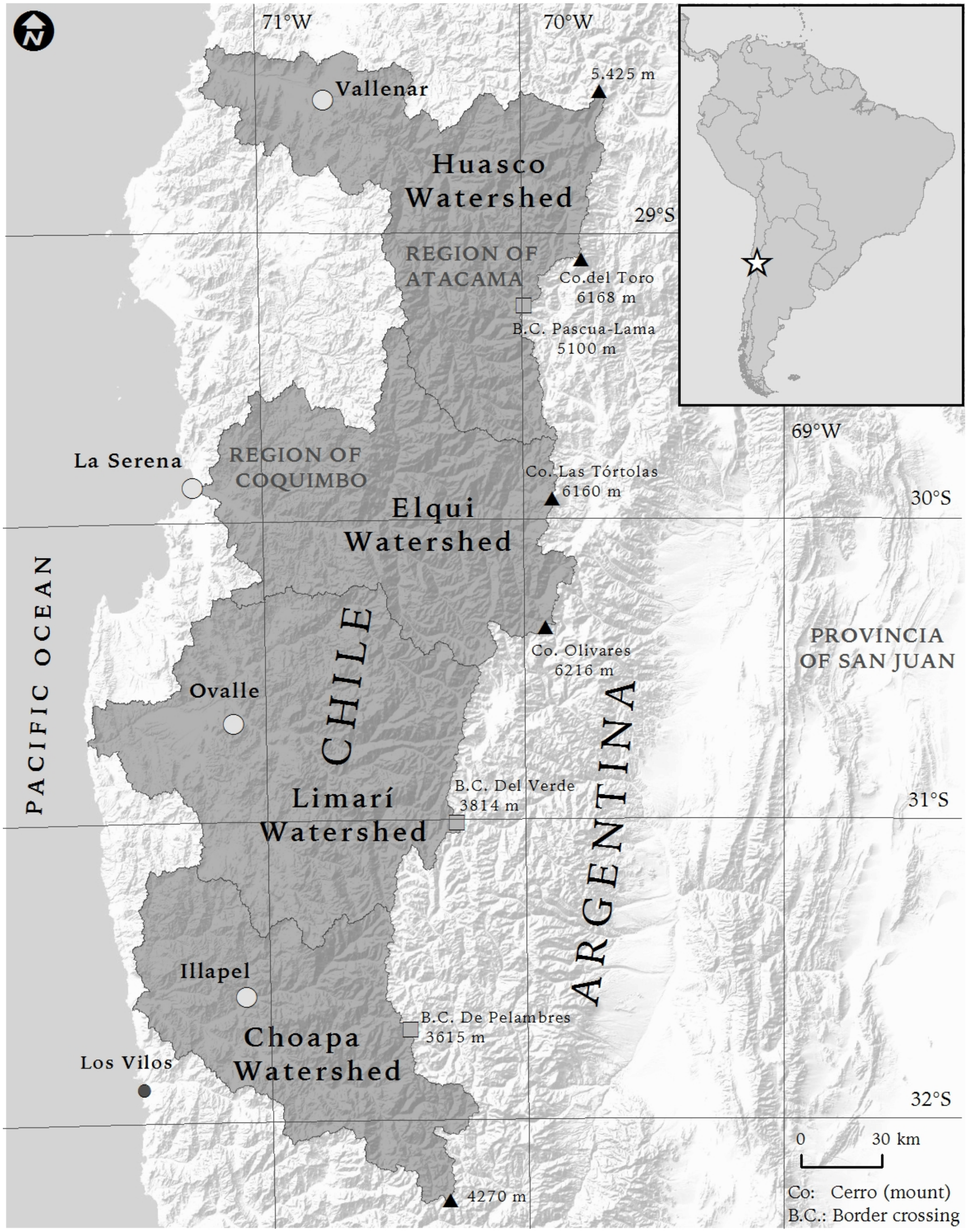

Figure 4. Overview map of the study area. Dark grey areas represent the chosen watersheds

3.2 Geology and Topography

The Andes are a result of plate tectonic processes, caused by the subduction of the Nazca plate beneath the South American plate (Pankhusrt & Hervé, 2007). They are generally divided into several mountain chains running in a north-south direction. The study area is located on the west side of the Andes. The direction of the drainage basins is mainly controlled by geological structures oriented transverse to the main mountain chain. As a consequence of this structural position, the runoff tends to flow an east-west. This section of the semi-arid Chilean Andes varies considerably in elevation from south to north. The southern part is mainly characterized by elevations below or up to ~4250 m a.s.l., in contrast, in the northern part, there is a marked increase in elevation, and summits reach to more than 5500 m a.s.l., grouping the highest peaks of the study area such as Cerro El Toro (6168 m a.s.l.), Las Tórtolas (6160 m a.s.l.) and Olivares (6216 m a.s.l.). Because of the high elevations, most glaciers are concentrated in the northern section (e.g., El Tapado Glacier 5538 m). This section of the Andes is mainly composed of intrusive rocks from the Permian-Triassic periods (i.e., porphyry granite) and volcanic sequences from the Miocene epoch (Sernageomin, 2003). Quaternary volcanism is absent along this section. Several mining projects are located along a mineralised zone known as the El Indio belt that contains large quantities of gold, silver and copper (Maksaev *et al.*, 2007).

3.3 Climate and Vegetation

In general terms, the study area is located in a transition zone between arid and semi-humid climates. The presence of the South Pacific anticyclone, a high-pressure system located in the south east of the Pacific Ocean where the atmospheric pressure is greater than its surrounding area, produces a downward movement of air in the atmosphere that inhibit the develop of cloudiness and precipitation, favoring clear skies, and high solar radiation (Escobar & Aceituno, 1998; Schrott, 1998). Another circulation pattern that has a strong influence on the climate conditions is El Niño–Southern Oscillation (ENSO), which is a rearrangement of atmospheric-oceanic circulation patterns in the tropical Pacific that produces an increase in the amount of precipitation, in the midlatitudes, among other effects; in contrast, the opposite process is called La Niña and typically causes decreased precipitation exacerbating the drought conditions in the study area (Garreaud & Aceituno, 2007). In addition, local weather conditions are influenced by a strong diurnal temperature variation between day and night, and a strong altitudinal effect on the temperature. The Western semi-arid Andes have a continental climate, with large daily and seasonal temperature ranges. The winters are cold and the summers are dry (Fiebig-Wittmaack *et al.*, 2012). Most of the moisture that reaches this area is released as solid precipitation (snow) between May and August (Gascoin *et al.*, 2011). However, during the summer, small snowfalls caused by humid air masses from the Eastern side of the Andes are observable, mainly between the months of January and March (Garreaud & Rutllant, 1997). Measurements of snow depth near the Pascua-Lama mining camp site show that the amount of snow pack thickness varied between ~1m and 4.4 m during the winter seasons between 2001 to 2006 (Azócar , 2013).

Meteorological information is scarce because weather stations tend to be located near the coast and in lower valleys rather than in mountainous areas; however, information from a few weather stations is available. Based on meteorological records from La Olla (3975 m a.s.l.; 1.3°C) and Frontera (4927 m a.s.l.; -6.2°C) weather stations from 2002 to 2006, it is estimated that the modern 0°C isotherm of the mean annual air temperature (MAAT) is situated at ~4150 m a.s.l. in the northern section (~29°S). In contrast, according to estimations made by Brenning (2005), the 0°C isotherm of MAAT tends to decrease altitudinally until ~3600 m a.s.l. in the southern section (~32°S). Furthermore, in the north section, the 0°C isotherm MAAT tends to be located at ~3700 m a.s.l. during the coldest month (July) and over 4800 m a.s.l. in the hottest month (January; Azócar, 2013). Winds tend to be moderate, with monthly average speeds between 16 and 23 km/h; however, the maximum absolute wind speed can reach between 100-300 km/h during the summer-fall seasons (Azócar, 2013). The high wind speeds are expected to strongly influence snow accumulation patterns.

In the semi-arid Chilean Andes, vegetation is scarce and tends to be concentrated along river terraces and in some areas where ground surface and topographic factors are favorable for vegetation growth; however, vegetation almost disappears above 3000 m a.s.l. (Bahre, 1979; Squeo *et al.*, 1993). Graminoids such as the *Cyperaceae, Juncaceae, Adesmia aphylla* and *Baccharis spp*. are found near main streams. Above 2000 m, the slopes are populated by scattered low dwarf shrubs such as *Ephedra Andina*, *Fabiana* sp., and *Tetraglochin* sp. and some pillow plant such as *Acaena* spp. and *Cryptantha* spp; on the other hand, in areas where water is abundant in summer, it is possible to find marshes (*vegas*), mainly dominated by members of genera *Werneria, Hypsela* and *Gentiana* (Bahre, 1979). The *vegas* areas are of great economic importance for seasonal grazing of animals in the study area (Westriecher *et al.* , 2006).

3.4 Modern Glacial and Periglacial Environment

Glaciers are rare in the semi-arid Chilean Andes because of low precipitation and high radiation (Nicholson *et al.*, 2009). Glaciers are present, however, under modern climatic conditions in the northern section of the study area (i.e., the Huasco and Elqui watersheds), where the modern equilibrium line altitude (ELA) of glaciers surpasses 5000 m a.s.l. (~30°S; Kull *et al.*, 2002; Brenning, 2005a; Azócar & Brenning, 2010). According to recent inventories, a total of 282 ice-bodies, covering an area of about 27.2 km^2, have been identified (Nicholson *et al.*, 2009; Dirección General de Aguas [DGA], 2009) but over 82% of the ice-bodies correspond to small ice features (<0.1 km^2) such as perennial snow cornices and snowbanks. In contrast, ice-bodies greater than 1 km^2 represent only 2% of the glacier population. The Estrecho (1.5 km^2), Guanaco (1.9 km^2) and Tapado (1.3 km^2) glaciers are the three largest glaciers into the study area (Nicholson *et al.*, 2009; DGA, 2009). In general, the glaciers are distributed only along to ridgelines and in shallow cirques, and tend to be limited to south -facing lee slopes, suggesting that shelter from wind ablation could control glacier survival (Nicholson *et al.*, 2009). Although debris-covered glaciers have been officially inventoried only in the Huasco watersheds (n=1; Nicholson *et al.*, 2009), the presence of a debris-covered glacier in the Tapado catchment, upper Elqui valley is very well known (Brenning, 2005a; Milana & Güell, 2008). Evidence of glacier retreat has been observed near to the Pascua-Lama region (29°S), where glaciated surface areas have reduced by ~29% since the mid-twentieth century, showing strongest loss in the later decades (Rabatel *et al.*, 2011).

The relatively lower number of glaciers in the study area indicates that snow makes the largest contribution to discharge in the high-altitude semi-arid Andes (Favier *et al.*, 2009). Glacier contribution to streamflow has barely been studied, however; some studies have pointed out that the runoff contribution from glaciers could contribute between 3% and 23% of the discharge to the upper part of the Huasco River at 29°S (Pascua-Lama area; Gascoin *et al.*, 2011), and between 5% to 10% to Laguna Embalse basin of the upper Elqui River at 30°S (Favier *et al.*, 2009).

Late Quaternay glaciation left widespread evidence marked by cirques, U-shape valleys and morainic deposits across the study area. According to Caviedes & Paskoff (1975), the semi-arid Chilean Andes was affected by several glaciations during the Quaternary period. Evidences of two major glacier advances are still visible in the Elqui Valley at 3100 m a.s.l., where the river is dammed by a large end moraine (in an area known today as Laguna Embalse) and in Quebrada Tapado 15 km down-stream from the Laguna sites, where older moraine deposits have been found at 2500 m a.s.l. (Caviedes & Paskoff, 1975).

Periglacial features, such as intact rock glaciers that represent current ice-rich permafrost areas have a more widespread distribution within the study region. According to the most recent inventories (UGP UC, 2010; Azócar, 2011,2013), there are 1290 intact rock glaciers covering an approximate area of 60.3 km^2. Almost 90% of these rock glaciers are smaller than 0.1 km^2 and are altitudinally distributed between ~3700-4800 m a.s.l (UGP UC, 2010; Azócar, 2011, 2013). Rock glaciers tend be more numerous and bigger towards the north rather than south within the area of interest; most of them are derived from talus rather than moraine deposits (UGP UC, 2010; Azócar, 2013). If the distribution of active rock glaciers is considered as an indicator of the lower limit of modern permafrost conditions, discontinuous mountain permafrost can potentially occur above ~4000 m (32°S) in the southern section, and at elevation above ~4600 m a.s.l. (28°S) northwards (Brenning, 2005a; Azócar, 2013). Recent comparison of water equivalents between rock glaciers and glaciers in the semi-arid Chilean Andes show that rock glaciers are potentially more significant stores of frozen water than glaciers (Azócar & Brenning, 2010); however, more research into the ice volume of glaciers and rock glaciers is needed.

Other periglacial features that can be commonly observed are patterned ground, solifluction lobes and blockfields. In addition, several mountain slopes, mostly situated at watershed headers, such as free-face or talus slopes and rectilinear debris-mantled slopes, may be related to periglacial processes (Brenning, 2005a; French, 2007).

In general, the occurrence of glaciers and rock glaciers is mainly controlled by topographic and climatic factors; the catchment area, slope, MAAT and altitudinal variation of PISR have been recognized in previous studies as important controlling factors in the rock glacier development in this area (Brenning & Azócar, 2010a). On the other hand, the occurrence of glaciers in the semi-arid Andes as well as in the Andes of Santiago (Brenning & Trombotto, 2006), is also related to topoclimatic factors such as PISR and orientation.

Section 5.1 and 6.1 provide more detailed and up-to-date information about the number and altitudinal distribution of rock glaciers with respect previous inventories. Current estimations of permafrost distribution areas are presented and discussed in sub sections 5.3.3 and 6.3.2.

Chapter 4
Methods

4.1 General Overview

To create a model of permafrost distribution, several preprocessing methodological steps are necessary. First, in order to create an indicative variable of permafrost conditions (or response variable), intact and relict rock glaciers need to be inventoried. In addition, criteria for recognizing new intact and relict rock glaciers must be clearly established. Considering the Potential Incoming Solar Radiation (PISR) and Mean Annual Air Temperature (MAAT) as potential predictor variables in the permafrost distribution model, a set of techniques designed to obtain these variables are described. At the end of this section, a statistical modeling approach using Generalized Additive Model (GAM) is presented to predict the probability of mountain permafrost distribution over the study area. To avoid the overestimation of permafrost areas due to the nature of rock glacier characteristics, model adjustment strategies based on surface classification and temperature offset are proposed and explained in detail. A schematic representation of the permafrost and temperature models is depicted in Figure 7.

4.2 Rock Glacier Inventory

Previous inventories of rock glaciers for the Elqui, Limarí and Choapa watersheds were created by UGP UC (2010); however, relict rock glaciers were not included in these inventories. Additionally, active and inactive rock glaciers were recognized and mapped using air photos and satellite images of moderate resolution (Landsat images 7, resolution 15-30 m; air-photos GEOTEC 1:50,000 scale). Attributes that can be useful for permafrost zonification, such as the altitude at the toe of rock glaciers were not collected. For the Huasco watershed, a previous inventory of rock glaciers was realized by Azócar (2013) using a set of air photos and high resolution imagery. This inventory includes intact as well as relict forms, and it is substantially more complete in terms of the number of rock glaciers inventoried that the work realized by Nicholson *et al.* (2009).

Based on these rock glacier inventories, a new inventory of rock glaciers was prepared using the Bing Maps Aerial imagery collection provided by Microsoft and accessible through the Geographic Information System (GIS) ESRI-ArcGIS 10.1. Bing Map provides high-resolution imagery of the semi-arid Chilean regions, with a ground resolution of less than 2 m, and its horizontal geometric accuracy is better than 10 m (Ubukawa, 2013). Using high-resolution imagery with consistent quality across the whole study ensures comparable and homogeneous recognition of active, inactive and relict rock glaciers. Each rock glacier was mapped as a point mark at the end of the rock glacier front. A scale of 1:7,000 was used to delineate rock glaciers. Because the inventory was carried out for the purposes of modeling permafrost distribution, only attributes related to location, altitude and PISR were calculated.

4.2.1 Mapping Methods

4.2.1.1 Rock Glacier Recognition

Rock glaciers in air photos and satellite images present particular visual features and distribution patterns that have been used by several authors to identify rock glaciers in mountain areas (Barsch, 1996; Roer & Nyenhuis, 2007):

- Generally, rock glaciers present a tongue or lobe shape, with ridges and furrows on their surface that are indicative of their present or past deformation; moreover, they exhibit a steep front slope near the angle of repose. The shape of a rock glacier is mainly controlled by its surrounding topography.
- Most rock glaciers are located underneath talus slopes and at the end of terminal moraines surrounded glacier cirques.
- Some rock glaciers can be located in a geomorphic continuum at the end of a glacier system, normally in the distal part of debris-covered glaciers.
- Frequently active, inactive and relict rock glaciers are situated in different altitudinal bands. Active and inactive rock glaciers are situated at higher altitudes than relict forms.

Even though rock glaciers can be easily detected visually, classification of their dynamic status (see section 2.7.2.3) as active, inactive and relict requires a more detailed analysis of several geomorphological and environmental characteristics. In general, the dynamic status of rock glaciers has been evaluated based on geomorphological criteria (i.e., surface relief, appearance of the rock glacier front), environmental attributes (i.e., the presence of vegetation) and direct measurements of velocity and thermal conditions (Janke *et al.*, 2013). A steep front (>35°) with unstable rocks and without vegetation has usually been used as a characteristic indicative of an active rock glacier; in contrast, a smooth front slope with stable boulders indicates that a rock glacier is inactive (Burger *et al.*, 1999). On the other hand, an irregular and collapsed surface due to thawing of the ice commonly indicates that a rock glacier is a relict form (Putnam & David, 2009).

In-situ measurements of surface velocity through GPS survey and photogrammetry permit the quantification of rock glacier creep. Based on this kinematic information, it is possible to distinguish an active glacier from an inactive or relict forms very easily; however, GPS measurements are not suitable for making a clear distinction between inactive and relict rock forms. BTS measurement and monitoring of GST are appropriate methods to distinguish between intact and relict forms but not between active and inactive forms (see section 2.9).

For this study, the relevance of different geomorphological, geomorphometric and environmental characteristics that indicate the dynamic status of rock glaciers is summarized in Table 2, based mainly on the studies of Roer & Nyenhuis (2007), Barsch (1996), Burger *et al.* (1999) and Janke *et al.* (2013). Each criterion presented in Table 2 can be used to evaluate a rock glacier's dynamic status. The characteristics criteria were adapted for the specific environmental conditions of rock glaciers in the semi-arid Andes.

Table 2. Evaluation of geomorphological, geomorphometric and environmental characteristics for the determination of rock glacier activity in the semi-arid Chilean Andes (Slightly modified after Roer & Nyenhuis, 2007)

			Suitable indicator of rock glacier activity?		
Method/indicator	**Determined by**	**Data type**	**Active vs. inactive**	**Inactive vs. relict**	**Active vs. relict**
Slope angle of rock glacier front	Slope angle: steep/flat	Quantitative	Not suitable	Deficient	Good
Geomorphological appearance of rock glacier front	Micro-scale geomorphic forms indicating movement	Descriptive	Very good	Deficient	Very good
Tonal appearance of rock glacier front on air-photos or satellite images	Presence of light tones on slope front	Descriptive	Very good	Good	Very good
Vegetation or lichen abundance	Spatial distribution	Descriptive	Not suitable	Not suitable	Not suitable
Geomorphological appearances of the surface relief	Presence of ridges and furrows	Descriptive	Deficient	Deficient	Good
Appearance of rocks on rock the rock glacier surface	Degree and position of rock weathering	Descriptive	Deficient[1]	Good[1]	Very good[1]
The stability of large rocks on the rock glacier surface	Large rocks moveable by hand	Descriptive	Deficient[2]	Good[2]	Very good[2]
Ocurrence of ice outcrops	Location of feature	Descriptive	Not suitable	Very good[3]	Very good[3]
Occurrence of thermokarst	Location of feature	Descriptive	Not suitable[4]	Very good[4]	Very good[4]

			Suitable indicator of rock glacier activity?		
Method/indicator	**Determined by**	**Data type**	**Active vs. inactive**	**Inactive vs. relict**	**Active vs. relict**
Basal Temperature of snow(BTS) Ground Surface Temperature (GST)	Temperature measurements under a cover snow of at least 0.8 m	Quantitative	Not suitable[5]	Good[5]	Good[5]
Measurements of velocity	GPS survey	Quantitative	Good	Very good	Very good
Perennial snow patches	Location of feature	Descriptive	Not suitable[6]	Not suitable/ Good[6]	Not suitable/ Good[6]
Measurements of water temperature coming from the rock glacier	Temperature measurements of spring water	Descriptive	Not suitable[7]	Good[7]	Good[7]

[1] In general, active and inactive rock glaciers tend to have rocks that do not appear weathered; moreover, there are clear signs of overturning on the rock surface. On the other hand, relict rock glaciers have rocks fragments that appear to be weathered and have lichen growth.

[2] In active and inactive rock glaciers, it is possible that some large rocks can be moved by hand; in contrast, in a relict rock glacier, large rocks have settled and are impossible to move with the force of one person.

[3] The occurrence of ice shows that a rock glacier is not a relict but active or inactive; in contrast, the absence of ice outcrops is irrelevant to state rock glacier activity.

[4] The absence of thermokarst does not necessarily mean that the rock glacier is active or inactive; in contrast, the presence of thermokarst might indicate that a rock glacier is active or inactive, but not a relict.

[5] In the Alps, BTS >-2°C indicates the absence of permafrost conditions; in contrast, BTS <-3°C indicates the probable presence of permafrost. Thus, BTS can be used as indicator to distinguish active-inactive rock glaciers from relict forms; however, the interpretation

of BTS and GST temperature thresholds in the semi-arid Andes should be calibrated in the context of local conditions (Lewkowicz & Ednie, 2004; Brenning *et al.*, 2005).

[6] The absence of perennial snow patches does not necessarily indicate the dynamic status of rock glaciers; however, perennial snow patches are indicators of permafrost conditions and thus of active-inactive rock glaciers (Haeberli, 1975).

[7] A temperature near 0°C implies that water is flowing over ice; thus, it indicates an active or inactive rock glacier's dynamic status; however, a high temperature does necessarily mean that there is no ice within the rock glacier (Haeberli, 1975).

4.2.1.2 Inventory Variables and Data Sources

The rock glacier inventory for the purpose of modeling permafrost distribution was based on the description of three attributes: location, altitude and PISR. For each rock glacier, the horizontal and vertical location was extracted from several Aster Global Digital Elevation Models version 2 (ASTER GDEMs) that cover the study area (Tachikawa *et al.*, 2011); the ASTER GDEM product has a spatial resolution of 30 m and approximate vertical root mean square error of 15.1 m (Table 3). PISR was calculated from ASTER GDEMs (for more detail, see section 4.3). The geodetic reference system used was WGS84, zone 19 South. Watershed boundaries were derived from ASTER GDEMs using hydrological and calculator tools in ArcGIS.

Table 3. Geometric error levels of Bing Maps Aerial images and ASTER GDEM v.2

Product	**Resolution**	**Horizontal standard error**	**Vertical standard error**
Bing Maps Aerial	2 m	-2.6 m westward -7.9 m northward*	-
ASTER G DEM v.2	30 m	3.9 m westward 5.7 m northward**	15.1 m

* According to Ubukawa (2013) for Santiago city area

**According to Tachikawa *et al.* (2011) for Japanese mountain areas

4.3 Statistical Temperature Model

4.3.1 Model Overview

To determine the spatial temperature distribution within the study area, a Generalized Linear Mixed-Effects Model (LMEM) was used. The Annual Average Temperature (AAT) from selected weather stations across years was chosen as the response variable, and the altitude and latitude were used as predictor variables. In the statistical temperature distribution model (M_{temp}), the interannual random variation in the response variable is modeled as random effects in the model. The overall fit of the M_{temp} is assessed examining the residual variation and the proportion of variance explained by predicted values (marginal and conditional R^2). In addition, the relationships between variables were explored through correlation. The regression coefficients were used to map the AAT distribution throughout the study area. The predictions from the statistical temperature model will be used in the next section as an input variable for the permafrost occurrence model.

The statistical temperature models were implemented using the statistical analysis software R and its packages 'nlme' (Pinheiro *et al.*, 2013) for linear mixed models and 'stats' for correlations (R Core Team, 2013). In order to produce a temperature raster layer, the 'RSAGA' package was used (Brenning, 2011).

4.3.2 Model Development

4.3.2.1 The Response Variable

The response or outcome variable, Annual Average Temperature (AAT), was calculated for selected weather stations for a thirty year climate period (1981-2010). In general a thirty year period is used by climatologists as a reference time period as “it is long enough to filter out any interannual variation or anomalies, but also short enough to be able to show longer climatic trends” (World Meteorological Organization [WMO], 2013). The number of weather stations with complete AAT records available per year is shown in Table 4.

4.3.2.1.1 Source of the Annual Average Temperature Values

Temperature data from eight weather stations were provided by DGA. In addition, meteorological data available from secondary sources for Los Bronces, La Olla and Frontera weather stations were used (Contreras, 2005; Azócar, 2013). AAT was calculated as the sum of mean monthly temperatures in the year divided by twelve. For weather stations belonging to DGA, mean monthly temperatures were calculated as the total of the mean daily temperatures of the month divided by the number of days in the month; the daily mean temperatures is determined by adding the maximum and minimum temperatures for a 24 hour period and dividing by two. Temperature data were measured using a thermometer for maximus and minimas and an electronic temperature data logger (DGA, personal communication, May, 05, 2013). The data were collected following the WMO processes and standards (WMO, 2000). For the remaining stations, it is mostly unknown how the daily and monthly temperature are calculated, and what procedure is used to collect the data. However, it is probable that similar procedures have been used for collecting and processing data. In regard to the location of weather stations (Table 5), even when the locations of weather stations are known, no clear references are given about the precision of the coordinates (DGA, personal communication, June 03, 2013). In order to reduce the inaccuracy of altitude values obtained from various sources, altitude values for each weather station were extracted from ASTER GDEM.

The weather stations were chosen based on two criteria: first, to avoid the moderating effect of the ocean on the atmospheric temperature, every weather station had to be located at a minimum of 100 km from the coast (Hiebl *et al.*, 2009). Second, to account for a greater effect of mountain areas on weather conditions, stations located above 2000 m a.s.l. were selected. In addition, weather stations outside of the study area were used to account for the influence of latitude changes in the northern as well as southern borders of the study area. Based on these criteria, Table 5 shows the location of meteorological stations and the number of annual observations used in this study. The spatial distribution of the weather stations chosen is depicted in Figure 5.

4.3.2.2 Predictor Variables

As predictor variables of the MAAT temperature, two variables derived from ASTER GDEM were used: elevation (m) and latitude (northing coordinate in m). Both variables are known to have a strong influence on mountain weather and climate, especially in the semi-arid Andes (Azócar & Brenning, 2010). The effects of these factors are described in detail in chapter section 2.4.

Table 4. Number of weather stations with complete AAT record per year

Year	Number of weather stations with complete AAT records
1981	3
1982	3
1983	4
1984	3
1985	3
1986	3
1987	3
1988	3
1989	3
1990	4
1991	4
1992	4
1993	4
1994	4
1995	4
1996	4
1997	4
1998	4
1999	4
2000	4
2001	6
2002	7
2003	4
2004	10
2005	4
2006	4
2007	1
2008	3
2009	3
2010	2

Table 5. Location of weather stations, source of the data and the number of annual observations between 1981-2010

Weather stations	Watershed	Number of annual observations	North* (Y) m	East* (X) m	Altitude m**	Data Sources
Portezuelo el Gaucho	Huasco	1	6,833,284	397,842	4000	DGA (2013)
La Olla	Huasco	2	6,758,225	397,772	3975	Azócar (2013)
Frontera	Huasco	4	6,756,677	401,489	4927	Azócar (2013)
Junta	Elqui	17	6,683,217	394,411	2150	DGA (2013)
La Laguna Embalse	Elqui	29	6,658,175	399,678	3160	DGA (2013)
Cerro Vega Negra	Limarí	4	6,580,076	355,129	3600	DGA (2013)
El Soldado	Choapa	3	6,458,009	375,186	3290	DGA (2013)
Cristo Redentor	Aconcagua	1	6,367,611	399,713	3830	DGA (2013)
Los Bronces	Mapocho	24	6,331,719	380,444	3519	Contreras (2005)
Laguna Negra	Maipo	1	6,274,286	397,293	2780	DGA (2013)
El Yeso Embalse	Maipo	30	6,273,104	399,083	2475	DGA (2013)

* WGS84, zone 19 South

** Extracted from ASTER GDEM in m a.s.l.

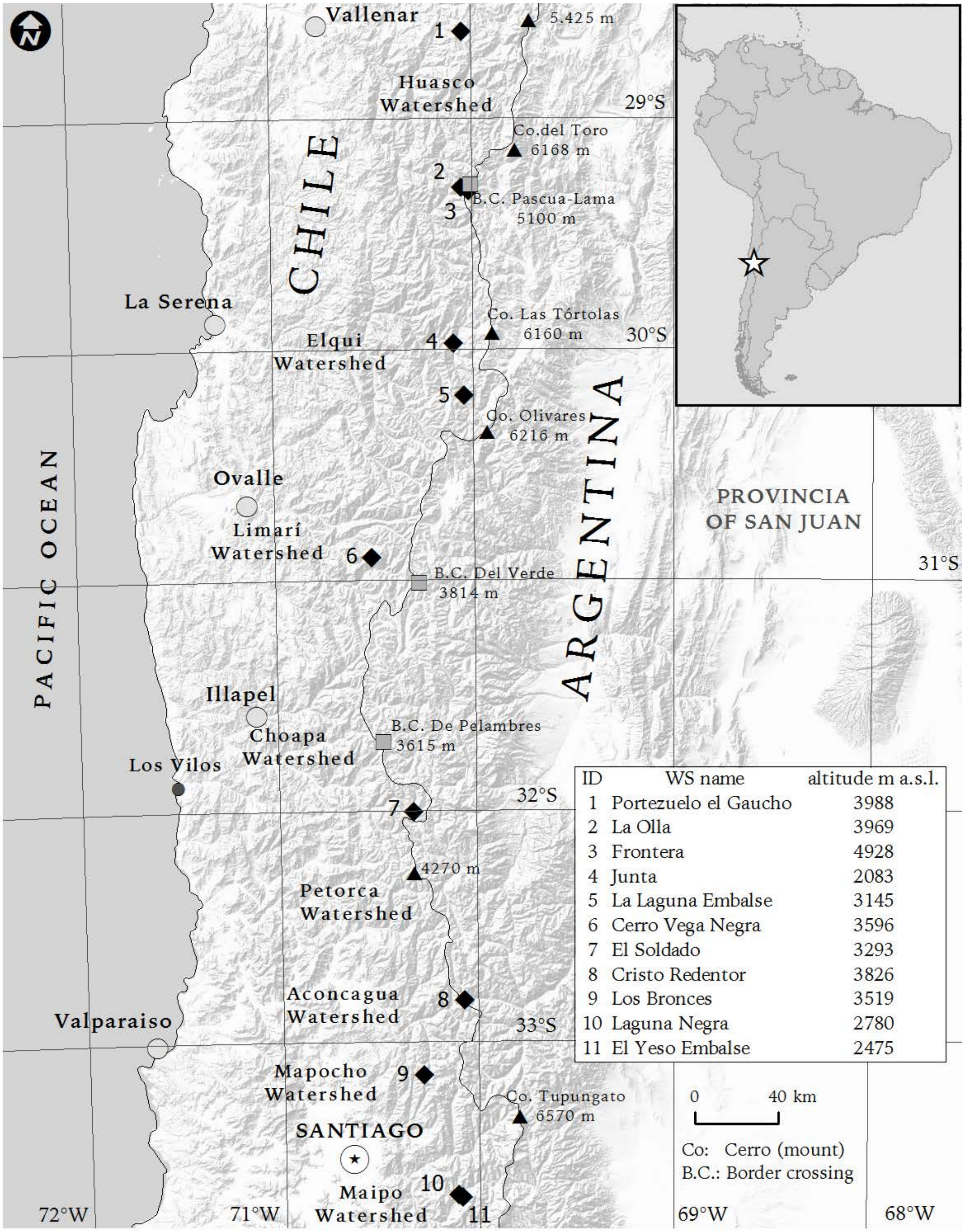

Figure 5. Weather stations (WS) chosen for the statistical temperature model

4.3.2.3 Linear Mixed-Effects Model

The statistical temperature distribution model for AAT was studied through Linear Mixed-Effects Models (LMEMs), also referred to as multilevel/hierarchical models (Raudenbush & Bryk, 2002). These models are an extension of linear regression and are appropriate when data are organized in hierarchical levels, i.e., when some observational units are clustered or nested within other variables (Pinheiro & Bates, 2000). The goal of a multilevel model is to predict values of some response variable as a function of predictor variables at more than one level (Luke, 2004). In other words, it takes into account the dependency of the observations (Twisk, 2006).

In an LMEM, the predictor variables can contain random and fixed effects. Commonly, the varying coefficients $(\alpha_j \text{ or } \beta_j)$ in a multilevel model are called *random effects*; in contrast, *fixed effects* are usually defined as the coefficients that do not vary by group (thus they are fixed, not random; Gelman & Hill, 2007). In multilevel modeling, random effects can also be thought of as additional error terms or sources of variability that are tied to different level units (Luke, 2004). *Fixed effects* are associated with continuous or categorical predictors, and *random effects* are associated with a categorical variable with levels that can be thought of as being randomly sampled from a population (West *et al.*, 2007). *Random effects* can be introduced into the model by assuming that the intercepts vary across groups (*random intercepts*) or by adding *random slopes* (Field *et al.*, 2012). Unlike classical linear regression, where regression coefficients is estimated using an ordinary least-squares estimation, in an LMEM, estimates are obtained by maximum likelihood (ML) estimation. An ML estimation determines the unknown parameter (α, β, σ) by optimizing a likelihood function (Zuur *et al.*, 2009). The maximum likelihood estimates (MLE) of the parameters are the values of the arguments that maximize the likelihood function (West *et al.*, 2007).

4.3.2.4 Model Specification

4.3.2.4.1 Hierarchical Model Structure

For this study, the structure of the data was considered in the two hierarchical structures or two levels of data: AAT and YEAR. Essentially, AATs are denoted as Level 1 and represent the subject or units of analysis at the most-detailed level of the data. AAT records are not independent of each other because they are clustered within a specific year. As such, YEAR represent the next level of the hierarchy (Level 2). In total 116 AAT records (total number of observations) taken between the years 1981-2010 (equal to 30 groups) were used for the LMEM analysis. Figure 6 shows a diagram with the hierarchical structures of the data set used in this research.

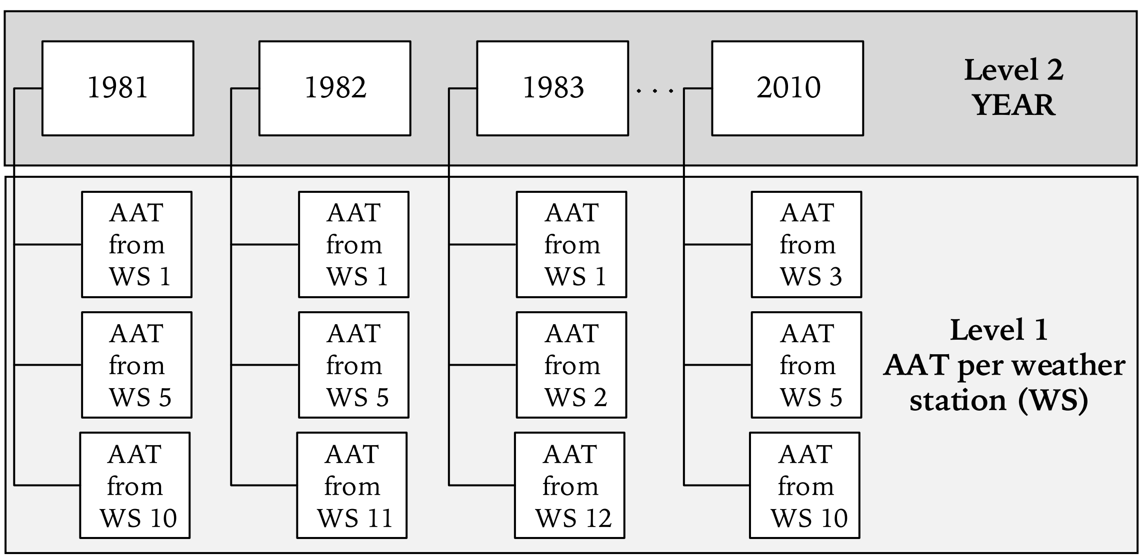

Figure 6. Diagram of hierarchical structure of statistical temperature model. AAT are clustered within years (Note: for each AAT, there are a series of variables measured, such as altitude and latitude)

4.3.2.4.2 General Model Specification

The general model specification of the statistical temperature distribution model (M_{temp}) for AAT (i) within YEAR (j) is shown in the following model equation:

$$AAT_{ij} = b_{0j} + b_{1j} altitude_{ij} + b_{1j} latitude_{ij} + \varepsilon_{ij} \quad (1)$$

$$b_{0j} = b_0 + u_{0j} \quad (2)$$

In the model (M_{temp}), AAT_{ij} is the annual average temperature for a particular weather station (i) within a particular year (j); b_{0j} represents the overall mean intercept varying (u_{0j}) across years when changed from a fixed effect (b_0) to random one ($b_0 + u_{0j}$); the parameters $b_{1j} altitude_{ij}$ and $b_{1j} latitude_{ij}$ represent the fixed effects across stations and years; and ε_{ij} denotes the residual error as a function of each year and weather station. Thus, the residual error is split into two components the variability between years (u_{0j}) and the variability between weather stations within a particular year (ε_{ij}).

AAT_{ij} calculated at different years represents at the same time the spatial variability of the temperature records throughout the study area; however, not all combinations of i and j have a AAT_{ij} for each year during the selected period of time.

It is expected that altitude is the most influential topographic factor that spatially control the AATs. In addition, solar radiation and temperature tend to decrease with increasing latitude; thus, a latitudinal temperature gradient is also expected. Consequently, the temperature model analyzes AATs based on altitude and latitude values.

4.3.2.4.3 Assessing the Model Fit

Testing the goodness-of-fit of LMEMs is not straightforward since traditional measures such as the coefficient of determination R^2 cannot be easily calculated due to the decomposition of variance in random-effect terms (Nakagawa & Schielzeth, 2013); however, the overall fit of the LMEMs has commonly been assessed by examining the residual variation and using the modified coefficient of determination R^2_{LMM} for LMEMs.

In a linear regression model, the deviations given by the observed value of y minus the predicted values $(y - \hat{y})$ are known as the *residuals* from the regression. Clearly then, if the residuals are small, the regression line is a good fit (Ebdon, 1985). The *residual standard error* (RSE) is the standard deviation of the residual values. The RSE estimates how well the fitted equation fits the sample data. The size of the RSE depends on the particular quantities being analyzed. Therefore, RSE is sensitive to the unit of measurement of the response variable, here, temperature in degrees Celsius.

R^2_{LMM} is a statistical approach recently developed by Nakagawa and Schielzeth (2013) to obtain a goodness-of-fit measure near to the traditional meaning of the R^2 i.e., the proportion of variance of the outcomes explained by the predicted values (Field *et al.*, 2012). In this approach, a conditional R^2 ($R^2_{\mathrm{LMM(c)}}$) can be interpreted as the variance explained by the entire model. In comparison to the commonly used R^2 (i.e., pseudo R^2) in LMEMs, this method has the advantages of being less susceptible to the common problems of alternative measures of R^2 for LMEMs in relation to the variance associated with each random factor and the residual variance, and also the variance at multiple levels and the risk of negative R^2. Basically, Nakagawa and Schielzeth (2013) solved the issues of negative *pseudo-R^2* when more predictors are added, while still keeping the random structure of the data. It is worth mentioning that the authors suggest showing the conditional $R^2_{\mathrm{LMM(c)}}$ in conjunction with marginal $R^2_{\mathrm{LMM(m)}}$; the latter describes the proportion of variance explained by the fixed factors(s) alone (Appendix A).

4.4 Statistical Permafrost Model

4.4.1 Model Overview

In recent years, several studies have used rock glacier activity status to model the probability of permafrost occurrence in mountain areas (Janke, 2005a,b; Boeckli *et al.*, 2012a,b; Azócar *et al.*, 2012). In these studies, Generalized Linear Models (GLMs) and Generalized Additive Models (GAMs) using logistic function are commonly chosen as the main statistical approaches for predicting permafrost occurrence. For this study, to determine the occurrence of permafrost distribution throughout the study area, a GAM was chosen to relate a dichotomous variable indicative of the presence or absence of permafrost condition derived from the inventory of rock glaciers executed in this work (Section 4.2), with the predictor variables PISR and MAAT which also were obtained in this study (Section 4.3-4.4; Figure 7). Model adjustments in relation to surface classification and temperature offset were introduced into the permafrost model. The predictive performance of the model was assessed using cross-validation estimates of the area under the receiver operating characteristics (ROC) curve (AUROC). The result of the model was expressed as a of a probability score of permafrost occurrence.

Even though the permafrost model is based on two predictor variables (PISR and MAAT) that are representative of permafrost conditions, the model does not explicitly include, for example, the influence of snow cover and soil properties and their effect on permafrost distribution. However, the model indirectly accounts for the influence of snow cover thickness and duration because MAAT and PISR are proxies for snow distribution as well as of permafrost occurrence. Otherwise, the environmental relationships being modeled operate over a temporal scale for current climatic conditions (1981-2010). Thus, the model is not suitable for future prediction and does not account for transient behavior of thermal conditions of the permafrost. The spatial scale of the permafrost probability model is defined by the spatial resolution of the DEMs (approximately 30 m) and the boundaries of the watersheds. An error assessment by comparing the probability of the permafrost distribution model against a set of independent measurements or independent observations of the presence or absence of permafrost conditions was not carried out due to a lack of suitable control sites.

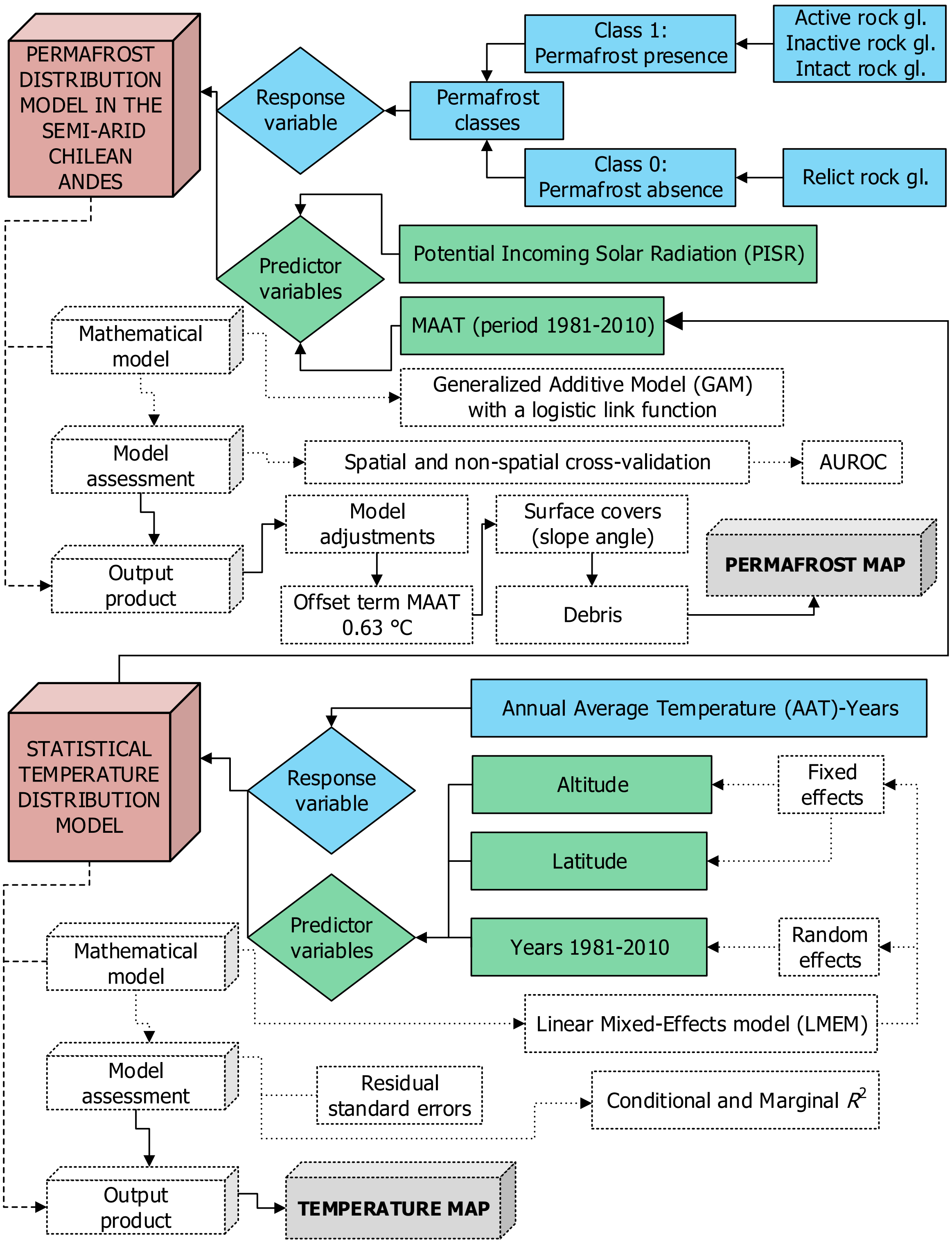

Figure 7. Schematic representation of the permafrost and temperature models

4.4.2 Model Development

4.4.2.1 Response and Predictor Variables

As a first step in permafrost modeling, rock glacier dynamic status, obtained from the inventory, was reclassified into two classes. Active, inactive and intact rock glaciers were grouped into the class indicative of permafrost presence (Y=1; intact rock glaciers). On the other hand, relict rock glaciers were reclassified into the class indicative of an absence of permafrost (Y=0). These classes were used as response variable in the model. As predictor variables were used PISR and MAAT obtained in this research; moreover, an interaction term for PISR and MAAT was considered as a potential additional predictor variable because such interaction had a significant influence on the distribution of forms related to permafrost areas, such as rock glaciers in the Chilean Andes (Brenning & Trombotto, 2006; Brenning & Azócar, 2010a). An interaction effect exists when the effect of an independent variable on a dependent variable differs depending on the value of a third variable (commonly called "the moderate" variable; Jaccard, 2001). Because in a regression analysis with an interaction effect, the variables need to be on a commensurable scale, PISR values were centered in relation to the mean of PISR [PISR-mean(PISR)= relative PISR(CPISR)].

4.4.2.2 Estimation of Solar Radiation

The particular differences of insolation over a geographic area for specific time periods can be theoretically estimated for a site using computational radiation models that account for atmospheric effects, site latitude and elevation, temporal variation in sun angles influenced by slope and aspect, and the effect of the shadows cast by surrounding topography (Wilson & Gallant, 2000). The Potential Incoming Solar Radiation (PISR) across the study area was estimated through the lighting terrain analysis module available in SAGA GIS version 2.1.0. The total potential insolation (the sum of direct and diffuse incoming solar radiation; Figure 8) was derived from ASTER GDEM. PISR was calculated for one year at intervals of ten days, using a daily temporal range of 18 hours (4 to 22) with a time resolution of 30 minutes. In addition, because the semi-arid Andes tend to have extremely clear and dry skies, a lumped atmospheric transmittance of 0.9 was used in the radiation model (Gates, 1980); moreover, to account for the effect of latitude on solar radiation, a latitudinal effect was included in the model. Reflected radiation from surface features as a function of surface albedo is not considered in the model. The PISR raster (measured in kWh/m^2, 30 m resolution) is used as a predictor variable for the permafrost occurrence model.

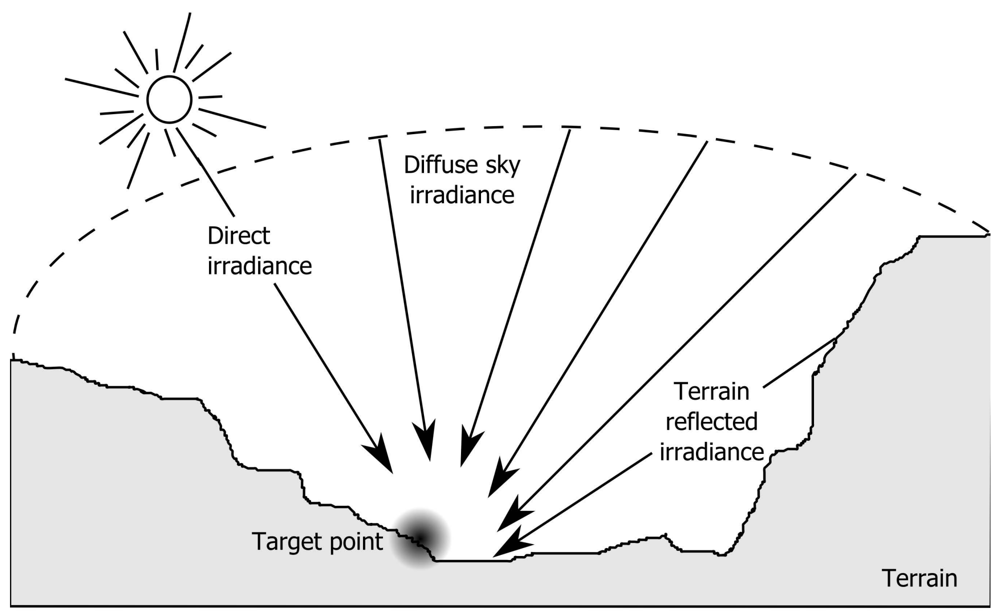

Figure 8. Simple scheme of the main components of solar irradiance that reaches the Earth's surface in mountain terrain (Modified based on Duguay, 1993)

4.4.2.3 Statistical Model Approach

A generalized additive model was chosen as the statistical or mathematical approach to study permafrost distribution. This type of statistical model has been successfully used in environmental sciences, including ecology (Guisan & Zimmermann, 2000; Guisan *et al.*, 2002), forestry (Janet, 1998), periglacial geomorphology (Brenning *et al.*, 2007; Brenning & Azócar, 2010a) and landslide research (Goetz *et al.*, 2011).

A GAM can be defined as a generalized linear model in which part of the linear predictor is specified in terms of a sum of smooth functions of predictor variables (Wood, 2006). In its simplest form, it is a generalization of the linear regression model, where the classical linear function of the covariates is replaced with a smooth function (Hastie & Tibshirani, 1990). Like the GLM, the GAM can be applied to data other than quantitative data, such as categorical data. In the case of the dichotomous response variable Y such as the presence (Y=0) versus absence (Y=0) of permafrost conditions, the probability $P(\boldsymbol{X})$ of permafrost occurrence in binary logistic regression (GLM with a logistic link function) can be modeled as:

$$ln\left\{\frac{P(\boldsymbol{X})}{1-P(\boldsymbol{X})}\right\} = \beta_0 + \beta_1\, MAAT_1 + \beta_2 PISR_1$$

where $P(\boldsymbol{X}) = P(Y = 1|MAAT_1, PISR_2)$ is the probability that Y takes the value of 1(permafrost presence) given known values of predictors $MAAT_1$ and $PISR_1$, where β_1 and β_1 are the regression coefficients and β_0 is the intercept. GLMs are linear models because their response variable is described by a linear combination of predictors. On the other hand, GAMs replace the usual linear function of quantitative predictors with smooth function:

$$ln\left\{\frac{P(\boldsymbol{X})}{1-P(\boldsymbol{X})}\right\} = \beta_0 + f_1(MAAT_1) + f_2(PISR_1)$$

where, f_1 and f_2 are the smooth functions of the covariates $MAAT_1$ and $PISR_1$.

When an interaction effect between $MAAT$ and $PISR$ is included in the above equation, the model can be conceptualized as:

$$ln\left\{\frac{P(\boldsymbol{X})}{1-P(\boldsymbol{X})}\right\} = \beta_0 + f_1(MAAT_1, PISR_1)$$

Now the predictors are described in term of a dependency between the values of $MAAT_1$ and $PISR_1$.

The GAM has the advantage of providing flexible methods for fitting a nonlinear predictor variable (Wood, 2006). A smoother function can be defined as a tool for summarizing the trend of a response measurement Y as a function of one or more predictor measurements X_1,..., X_P (Hastie & Tibshirani, 1990). A variety of smoothers can be applied in nonparametric regression (Hastie & Tibshirani, 1990). In this study, the smooth terms are represented using a local regression smoother called LOESS with two degrees of freedom. This method is based on the principle of moving windows, where a localized set of data are fitted using local linear regression to build up a function that describes the predicted values. Repeating this whole process for a sequence of data produces the smoothing curve that fits the data. One of the advantages of this method is that assumptions about the form of the relationship are not previously made, allowing the form to be discovered using the data itself. The main disadvantages of this method are associated with the definition of the size of the window (also referred as the span width) and what happens at the edges. Each section of the fitted curve is obtained using the ordinary least squares (OLS) method.

The statistical permafrost model was implemented using the software R and its package 'gam' for generalized additive models (Hastie, 2013), and the 'stats' package for generalized linear models (R Core Team, 2012) was used to compare results between GAM and GLM models. A permafrost index raster layer was created using the 'RSAGA' package (Brenning, 2011). Areas with a MAAT values greater than 2°C were excluded from the prediction map due to a low probability of finding permafrost below this temperature threshold.

4.4.2.4 Performance Assessment

The performance assessment of the predictive permafrost models as well as landslide susceptibility models can be evaluated in terms of reliability, robustness, goodness-of-fit and prediction skills (Guzzetti *et al.*, 2006).

To evaluate whether the model actually produces acceptable results, many recent studies that predict the probability of permafrost occurrence using GLMs and GAMs (Azócar & Brenning, 2010; Boeckli *et al.*, 2012a,b) and similar methods (Zhang *et al.*, 2012; Deluigi & Lambiel, 2012) have used indicators derived from comparing the predicted class with the actual class through a classification table. Among these indicators are the misclassification error (total proportion of wrongly classified observations), overall accuracy (total proportion of correctly classified observation), sensitivity (proportion of positives observations that are correctly classified) and specificity (proportion of negatives observations that are correctly classified). A more complete description of classification accuracy is given by the area under the ROC (Receiver Operation Characteristic, AUROC). This curve shows the probability of detecting true values (1-sensitivity) and false values (specificity) for an entire range of possible cutpoints (Hosmer & Lemeshow, 2000). The AUROC can range from zero (no separation) to one (complete separation of presence and absence by the model). A cutpoint of 0.5 was chosen for purpose of classification of permafrost condition.

A common method used to estimate the performance of predictive models on independent test data sets is *k*-fold cross-validation. In *k*-fold cross-validation, the data are divided randomly into *k* subsets of equal size, where one of the subsets is used for testing the models and the remaining (*k* -1) subsets are used as training data. In *k*-fold cross-validation does not consider the spatial distribution of testing and training data sets (Brenning, 2005c). Consequently, the error estimates may be overoptimistic due the spatial dependencies between both data sets (Brenning, 2012). This can be overcome by using a spatial cross validation method where testing and training data sets are spatially separated (Brenning, 2005c). This method has successfully been applied in studies of landslides and in remote sensing (Brenning, 2005c; 2012; Goetz *et al.*, 2011). Thus, for this study, spatial and non-spatial cross validation with different sets of data are used to evaluate the performance of the permafrost model. *k*-means clustering was used to partition the subsets randomly into *k*=10 equally-sized subsamples (*k*-fold). The spatial and non-spatial cross validation process was repeated 100 times with each of the subsamples (*k*-repeated).

All performance assessments were carried out using R software and its package ‘verification’ for plotting the ROC curve of the logistic regression (Gilleland, 2012). Spatial and non-spatial cross validation were obtained using the ‘sperrorest’ package (Brenning, 2012).

4.4.3 Model Adjustments

4.4.3.1 Surface Classification

The substantial differences in surface temperature regimes and their effect on permafrost distribution (Section 2.3) were addressed in this study through a distinction between steep bedrock and debris-cover areas. This difference is necessary because the actual model is based on rock glacier forms (a debris surface) as evidence of permafrost conditions. Thus, the model cannot extrapolate permafrost predication to other non-debris surface areas such as steep bedrock slopes.

In one recent permafrost model (Boeckli *et al.*, 2012b), steep bedrock is described as terrain only marginally affected by snow cover during winter periods, one that does not accumulate rock blocks, debris and vegetation. Commonly, a slope angle criterion is used in different studies to distinguish between steep bedrock and debris areas. According to Gruber and Haeberli (2007), a slope angle greater than 37° is normally used as a definition of "steep slope". In one investigation of the influence of snow cover on GST in the Italian Alps, Pogliotti *et al.* (2010) states that a slope angle of 35-37° represents the upper limit of snow-cover areas as well as the lower limit of steep bedrock zones. In this study, and partially following the criterion stated by Boeckli *et al.* (2012b), a slope angle ≥ 35° assumed to be as indicative of steep bedrock surfaces and therefore excluded from predictive modeling. Thus, less steep slopes were considered as debris zones. Slope angle values (measured in degree) were derived from the ASTER GDEM using the morphometric terrain module available in SAGA GIS (version 2.0.8, using 2nd Polynomial Adjustment algorithm of Zevenbergen & Thorne, 1987).

4.4.3.2 Temperature Offset

Even though rock glaciers are good geomorphological indicators of permafrost conditions in mountain areas, calculating permafrost areas based on rock glacier distribution overestimates the permafrost areas for several reasons (Boeckli *et al.*, 2012b):

- *A cooling effect occurs in coarse block* material that is often present on the surface of rock glaciers (section 2.2). Thermal conductivity of the block layer modifying the warming influence of snow cover (Gruber & Hoezle, 2008) and the so-called *chimney* effect that produces a strong overcooling of the ground due to the ascent of warm air toward the top of the block deposit in winter, thus facilitating the aspiration of cold air deep inside of coarse block deposits (Delaloye & Lambiel, 2005).
- *The terminus of active rock glaciers creeps downslope*; thus, cold and ice-rich masses from the upper areas of the rock glaciers move to lower areas where the environmental conditions are less favorable for the existence of permafrost. Thus, an increase of the active layer as a result of melt acceleration produces a cooling effect that permits the existence of permafrost to a greater depth (Boeckli *et al.*, 2012b).
- The *response of ice-rich permafrost to climate forcing is delayed*; changes in the temperature profile within the permafrost may be delayed by decades to centuries due to the influence of high ice content that strongly reduces the thermal conductivity of the ground. Therefore, ice-rich permafrost is less sensitive to climatic forcing than “dry” permafrost (Fitzharris, 1996; Kellerer-Pirklbauer *et al.*, 2011).

The last two effects can be compensated for by the use of a temperature offset term (Boeckli *et al.*, 2012b); however, the first effect cannot be easily accounted for due to lack of information about the surface characteristics of rock glaciers. In this work, the magnitudes of last two effects were estimated by a *mean altitudinal extent of the rock glaciers*. This value represents a systematic altitudinal difference for each rock glaciers assuming that only in the rooting zone of rock glaciers have conditions more favorable for the existence of ice-rich permafrost. To account for these effects, the *mean altitudinal extent of the rock glaciers* is added to altitude values measured at the front of rock glaciers.

In order to estimate this bias, the *mean maximum length* and the *mean slope angle* of intact rock glaciers inventoried by Azócar (2013) for the Huasco watershed and UGP UC (2010) for the Elqui, Limarí and Choapa watersheds (Table 6) were used to calculate the $mean\ altitudinal\ extent\ of\ the\ rock\ glacier$, using the following trigonometric function:

$$mean\ altitudinal\ extent\ of\ the\ rock\ glaciers = \frac{\sin(mean\ slope\ angle) \times\ mean\ maximum\ length}{Number\ of\ watersheds}$$

where, the $mean\ altitudinal\ extent\ of$ the $rock\ glaciers$ of each watershed is determined by multiplying the sine of the $mean\ slope\ angle$ by the $mean\ maximum\ length$ of rock glaciers and dividing by the $Number\ of\ watersheds$. For the inventories mentioned above, the $mean\ altitudinal\ extent\ of$ the $rock\ glaciers$ is ~89 m (Table 6), which corresponds to an estimated temperature offset of -0.63 °C, assuming a lapse rate of -0.0071°C per one m increase in altitude (the temperature rate obtained in the present work, see section 5.2). This temperature offset was chosen and added to MAAT (renamed as 'MAAT adjusted') values for each permafrost class before model fitting.

Table 6. Mean altitudinal extent of intact rock glaciers

Watershed	Mean maximum length of intact rock glaciers (hypotenuse)*	Mean slope angle of intact rock glaciers (angle)	Mean altitudinal extent of intact rock glaciers (opposite)
Huasco	297 m	20 °	103 m
Elqui	316 m	18 °	98 m
Limarí	234 m	20 °	80 m
Choapa	207 m	21 °	74 m
			Mean: 89 m

* Length in these inventories was measured tridimensionally, not planimetrically

Chapter 5

Results

5.1 Rock Glacier Inventory

An inventory comprising 3575 rock glaciers was compiled based on existing inventories and the identification of additional rock glaciers in the study area (~29-32°S). Of these, 1075 were classified as active, 493 as inactive, 343 as intact and 1664 as relict forms (Table 7 and Figure 9). Active rock glaciers are present at altitudes above 3349 m a.s.l. along the study area. They are most abundant in the Elqui (n=463), Huasco (n=252) and Limarí (n=224) watersheds (Table 8 and Figure 10).

Table 7. Total number of active, inactive, intact and relict rock glaciers inventoried and their general altitudinal distribution

Rock glacier dynamics	Number of rock glaciers	Mean Altitude (m)	Max. altitude (m)	Min. altitude (m)	Mean PISR (kWh/m^2)
Active rock gl.	1075	4123	5128	3349	1908
Inactive rock gl.	493	3974	4738	3022	1894
Intact rock gl.	343	4008	4885	3390	1879
Relict rock gl.	1664	3870	4498	2372	2023

Table 8. Total number of active, inactive, intact and relict rock glaciers inventoried within each watershed

Watershed name	Active rock gl.	Inactive rock gl.	Intact rock gl.	Relict rock gl.	TOTAL active, inactive and intact rock glaciers
Huasco	252	78	94	298	**424**
Elqui	463	179	39	659	**681**
Limarí	224	134	128	407	**486**
Choapa	136	102	82	300	**320**
TOTAL	**1075**	**493**	**343**	**1664**	**1911**

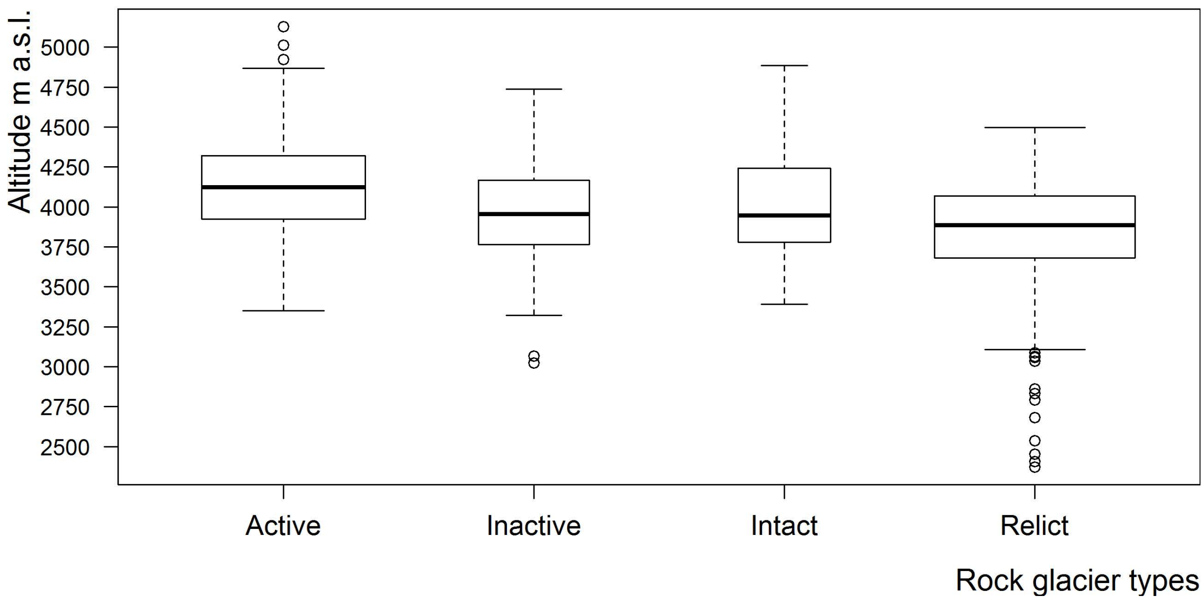

Figure 9. Altitudinal distribution of active, inactive, intact and relict rock glaciers inventoried. The box widths are proportional to the square root of the number of rock glaciers

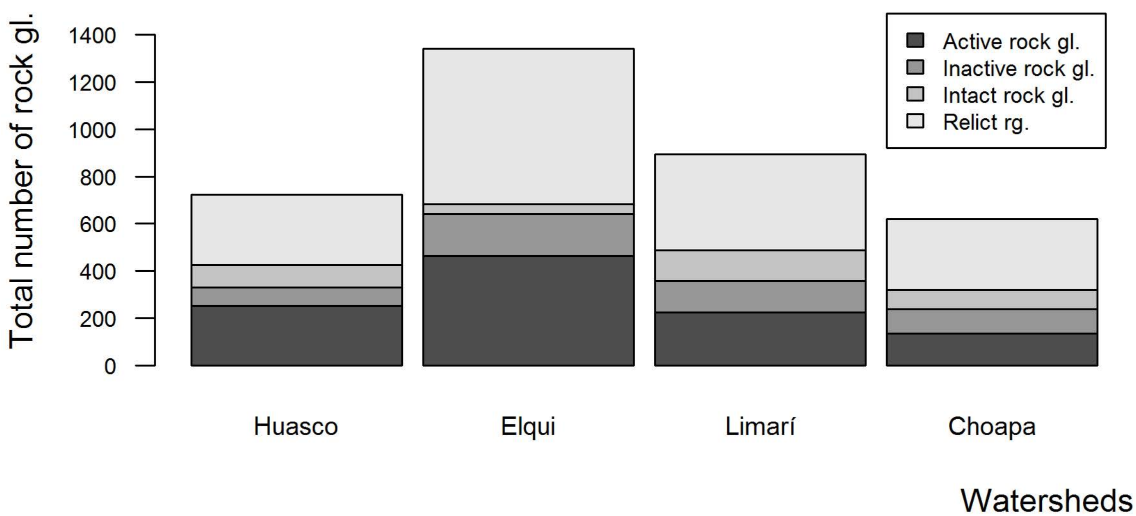

Figure 10. Total number of active, inactive, intact and relict rock glaciers inventoried within each watershed

The average elevation of the 1075 active rock glaciers is 4123 m a.s.l., which is about 149 m higher than that of inactive rock glaciers and about 253 m higher than that of the relict rock glaciers (Table 8). Around 80% of the active rock glaciers are situated at elevation between 3750 m and 4500 m a.s.l. (Figure 11). The average elevation of the lower limit of active rock glaciers is located at 4345 m a.s.l. in the north section of the study area, at~29°S (Huasco watershed; Appendix B), and drop altitudinally to 3779 m a.s.l. in the south section at 32°S (the Choapa watershed).

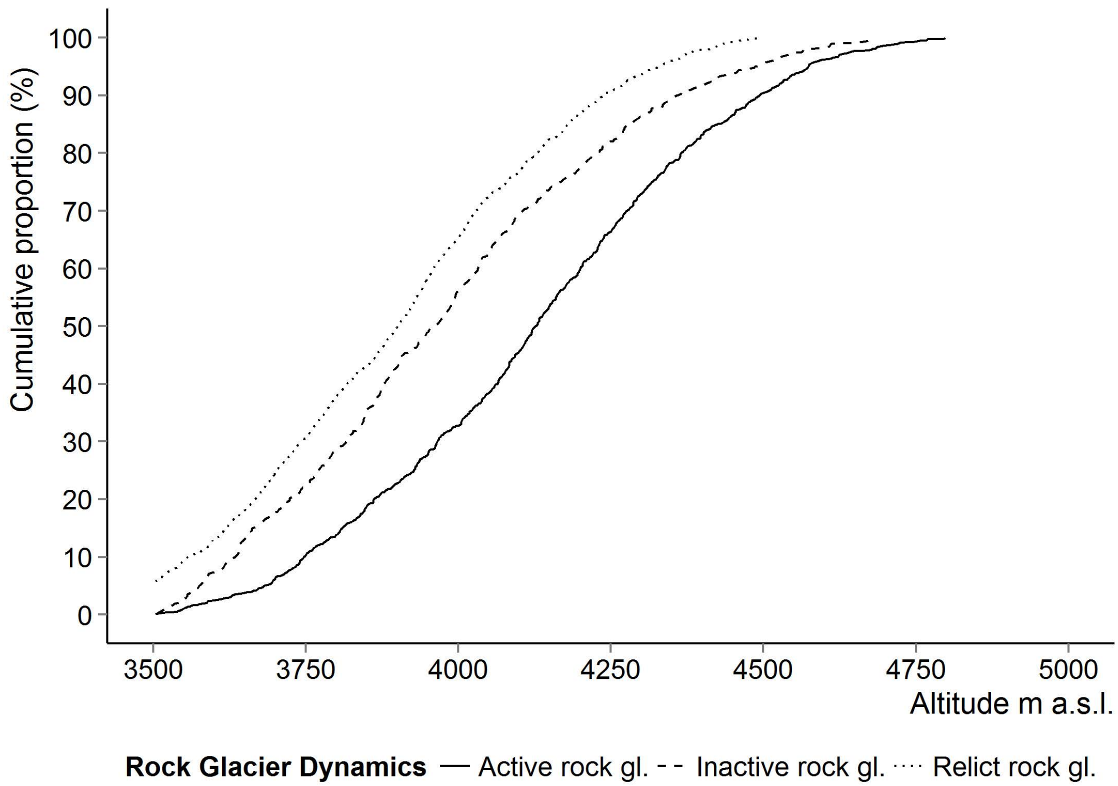

Figure 11. Cumulative distribution of rock glacier altitude by activity status

The average elevation of the 493 inactive rock glaciers is 3974 m a.s.l., which is not considerably lower than that of active rock glaciers (Table 8). They occur mostly between 3500 and 4250 m a.s.l. (~80%; Figure 11). The average elevation of the lower limit of inactive rock glaciers is 4280 m a.s.l. in the north section of study area, and decreasing to 3717 m a.s.l. in the south section (Appendix A). Inactive rock glaciers are less frequent in the Huasco watershed (n=78; Table 8), but they are abundant in the other watersheds (n=415).

Around 1664 rock glaciers were classified as relict, with an average elevation of 3870 m a.s.l., and most of them are located at lower elevations than active and inactive rock glaciers (Table 8). The front of 70% of relict forms is located between 3500 m and 4000 m a.s.l. (Figure 11). Relict rock glaciers are widespread in all watersheds (Table 8 and Appendix C); however, they are more abundant in the Elqui and Limarí watersheds (n=1066). Active and inactive rock glaciers tend to be less exposed to solar radiation than relict forms at watershed scale (Table 7).

5.1.1 Distribution of Rock Glaciers and MAAT

If the results of the statistical temperature distribution model from this work are used to characterize the spatial distribution of rock glaciers, the results reveals that a large part of the rock glaciers (~60-80%) are located below the 0°C MAAT isotherm, and 37% of active, 21% of inactive, 26% intact and 15% of relict rock glaciers are located above the 0°C MAAT isotherm (Figure 12 and 13). However, at watershed scale, these percentages tend to vary considerably; for example, in the Huasco and Elqui watersheds, nearly 50% of active rock glaciers are located at negative MAAT compared to less than 20% in the Limarí and Choapa watersheds, (Figure 14 and Appendix D). The proportion of rock glaciers above 0°C MAAT isotherm altitude greatly decrease from the north to south in the semi-arid Andes between ~29°S and 32°S (Figure 14).

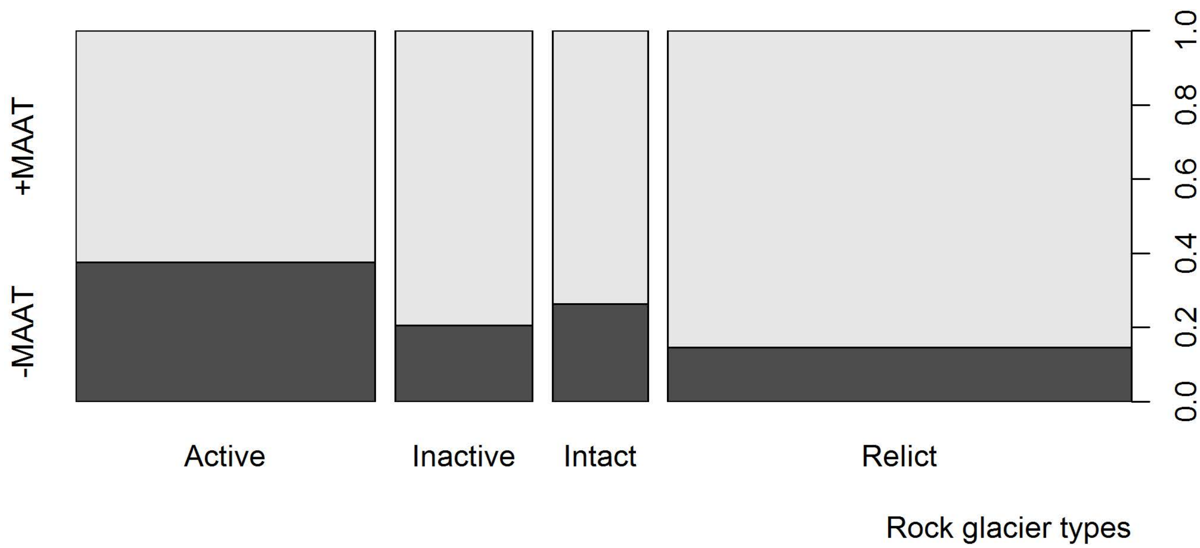

Figure 12. Proportion of active, inactive, intact and relict rock glaciers located below and above the 0°C MAAT isotherm altitude

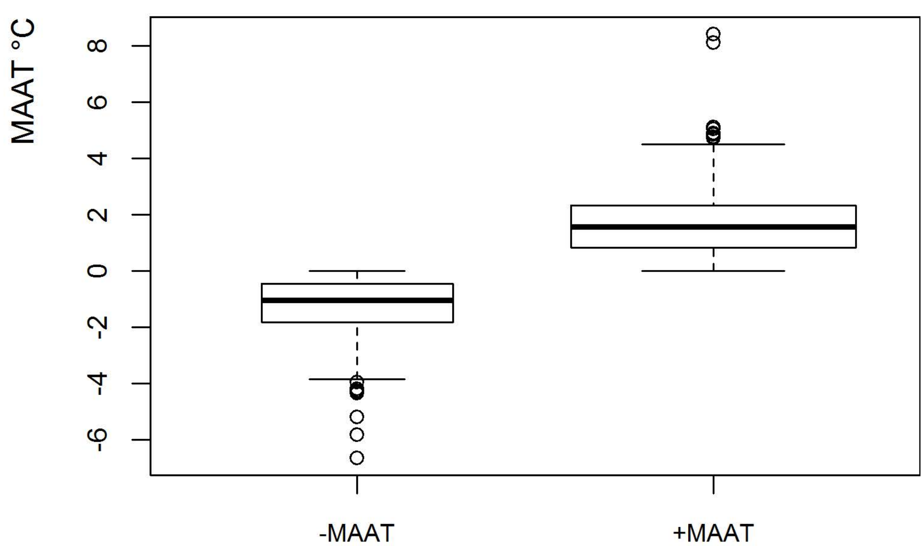

Figure 13. Number of intact rock glaciers located below (-MAAT) and above (+MAAT) the 0°C MAAT isotherm altitude

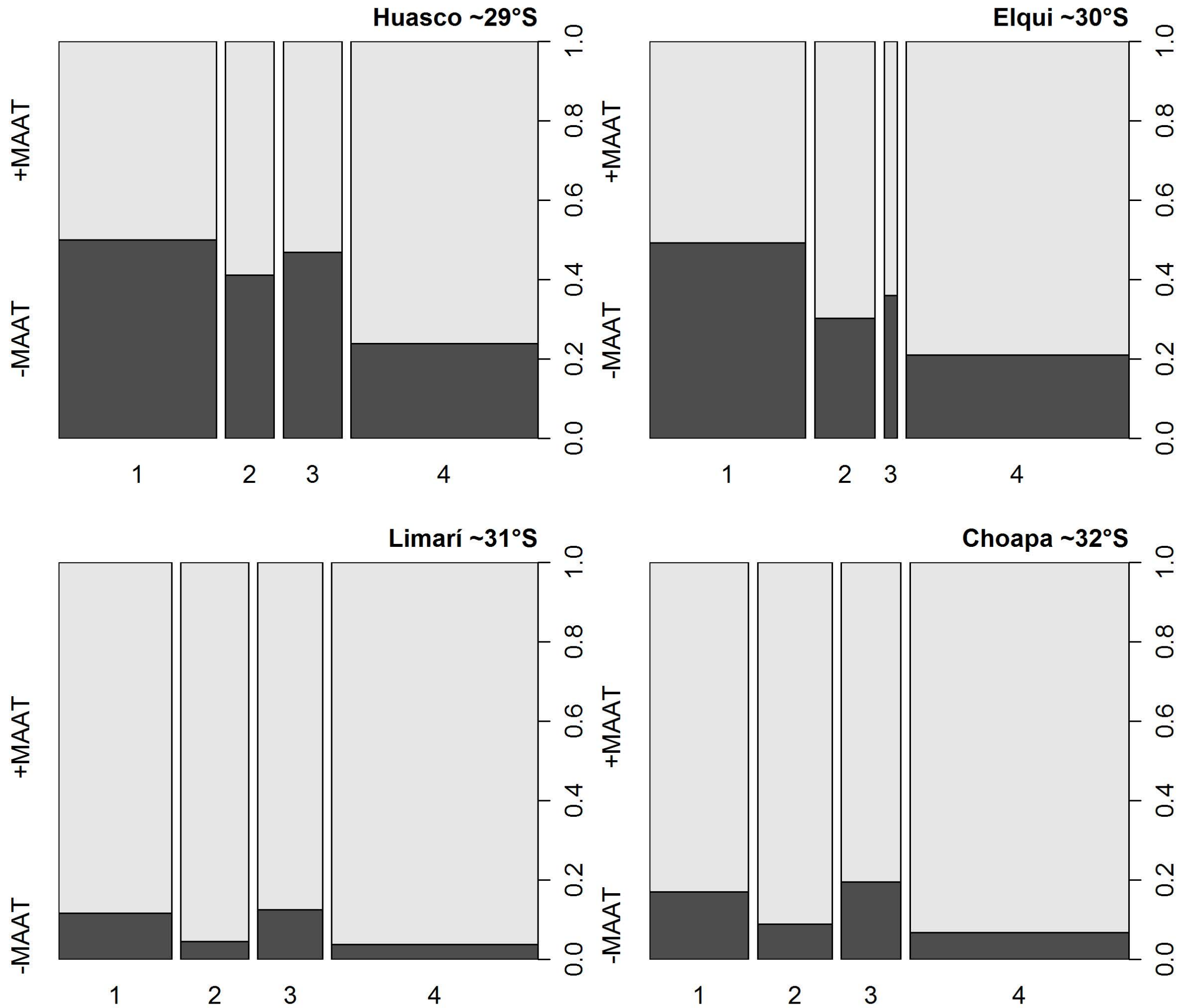

Figure 14. Proportion of active, inactive, intact and relict rock glaciers located below (+MAAT) and above (-MAAT) the 0°C MAAT isotherm altitude within each watershed. (1) Active, (2) inactive, (3) intact and (4) relict forms

5.2 Statistical Temperature Model

5.2.1 Exploratory Analysis of Predictor Variables

The dataset includes 116 AAT records ranging from -6.8°C to 15.4°C during a thirty year period since 1981 to 2010. The eleven weather stations are located between 2150 to 4927 m a.s.l. A search for correlations between the variables revealed that a strong negative correlation between AATs and altitude (Pearson correlation ρ=-0.95) indicating that the AATs drop increasing altitude. AAT and latitude exhibit moderate positive association (Pearson correlation ρ= 0.37), showing that the temperature tends to increase northward (Figure 15).

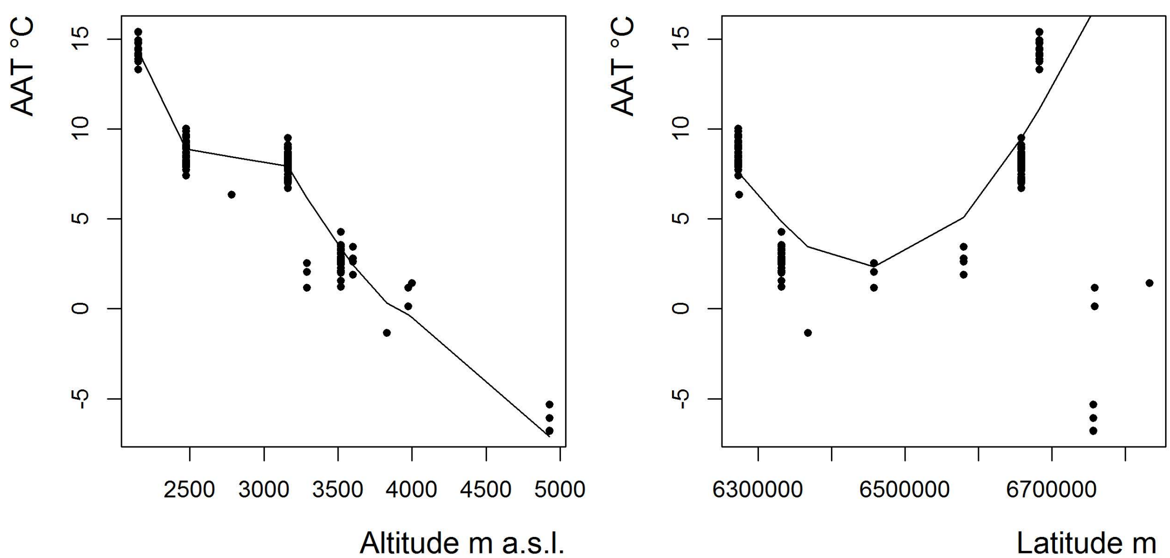

Figure 15. Relationships of AAT with the predictor variables altitude and latitude

5.2.2 Interpreting Parameter Estimates and Assumptions of the Model

Model coefficient estimates show that (Table 9), on average the AAT drop -0.71°C per 100 m increase in altitude (called also the Environmental Temperature Lapse Rate by meteorologists) while accounting for latitude and interannual variation. Over a 200 km northward distance the AAT increases on average by 1.6°C while accounting for altitude and interannual variation. Thus, on average there is a 4°C temperature difference is expected between the northern and southern limit of the study area. Both predictor were significantly different from zero (p values <0.001).

The estimates variance between years is 0.87 and within years of 0.19. The intraclass correlation coefficient (ICC) is then (0.87/[0.19+0.87])= 0.82. This means that years account for a large proportion of the variability of AAT records among weather stations. This high ICC value suggests that a linear-mixed model incorporating two levels of the data is useful.

On the other hand, the results of model shows that the proportion of AAT variance can be very well explained based on the predictors altitude and latitude, with conditional $R^2_{\mathrm{LMM(c)}}$ and marginal $R^2_{\mathrm{LMM(m)}}$ values ≥ 0.95 (Table 9). If the residual standard error (RSE) is used as measure of precision for temperature distribution model, the RSE vary between 0.26-0.76°C year to year (level 2) and 0.8-1.08°C AAT within years (level 1) at 95% confidence interval.

Table 9. Model coefficients and goodness-of-fit for the linear mixed-effects model for temperature distribution

	Coefficients (standard error)	95 % Confidence Interval
Intercept	-23.87(3.09)*	-2.99;-1.78
altitude	$-7.11*10^{-3}$ $(1.43*10^{-4})$*	$-7.39*10^{-3}$;$-6.83*10^{-3}$
latitude	$8.06*10^{-6}$ $(4.82*10^{-7})$*	$7.11*10^{-6}$; $9.01*10^{-6}$
Residual standard error within AAT records- level 1 [°C]	0.44	0.26;0.76
Residual standard error between years-level 2 [°C]	0.93	0.8;1.08
Total residual standard error [°C]	1.03	
Conditional $R^2_{LMM(c)}$	0.96	
Marginal $R^2_{LMM(m)}$	0.95	

Significance of the Wald test * <0.001.

Regarding one of the main assumptions of LMEM, the residual are independent and normally distributed with a mean of zero across the groups. This was evaluated using a boxplot of residuals by year. The residuals do seem to be centered at 0, although with a fair amount of variability (Appendix E). The normal quantile plot also indicates a nearly normal distribution of the residuals (Appendix F).

Figure 16 and 17 shows the altitudinal and spatial distribution of MAAT over the period 1981-2010, using the regression parameters from temperature distribution model. According to the model the 0°C MAAT isotherm is situated at ~4250 m a.s.l. in the northern (29°S) section and it drops altitudinally to ~4000 m a.s.l. in the southern section (32°S) of the study area.

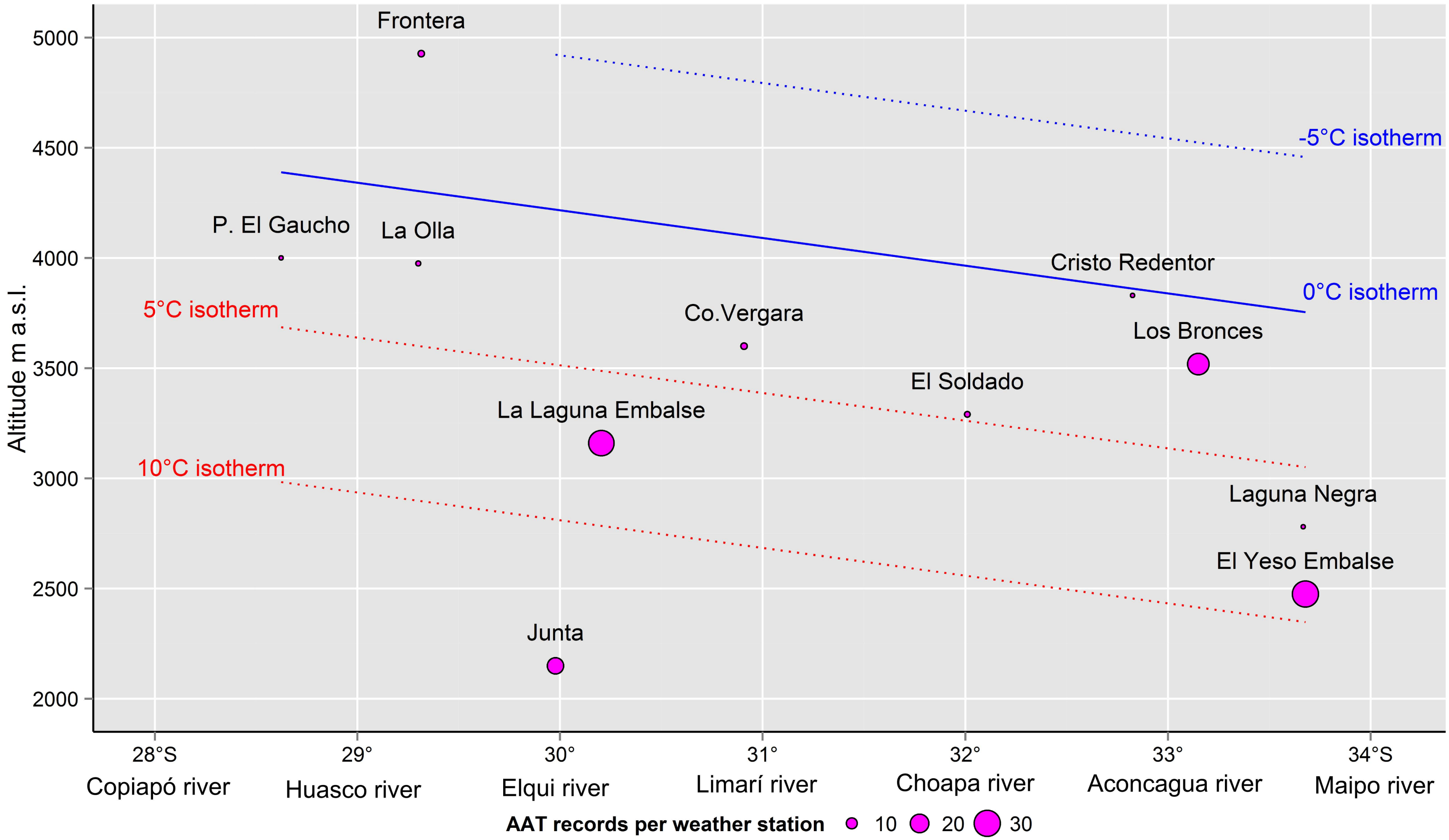

Figure 16. Altitudinal distribution of MAATs derived from the statistical temperature distribution model for a period of thirty years (1981-2010)

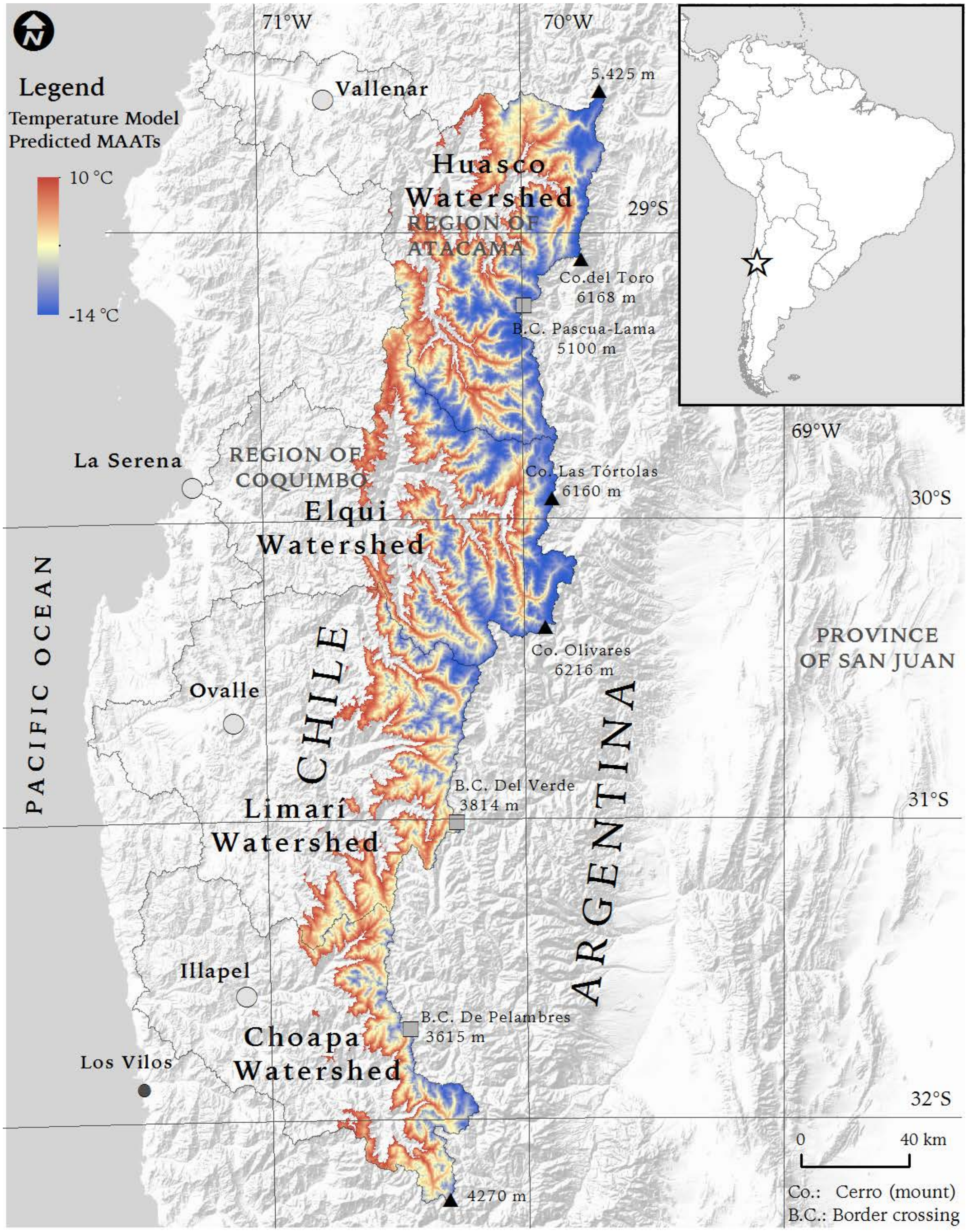

Figure 17. Mean annual air temperatures in the study area derived from the statistical temperature distribution model. The red color represents

warmer temperatures, while the light yellow and blue depict cooler temperatures

5.3 Permafrost Occurrence Modeling

5.3.1 Exploratory Analysis of the Response and Predictor Variables

In order to create a permafrost indicator variable, rock glacier activity status from the rock glacier inventory was reclassified into two classes: presence (*Y*=1) and absence (*Y*=0) of permafrost conditions. In total, 1911 active, inactive and intact forms were categorized under the class indicative of permafrost conditions, and 1664 relict rock glaciers were categorized under the class indicative of non-permafrost conditions. In addition, 51 rock glaciers were removed and excluded from the model analysis based on the following criteria:

- 34 rock glaciers located below 3250 m a.s.l. (0=23, 1=2) and 14 observation indicative of the absence of permafrost conditions situated above 4750 m a.s.l. were excluded from the total population due to being isolated observations, outside the main distribution.
- 12 rock glacier indicative of non-permafrost (*Y*=0), located at sites with MAAT below -2.5°C, were excluded. Normally, relict rock glaciers are located in areas with positive MAAT.

Thus, 3524 units of observations (1=1909; 0=1615) were used to model permafrost distribution in the study area. MAAT and PISR values at sites with permafrost are lower than to the sites without permafrost (Figure 18). In 75% of sites with permafrost (*Y*=1), the MAAT ranges between 5.1°C and -0.4°C and only 25%

of these sites have a MAAT lower than -0.4°C (Y=0). At sites without permafrost, the temperature ranges between 7°C and 0.8°C in 75% of the cases. In general, the sites with permafrost present lower values of PISR than sites without permafrost (mean, Y-0=2028; Y-1=1900; Table 10). MAAT and PISR were only weakly correlated (ρ=-0.12) indicating that collinearity is not issue. The distribution of MAAT and PISR per permafrost classes tends to be symmetrical (the range of the top and the bottom 25% of scores tend to be the same).

Table 10. Descriptive statistics of the predictor variables used for modeling permafrost occurrence

		Permafrost observations		Total observations; 3524 obs.
		Class = 0; 1615 obs.	Class =1; 1909 obs.	
	Unit	mean (Std dev.)	mean (Std dev.)	mean (Std dev.)
MAAT	°C	1.88 (1.61)	0.74(1.70)	1.27(1.75)
PISR	kWh/m^2	2028 (245)	1900(285)	1959(275)

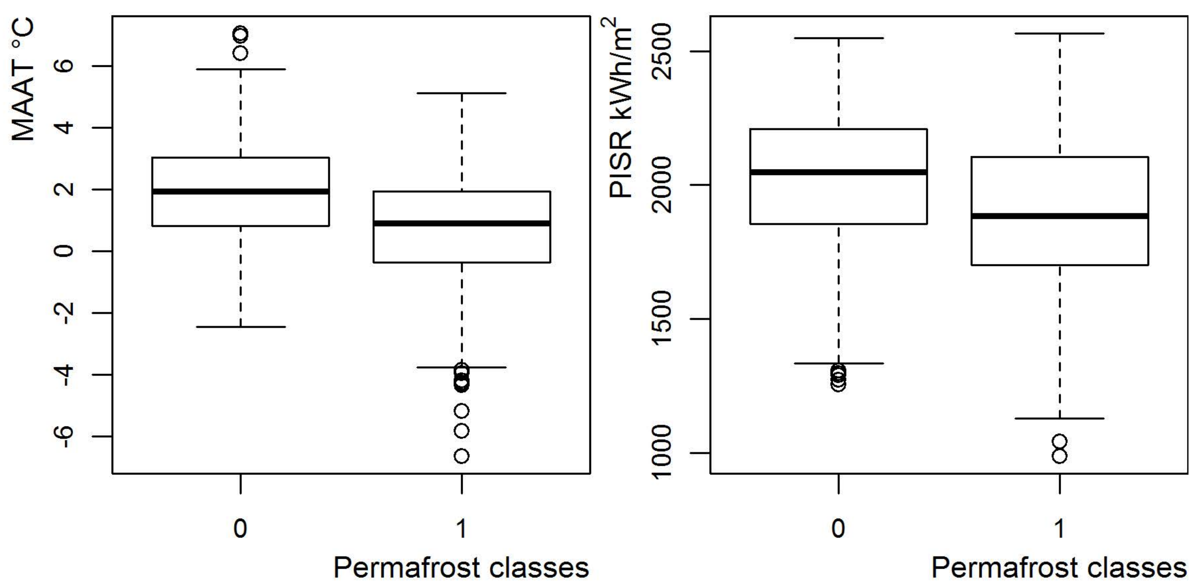

Figure 18. Boxplots of MAAT and PISR by per permafrost classes

In general, the proportion of permafrost classes changes considerably over different temperature levels (Figure 19). Permafrost sites are much frequent at MAAT lower than 2°C; in contrast, permafrost is less frequent at MAAT greater than 3 °C.

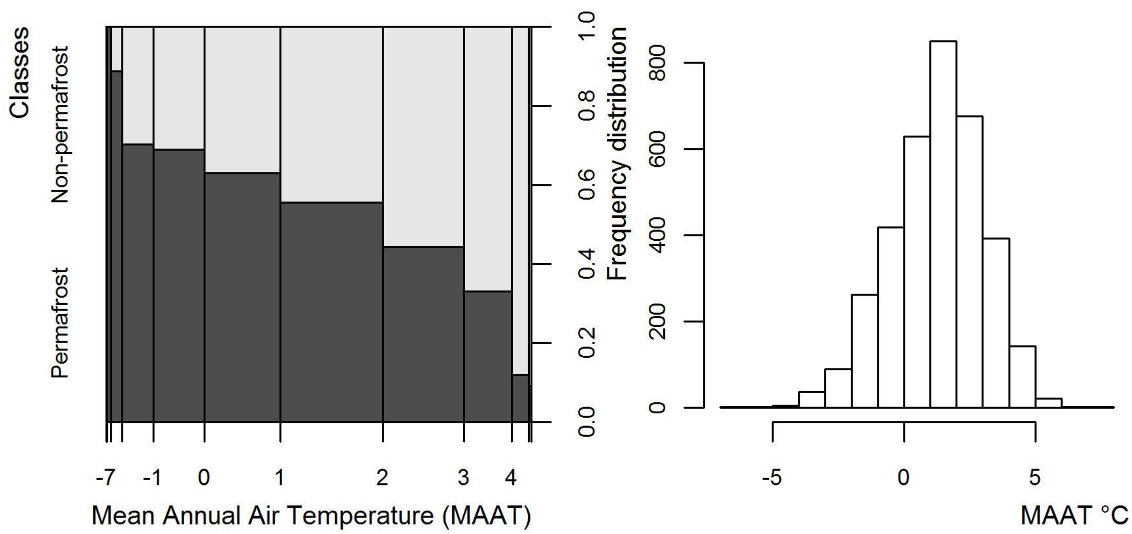

Figure 19. Proportion of permafrost classes by mean annual air temperature and histogram of MAAT

In terms of PISR, permafrost frequently occur in areas where the PISR values are below 2000 kWh/m^2; in contrast, permafrost is less frequent in areas where the PISR drops below 2100 kWh/m^2 (Figure 20).

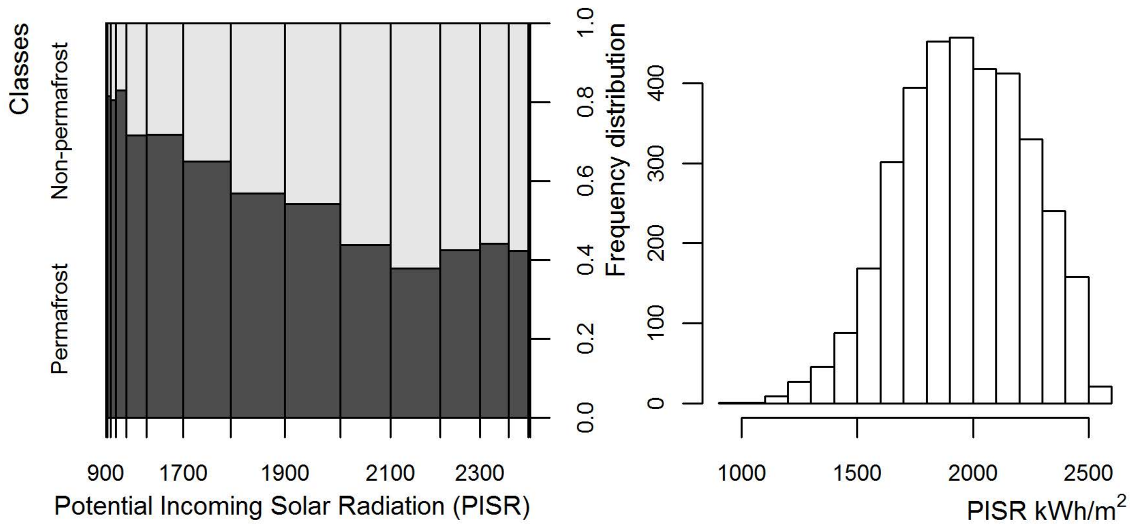

Figure 20. Proportion of permafrost classes by potential incoming solar radiation and histogram of PISR

5.3.2 Model Interpretation and Performance

According to the model results, at a mean relative PISR, a change in MAAT adjusted from 0°C to +1°C is associated with a ~33% decrease in the odds of permafrost occurrence (Figure 21), whereas the same change of MAAT but at sites with PISR two standard deviations above is associated with a ~73% decrease in the odds of permafrost occurrence. On the other hand, a high amount of relative PISR has a greater effect at higher MAAT levels than at lower MAAT levels; At -1°C MAAT, an increase in one standard deviation over the average relative PISR (Table 11) is associated with an approximately 27% decrease in the odds of permafrost occurrence, while the same change of relative PISR at +1°C MAAT is associated with an 57% decrease in the odds of permafrost occurrence. According to the result of Wald test, the interaction between the MAAT and relative PISR are statistically significant (p-value <0.001). For comparative purposes, a GLM is presented in Appendix G.

Table 11. Odds ratio corresponding to different combination of MAAT adjusted and relative PISR values for the permafrost distribution model

Predictor variables		odds	odds ratio	Effect on odds of permafrost occurrence
MAAT °C (adjusted)	Relative PISR			
1	1	1.17	0.43	a 57.1% decrease
1	1.14	0.50		
-1	1	2.19	0.73	a 26.8% decrease
-1	1.14	1.60		
0	1	1.74	0.67	a 32.7% decrease
1	1	1.17		
0	1.28	0.80	0.27	a 73% decrease
1	1.28	0.22		

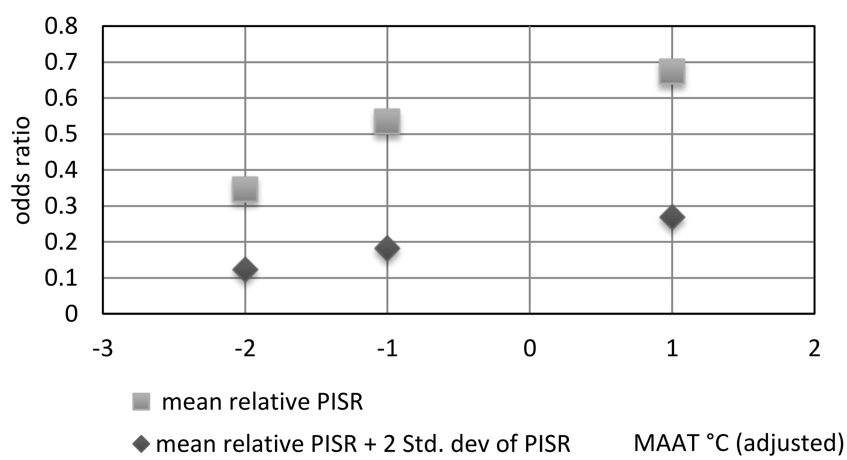

Figure 21. Illustration of odds ratio of permafrost occurrence at different levels of MAAT adjusted and relative PISR

5.3.2.1 Predictive Performance

The measures of predictive performance (Table 12 and 13) were obtained through cross-classification whose values derived from the estimated logistic probabilities of permafrost distribution model (using a cutpoint of 0.5). These measures of predictive performance were estimated using spatial cross-validation on the basis of training dataset (median value). The results show that 66% (overall accuracy) of sites indicative of permafrost conditions were correctly classified by the model and 34% of the sites were wrongly predicted. 60% of sites with permafrost were predicted as such; in contrast, 73% of sites without permafrost were predicted as sites with absence of permafrost conditions.

In addition, the results show that there is not an appreciable difference in the performance of the GAM using a method of spatial cross-validation (median AUROC: 0.757) that account for the presence of spatial autocorrelation in the data set (Brenning, 2012) in comparison to non-spatial cross-validation method for accuracy assessment (median AUROC: 0.756). This slight difference between AUROC values indicates that the model's performance is largely unaffected by a possible imbalanced spatial distribution of the observation sites. Consequently, it can be concluded that if the model achieved an AUROC above 0.75, the GAM permafrost distribution model has acceptable discrimination between observed and predicted values of permafrost conditions (Hosmer & Lemeshow, 2000). All possible combinations of specificities and sensitivities obtained using spatial-cross validation estimates of the area under the ROC curve are shown in Figure 22.

Table 12. Measures of predictive performance and spatial and non-spatial error estimations for the GAM for permafrost distribution

		Indices of predictive efficiency Permafrost distribution model	
Based on training set derived from the spatial cross-validation (median value)	Overall Accuracy	0.66	
	Misclassification error rate	0.34	
	Sensitivity	0.60	
	Specificity	0.73	
	Non-spatial cross validation AUROC	0.756 (median)	-
	Spatial cross validation AUROC	0.757 (median)	-

Table 13. Classification table based on the GAM for permafrost distribution, using a cutpoint of 0.5

Permafrost distribution model	Observed permafrost (obs.=1)	Observed non-permafrost (obs.=0)	**TOTAL**
Predicted permafrost (pred.=1)	1548	361	1909
Predicted non-permafrost (pred.=0)	714	901	1615
TOTAL	1548	361	3524

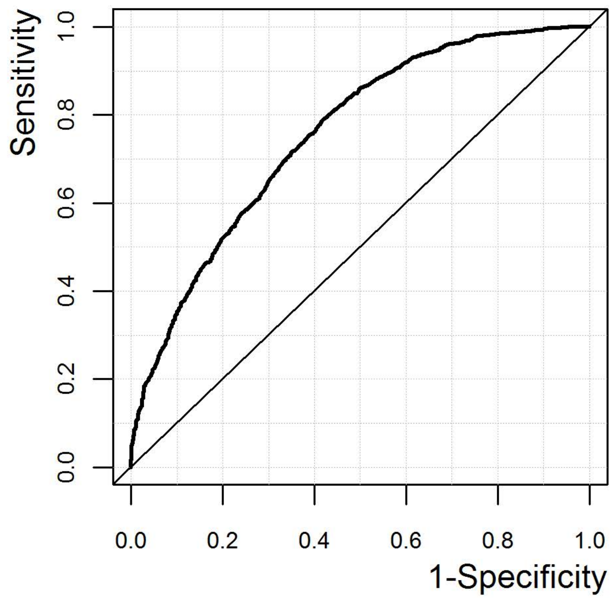

Figure 22. ROC curve for the GAM permafrost distribution model, estimated on the training data set (area under the ROC curve: ~0.76)

5.3.3 Spatial Distribution of Permafrost

Excluding steep bedrock and glacier surfaces and considering a permafrost probability score (PPS) ≥ 0.5, permafrost could cover around 6.8% of the semi-arid Chilean Andes (2636 km^2), whereas considering a PPS ≥ 0.75, the potential permafrost area decreases to 2.7% (1051 km^2; Table 14).

The largest spatial extension of potential permafrost surfaces are concentrated in the Huasco and Elqui watersheds, where the PPS ≥ 0.5 covers above 10% of each watershed surface (1150 km^2 in the Huasco; 1104 km^2 in the Elqui); whereas, in the Limarí and Choapa watersheds, areas with PPS ≥ 0.5 represent less than 3% of each watershed's surface (217 km^2 in the Limarí; 192 km^2 in the Choapa).

The spatial distribution of the predicted probability of permafrost occurrence in the study area is depicted in Figure 23. In general, the potential permafrost areas tend to decrease southward. Higher PPSs are spatially concentrated around the highest part of the study area, where the elevation rises considerably (i.e., Cerro El Toro 6168 m a.s.l., Las Tórtolas 6160 m a.s.l., and Olivares 6216 a.s.l.). On the other hand, lower PPSs (<0.5) are associated with lower hill slopes and valley bottom (Figure 24).

Table 14. Distribution of areas potentially influenced by permafrost per watershed in the semi-arid Chilean Andes

Permafrost Probability scores (PPS)	Watershed names [1,2,3]				Total area per PPS ranges km² (%)
	Huasco km² (%)	Elqui km² (%)	Limarí km² (%)	Choapa km² (%)	
0 to 0.25	242 (2.5)	199 (2.1)	86 (0.7)	63 (0.8)	**590 (1.5)**
0.25 to 0.50	317 (3.2)	296 (3.1)	94 (0.8)	81 (1.0)	**788 (2.0)**
0.50 to 0.75	662 (6.8)	656 (7.0)	141 (1.2)	126 (1.6)	**1585 (4.1)**
0 .75 to 1	488 (5.0)	448 (4.8)	76 (0.7)	66 (0.8)	**1051 (2.7)**

[1]The areal extent of drainage basin including low elevation areas: Huasco (9766 km^2), Elqui (9407 km^2), Limarí (11683 km^2) and Choapa (7795 km^2)

[2] Predicted permafrost occurrence areas, steep bedrock and glacier surface zones are excluded

[3] Glacier surface zones excluded from permafrost areas were obtained from: Nicholson *et al.* (2009) for the Huasco (16.9 km^2) and DGA (2009) for the Elqui (8.3 km^2), Limarí (1.7 km^2), and Choapa (0.3 km^2) watersheds

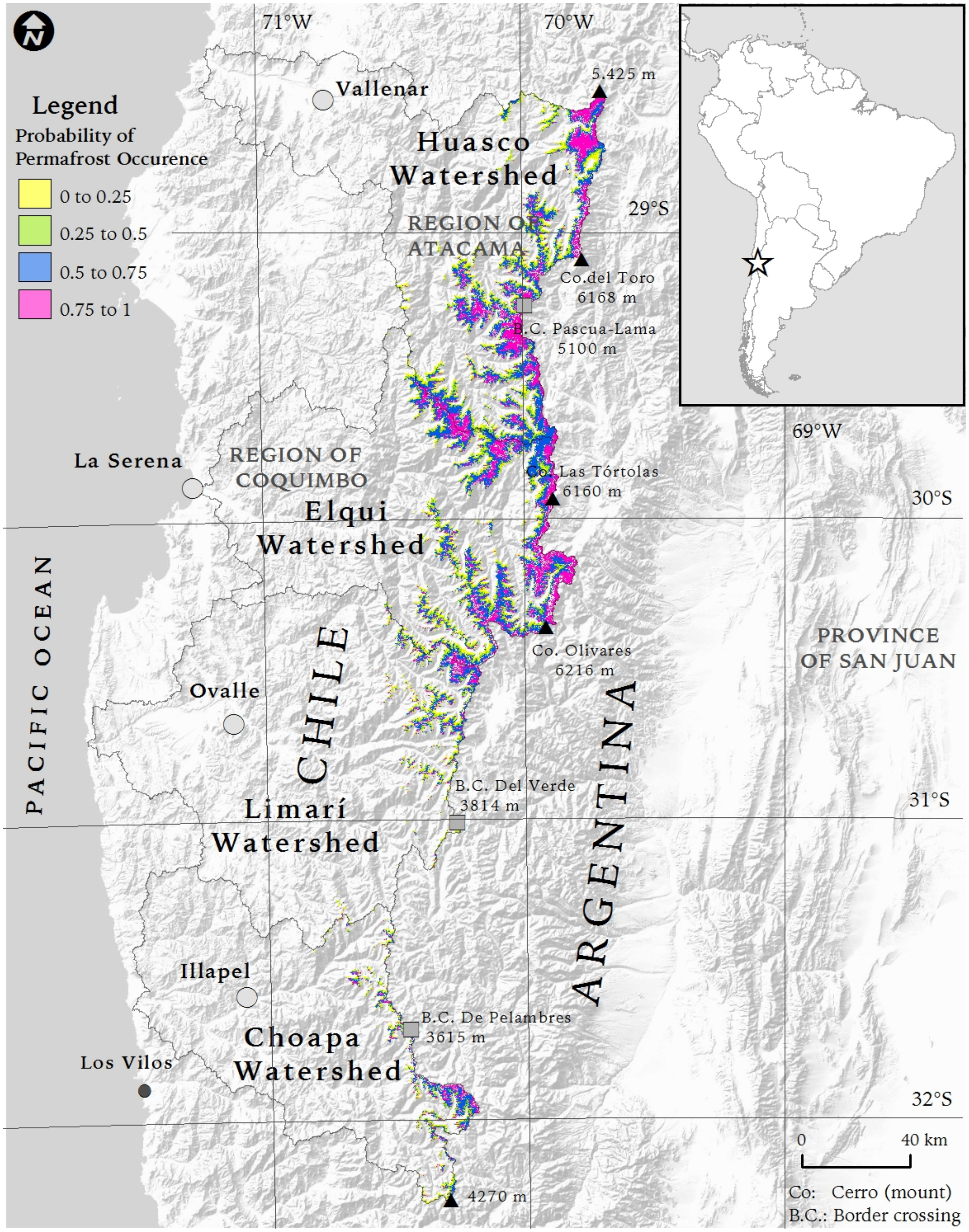

Figure 23. Potential permafrost distribution in the semi-arid Chilean Andes based on the permafrost distribution model, GAM permafrost for debris areas

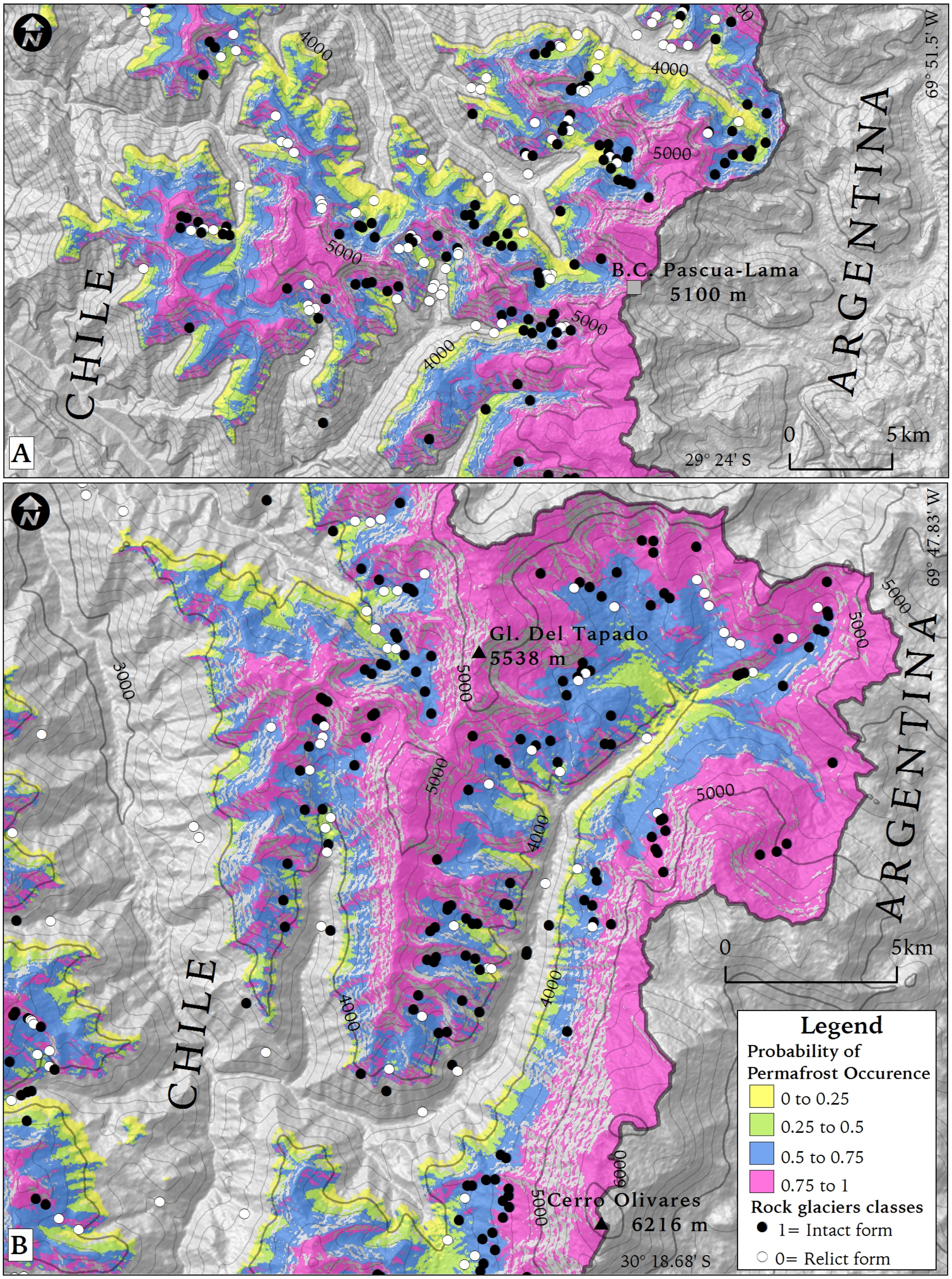

Figure 24. Detailed view of the potential permafrost distribution and rock glacier classes in (A) the upper Huasco and (B) upper Elqui Rivers (scale differ)

Chapter 6

Discussion

6.1 Rock Glacier Inventory

Rock glaciers along the study area are abundant, with an important presence of active (n=1075), inactive (n=493), intact (n=343) and relict rock glaciers (n=1664), together forming on of the largest concentrations in the Chilean Andes documented to date. This research has updated the number of rock glaciers estimated in previous studies (Brenning, 2005a,b; Brenning & Azócar, 2010a, Nicholson *et al.*, 2009; UGP UC, 2010). A similar abundance of rock glaciers has only been found before in the Alps (Krainer & Ribis, 2012; Scotti *et al.*, 2013), Sierra Nevada (Millar & Westfall, 2008) and Tien Shan mountains located in Central Asia (Bolch & Marchenko, 2006).

In comparison to the recent inventory of rock glaciers realized by UGP UC (2010) in the Elqui, Limarí and Choapa watersheds, the present inventory increases the number of active rock glaciers from 581 to 933 (increase 60%), inactive rock glaciers from 151 to 415 (increase 275%) and intact rock glaciers from 135 to 249 (increase 184%) within of these watersheds (Table 15). This has been possible because in the current work, rock glaciers are recognized using images with better resolution than in the previous work.

Although rock glacier surfaces were not considered in this work, it is probable that most of the new rock glaciers recognized in this inventory correspond to small landforms (below 0.1 km^2) that could not recognized in the previous inventories (Nicholson *et al.*, 2009 and UGP UC, 2010).

Table 15. Total number of active, inactive, intact and relict rock glaciers inventoried at watershed level

Watershed name	Active rock gl.	Inactive rock gl.	Intact rock gl.	TOTAL	
				Active, inactive and intact rock gl.	Relict rock gl.
Huasco**	252	78	94	**424**	298
Elqui	463 (220*)	179(80*)	39 (5*)	**681**	659
Limarí	224 (247*)	134(40*)	128(54*)	**486**	407
Choapa	136 (114*)	102(31*)	82 (76*)	**320**	300
TOTAL	**1075**	**493**	**343**	**1911**	**1664**

*Number of rock glaciers inventoried by UGP UC (2010)

**Rock glaciers inventoried by Azócar (2013)

Uncertain in classification of activity status of rock glaciers between different operators is discarded because rock glaciers were inventoried for all watersheds by the same operator. However a degree of subjectivity must be assumed in the inventory activity status results. Future integration of inventories of rock glaciers from different sources need to reduce the uncertain in classification status. Classification status of random rock glacier inventory samples by independent operators can be one of the solutions to estimate the uncertain itself (Curtaz *et al.*, 2010).

6.1.1.1 Distribution of Rock Glaciers and MAAT

Although it is well known that the distribution of rock glaciers at a regional scale is mainly controlled as a function of MAAT, PISR and precipitation (Brenning & Trombotto, 2006; Brenning & Azócar , 2010a; Owen & England, 1998), it is likely that most non-relict rock glaciers located in positive MAAT levels within the study area exist due to topographic factors related to the size of the catchment-area and the talus production that contributes to the occurrence of rock glaciers in unfavorable MAAT levels. In general, at the semi-arid Chilean Andes where there are not significant glacierizations, unglacierized headwalls supply abundant debris for rock glacier development (Brenning *et al.*, 2007). Moreover, the delayed response of intact rock glaciers to climate forcing can contribute to the occurrence of rock glaciers within the zone of positive regional MAATs (Brenning, 2005a).

The spatial distribution of non-relict rock glaciers with (active, inactive and intact forms) suggests that 31% (*n*=594) of these forms exist above the 0°C MAAT isotherm altitude, and around 20% (*n*=122) of these forms are situated up to the MAAT -2°C isotherm altitude (Figure 13). The above findings suggest that a uniform increase of 1°C due to of climate changes would not greatly impact rock glaciers situated above the MAAT -2°C isotherm altitude because they will remain under very cold conditions. However, rock glaciers located in MAAT isotherms that range between 0°C and -1°C (*n*=288) would become more sensitive to a rise in temperature because this warming would cause permafrost to thaw.

6.2 Temperature Distribution Model

The results of the temperature distribution model show that the modern 0°C isotherm of Mean Annual Air Temperature (MAAT) for a period of thirty years (1981-2010) is situated at ~4250 m a.s.l. in the northern (29°S) section and drops altitudinally until ~4000 m a.s.l. in the southern section (32°S) within the semi-arid Chilean Andes. Although the result cannot be directly compared with other studies due to the lack of research that characterizes the altitude of the 0°C isotherm within the study area during this time period, the altitudinal position of 0°C MAAT conforms to rough estimations suggested by Brenning (2005; 0°C MAAT ~4000 at 29°S, ~3750 at 32°S) for the semi-arid Chilean Andes. Furthermore, the environmental temperature rate obtained in this study (-0.71°C per 100 m) is partially similar to the average temperature decrease in the free atmosphere (~ -0.6°C per each 100 m; Barry, 1992).

In this study, the RSE in the prediction of MAAT is about 0.26° to 0.76°C between AAT records (level 1) and 0.8° to 1.08°C between years (level 2) at 95% of confidence interval which is in agreement with the uncertainty in MAAT prediction utilized in permafrost distribution and global temperature models for the European Alps (RSE ±0.5°C at 95% confident interval, in Hoelzle & Haeberli, 1995; RSE below 1°C, in Hiebl *et al.*, 2009).

6.3 Permafrost Distribution Model

6.3.1 Statistical Results

The statistical results of the permafrost distribution model shows that debris areas with a permafrost probability score ≥ 0.5 cover a spatial extension of 6.8 % (2636 km^2) of the study area. Although the model includes the main factors that control the regional permafrost distribution in the semi-arid Chilean Andes, such as the temperature and the potential amount of solar radiation in relation to the altitude and latitude changes (Brenning, 2005b; Brenning & Trombotto, 2006; Azócar & Brenning, 2010), the permafrost model does not account for the effect of specific local environmental factors in debris areas, such the soil properties and the effect of snow avalanches (and the distribution of snow patches) that can influence permafrost distribution (Hoelzle *et al.*, 2001; Gruber & Haeberli, 2009). Therefore, all these local factors must be considered when the results of a permafrost distribution model are interpreted (Boeckli *et al.*, 2012b).

6.3.2 Interpretation of Scores of Probability Permafrost Occurrence

Although the results of the permafrost distribution model for debris areas offer a useful overview of the potential permafrost zones within the study area, the model does not account for several local environmental factors that can also influence the presence and absence of permafrost across mountain areas such as the distribution of long-lasting snow patches and substrate properties such as the size and sort of rock clasts. Even though the model does indirectly take into account the influence of snow on permafrost occurrence due to that MAAT and PISR are proxies of snow distribution, the model does not consider how snow redistribution by avalanches affects permafrost distribution. Long-lasting snow patches at the toe of talus slopes can influence the energy budget of the ground by insulating the ground from atmospheric temperatures. On the other hand, it can also change the surface albedo. These changes can have a direct influence on the presence of isolated permafrost patches (Hoelzle *et al.*, 2001).

At a local scale, the temperature of a surface talus deposit is influenced by the sort and size of clasts, the air circulation within the talus slope, and the snow re-distribution along the talus surface. These local factors can cause strong differences in ground temperatures and therefore in permafrost distribution. Often, ground temperatures tend to be cooler at the toe of the talus deposit because it contains more coarse blocks that produce a cooling effect of the ground; in contrast, the areas at the top of a talus slope that contain smaller clasts as well as an infill of fine material, have warmer ground temperatures (Boeckli *et al.*, 2012b).

Although steep bedrock areas were excluded from the permafrost model distribution due to the lack of empirical evidence of permafrost conditions to use into the model, steep bedrock surfaces can be favorable or unfavorable for permafrost conditions depending upon the degree of rock fractures. According to Boeckli *et al.* (2012b) more strongly fractured surface promotes the accumulation of thin snow cover and the penetration of air, factors that locally contribute to cold conditions. On the other hand, flat steep bedrock surfaces without fractured areas are more favorable for warm conditions.

In summary, it is suggested that in areas with PPS ≥ 0.75, permafrost will occur in almost all environmental conditions; in contrast, in areas where PPS ranges between 0.5 and 0.75, permafrost will be present only in the favorable cold zones describe before. Finally, in areas with PPS < 0.5, permafrost may be present in exceptional environmental circumstances.

6.3.3 Comparison of Permafrost Predictions Models

In order to compare the statistical permafrost distribution model result from this study with those of the Global Permafrost Zonation Index model (PZI; Gruber, 2012), the PPSs resulting from this study (30 m resolution) were resampling to PZI resolution (1 km resolution) through a simple interpolation method based on averaging all PPS pixels that fall within a given PZI pixel. Judging from the boxplot and scatterplot (Figure 25) and mean and standard deviation values for each group of pixels, the results of this work (mean=0.53; SD=0.2) seem to predict more pixels with higher probability scores than the global PZI model (mean=0.18; SD=0.2), within the study area (difference of means 0.35±0.008 with 95% confidence). In addition, the potential permafrost areas with PPS ≥ 0.75 (1284 km^2) is larger than the area with PZI ≥ 0.75 (209 km^2). A visual comparison of PPS ≥ 0.75 between models for the area surrounding El Tapado Glacier (5538 m a.s.l; Elqui valley) is depicted in Figure 26.

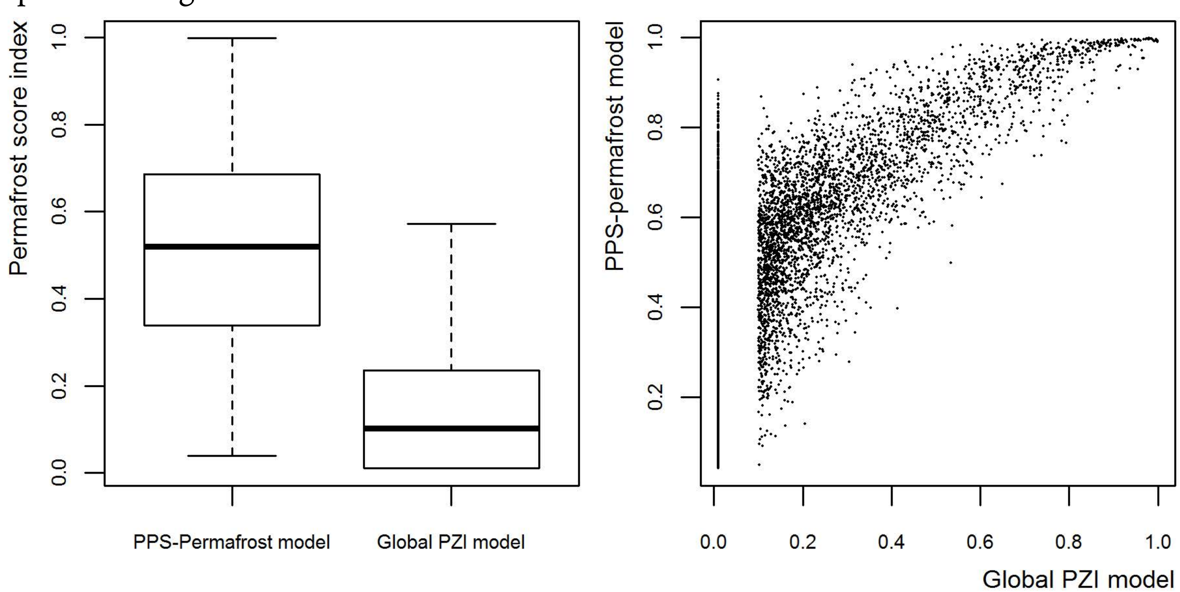

Figure 25. Comparison between permafrost probability scores (PPS) from this study with the Global Permafrost Zonation Index (PZI; Gruber, 2012) within the study area

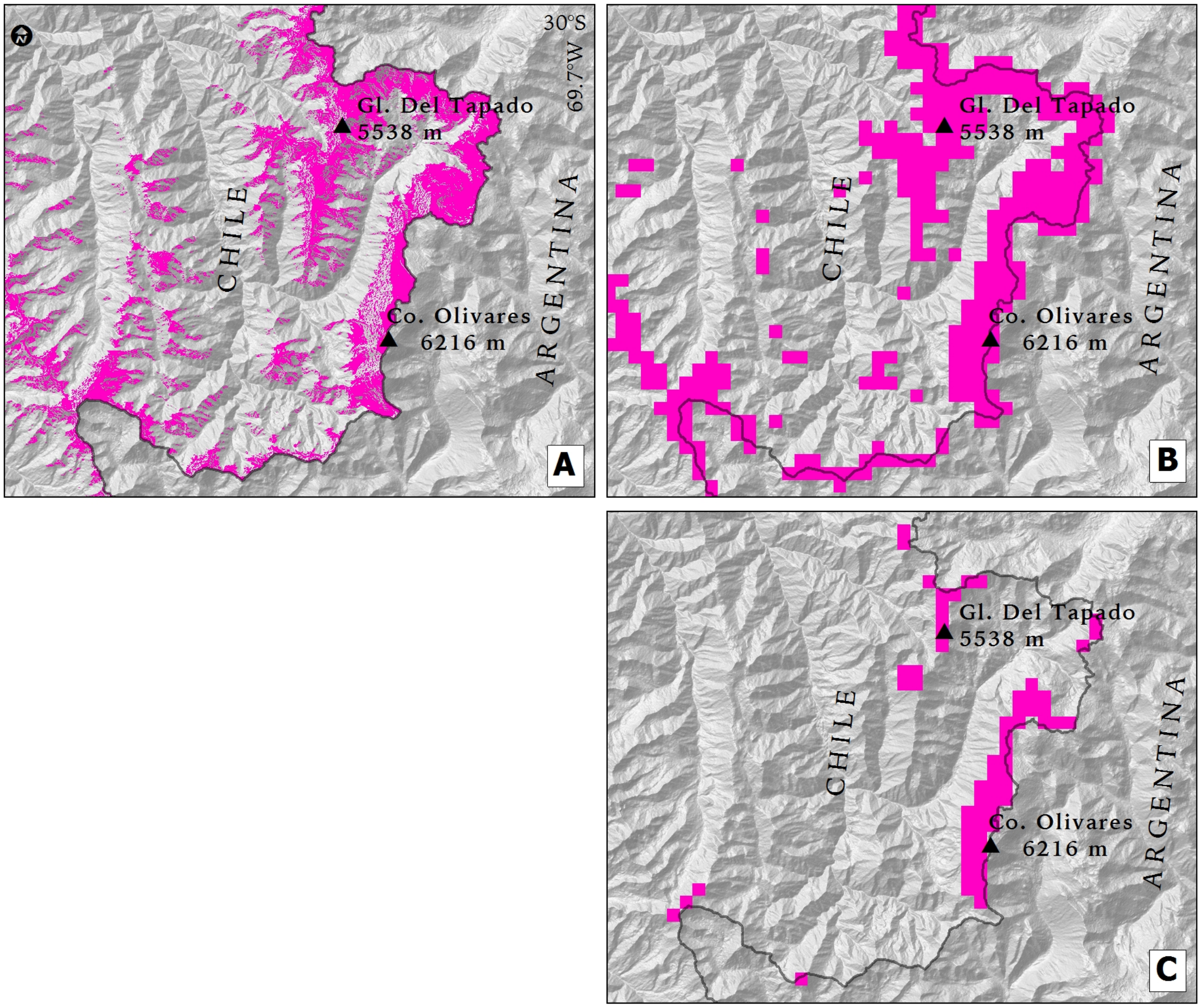

Figure 26. Visual comparison of permafrost probability scores (PPS) ≥ 0.75 between models around El Tapado Glacier zone. (a) PPS from this study, (b) PPS from this study resampling to 1 km and (c) Permafrost Zonation Index (PZI) model by Gruber (2012)

6.3.4 Permafrost Areas and Effects of Climate Changes

According to the model the occurrence of permafrost in the semi-arid Chilean Andes between 29° and 32° South is relative continuous above ~4500 m a.s.l. and discontinuous between ~3900 to 4500 m a.s.l. Permafrost areas near the lower boundary of permafrost distribution are more sensitive to degradation processes due to possible effect of climate changes (Haeberli, 1992). A rise in air temperature can potentially lead to thaw ice rich frozen ground (i.e., intact rock glacier). In addition, this warming could lead to geotechnical problems related to high-altitude infrastructure build by mining companies (Brenning, 2008; Brenning & Azócar, 2010b) or in connection with public infrastructures (i.e., border roads, tunnels). Moreover, an increase in the numbers of debris flow and rock fall activity would take place (Haeberli, 1992; Zimmermann & Haeberli, 1992).

6.3.5 Future Challenges for Permafrost Distribution Model in the Andes

The presented statistical approach to modeling permafrost distribution in the semi-arid Chilean Andes can be extended to other mountain regions of the South America Andes; however, some limitations need to be overcome. More complete inventories of rock glacier forms along to the Andes including relict forms. In this direction, some progresses have been made with build of new inventories of rock glaciers in the Argentine and Chilean Andes (UGP UC, 2010; IANIGLA-CONICET, 2010).

Temperature records are scarce in the Andes; most long-term weather stations are located in low altitudes and broadly distributed along i.e. the Chilean and

Argentine Andes. Given the limitation of temperature records, temperature distribution could be potentially be modeled at very fine resolution using inexpensive temperature sensors for monitoring surface and air temperatures, and empirically downscaling methods (i.e., mixed-effects models) that combine short-term data from inexpensive temperature sensors with long-term temperature observations available for some weather stations located at high altitudes (Fridley, 2009). Predictor variables such altitude and latitude can be easily measured through free high resolution DEM (i.e., ASTER GDEM). However, logistical limitation related to local relief characteristics and accessibility conditions must be considered. In addition, remote-sensing techniques to derive temperatures should also be evaluated as an additional method.

In recent permafrost model, the influence of precipitation has shown to being as a variable with a positive influence in the permafrost presence (Boeckli *et al.*, 2012a). Although precipitation data are scarce for the high Andes zones, West-East trend in precipitation can be potentially inferred through the study of the cloudiness with remote sensing techniques. According to Boeckli *et al.* (2012a) the precipitation variable can be seen as simple proxy for the reduction of short wave insolation by cloud cover.

Finally, the results showed that permafrost distribution can be successfully modeled with the data available for this area and using similar modeling approaches to those already applied in other mountain zones (Janke, 2005a,b; Boeckli *et al.*, 2012a.b; Deluigi & Lambiel,2012).

Chapter 7

Conclusion

The statistical permafrost distribution model proposed has enabled more detailed calculation as well as the inclusion of low-altitude permafrost in contrast to the global permafrost estimation model for the semi-arid Chilean Andes. The overall permafrost distribution within the study area is controlled by climate and topographic factors. However, local environmental factors (e.g., substrate properties) not included in the model, could determine permafrost presence locally.

Data from rock glacier inventories combined with topographic and topoclimatic attributes can be used to effectively model the probability of permafrost occurrences in the semi-arid Chilean Andes. The GAM using a logistic function is particularly suitable for modeling relationships, due to its ability to incorporate nonlinear relationships between predictor and response variables. Moreover, GAM has shown to be a reliable statistical method for modeling permafrost distribution for large mountain regions.

Using rock glaciers as indicators of permafrost conditions in areas with debris as surface type the result of the permafrost model cannot be extended to other types of surface covers. Therefore, future studies should address this limitation. Furthermore, the effect of a delayed response of rock glaciers with high ice content to climate forcings must be considered in future analysis.

The permafrost model was built based on indirect evidence of permafrost presence. In order to overcome this limitation, an inventory of empirical evidence of permafrost through field observations is highly recommended to improve the input data quality as well as to validate the model results.

The results show that linear mixed-effects models can be advantageous in determining temperature distribution with scarce and heterogeneous temperature records from weather stations. This finding suggests that in some instances, overall regression models can be an effective interpolation method. However, more research that evaluates the performance of interpolation methods for climate data in the semi-arid Andes is needed. The results of the statistical temperature distribution model can be used to thermally characterize other mountain phenomena (i.e. glaciers, vegetation patterns) and can be used also as input for other models in a variety of applications

The occurrence of rock glaciers is highly marked by an altitudinal zonation, in that relict rock glaciers occur at lower altitudinal positions than intact rock glaciers; therefore, they can signal how the distribution of cold environments has change through time.

The findings of this research contribute to increasing knowledge on permafrost in the semi-arid Chilean Andes, providing valuable information for local environmental planning, mining projects and study of the cryosphere in the Andes.

Appendices

Appendix A

Marginal and conditional R^2

$$R^2_{\text{LMM(m)}} = \frac{\sigma_f^2}{\left(\sigma_f^2+\sum_{l=1}^{u}\sigma_l^2+\sigma_e^2+\sigma_d^2\right)}$$

Where u is the number of random factors in LMM and σ_l^2 is the variance component of the lth random factor, and σ_f^2 is the variance calculated from the fixed effect component of the LMM. This equation can be modified to express conditional R^2 (i.e. variance explained by fixed and random factors).

$$R^2_{\text{LMM(c)}} = \frac{\sigma_f^2+\sum_{l=1}^{u}\sigma_l^2}{\left(\sigma_f^2+\sum_{l=1}^{u}\sigma_l^2+\sigma_e^2+\sigma_d^2\right)}$$

The equation above represents the variance explained by the entire model.

For more formulation detail see: Nakagawa & Schielzeth (2012)

Appendix B

Altitudinal distribution of rock glaciers

	Mean altitude (m a.s.l.)	Max. altitude (m a.s.l.)	Min. altitude (m a.s.l.)	Mean PISR (kWh/m^2)
Huasco watershed				
Active rock gl.	4345	4869	3911	2005
Inactive rock gl.	4280	4716	3627	2052
Intact rock gl.	4300	4885	3658	2018
Relict rock gl.	4133	4102	2537	2106
Elqui watershed				
Active rock gl.	4204	5128	3482	1948
Inactive rock gl.	4083	4738	3022	1913
Intact rock gl.	4160	4660	3837	1970
Relict rock gl.	4001	4328	2372	2038
Limari watershed				
Active rock gl.	3918	4710	3432	1805
Inactive rock gl.	3844	4358	3465	1834
Intact rock gl.	3885	4643	3390	1819
Relict rock gl.	3711	4397	2861	2000
Choapa watershed				
Active rock gl.	3779	4567	3349	1760
Inactive rock gl.	3717	4261	3322	1819
Intact rock gl.	3791	4341	3395	1771
Relict rock gl.	3654	4376	2406	1969

* Altitude measured in front of each rock glacier

Appendix C

Distribution of rock glaciers within the study area

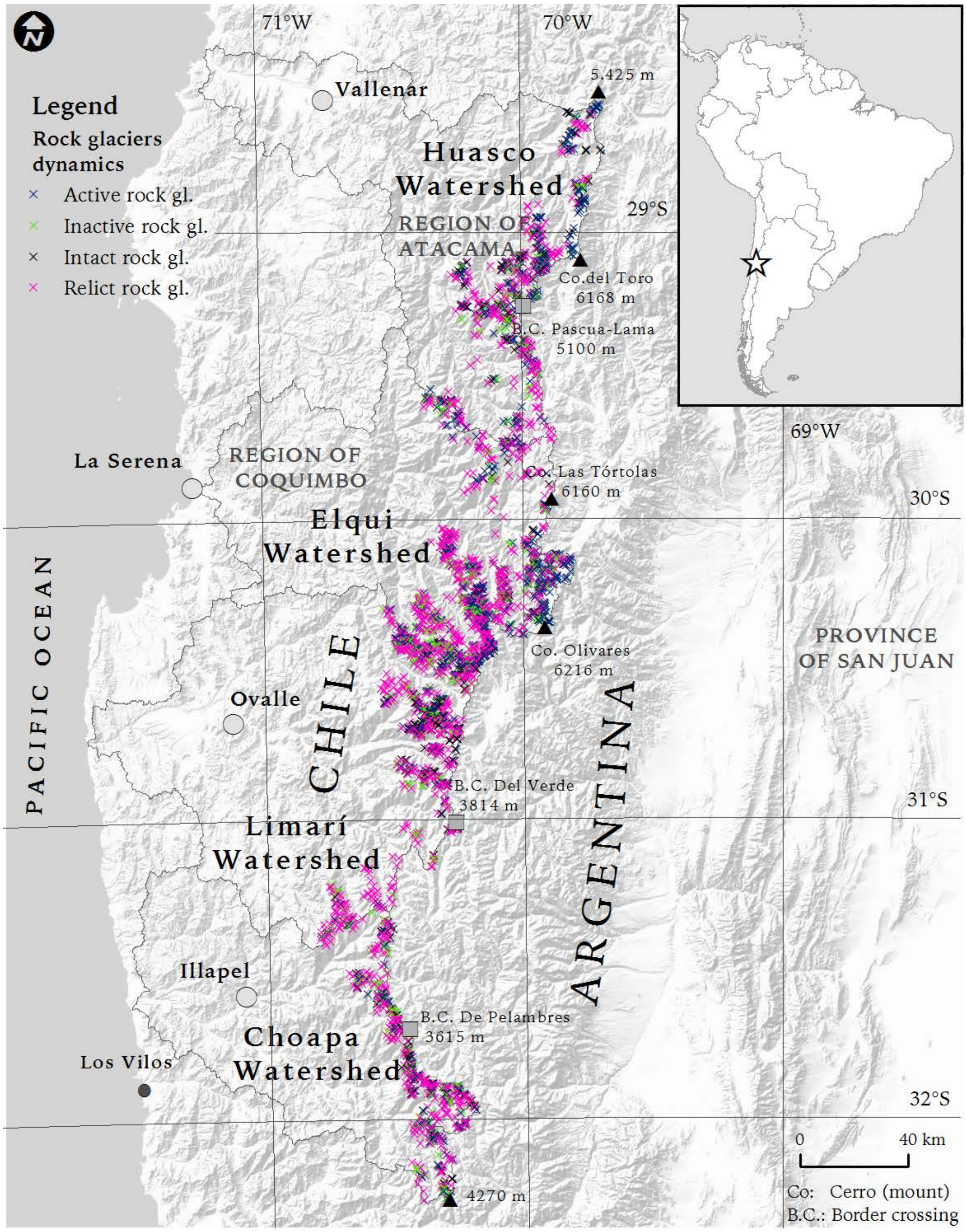

Appendix D

Number of active, inactive, intact and relict rock glaciers located above the 0°C MAAT isotherm altitude

Rock glacier dynamics	Total *	Huasco	Elqui	Limarí	Choapa
Active rock gl.	1075;403(37)	252;126(50)	463;228(49)	224;26(12)	136;26(19)
Inactive rock gl.	493;101(20)	78;32(41)	179;54(30)	134;6(4)	102;6(6)
Intact rock gl.	343;90 (26)	94;44(47)	39;14(36)	128;16(13)	82;16(20)
Relict rock gl.	1664;244(15)	298;71(24)	659;138(21)	407;15(4)	300;15(5)

* Total number of rock gl.; total number of rock gl. located above the 0°C MAAT isotherm altitude (%)

Appendix E

Statistical temperature distribution model, residual by year

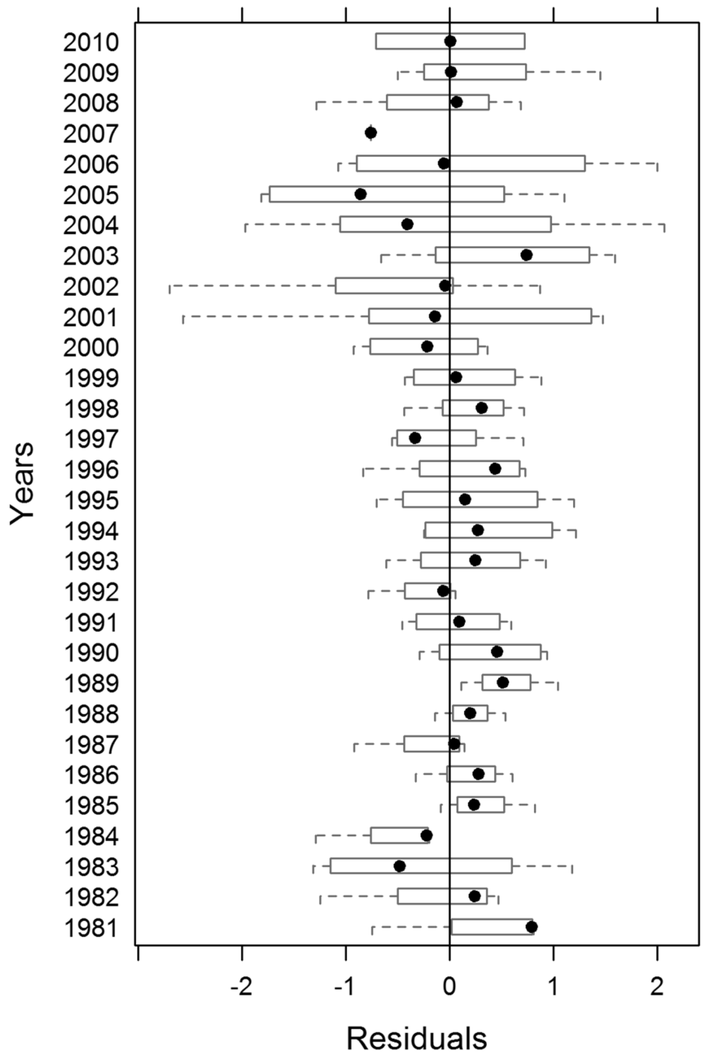

Appendix F

Statistical temperature distribution model, normal quantile-quantile plot

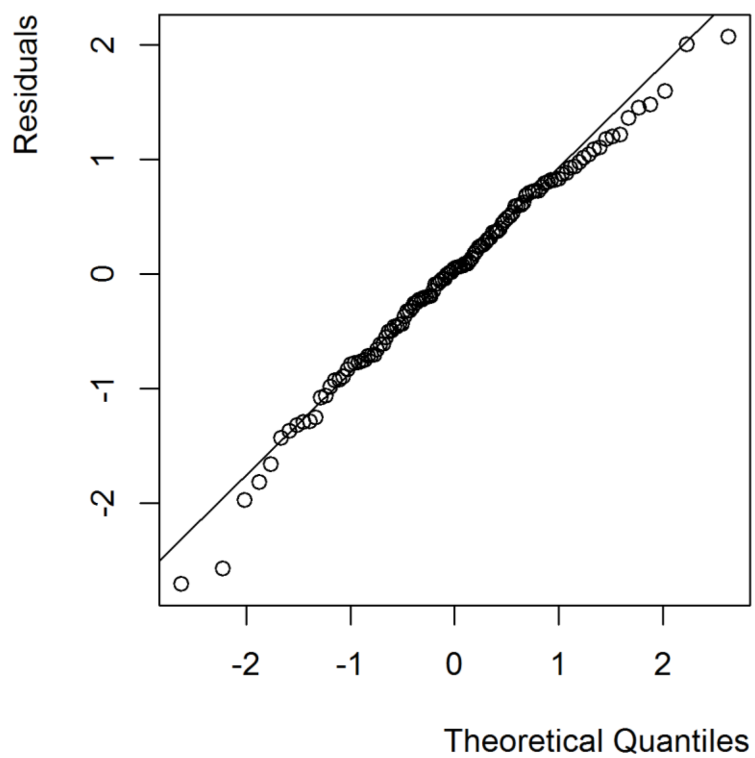

Appendix G

Estimated coefficients for the generalized linear model (GLM) model of permafrost distribution with interaction effect between the variables MAAT and relative PISR (CPISR)

	Coefficients (standard error)
Intercept	4.744 (0.315)
MAAT	0.6205 (0.186)
CPISR	-4.268 (0.305)
MAAT:CPISR	-1.118 (0.185)

Measures of predictive performance and spatial and non-spatial error estimations for the GLM for permafrost distribution

		Indices of predictive efficiency Permafrost distribution model
Based on training set derived from the spatial cross-validation (median value)	Overall Accuracy	0.65
	Misclassification error rate	0.35
	Sensitivity	0.55
	Specificity	0.76
	Non-spatial cross validation AUROC	0.748 (median)
	Spatial cross validation AUROC	0.749 (median)

Permafrost model using:	Degree of freedom	Akaike Information Criterion (AIC)
GAM (this work)	4	4126
GLM	3	4063

Bibliography

Allen, S. K., Gruber, S., & Owens, I. F. (2009). Exploring steep bedrock permafrost and its relationships with recent slope failures in the Southern Alps of New Zealand. *Permafrost and Periglacial Processes, 20*(4), 345-356. doi:10.1002/ppp.658

Apaloo, J., Brenning, A., & Bodin, X. (2012). Interactions between seasonal snow cover, ground surface temperature and topography (Andes of Santiago, Chile 33.5ºS). *Permafrost and Periglacial Processes, 23*(4), 277-291. doi:10.1002/ppp.1753

Arenson, L. U., & Jakob, M. (2010). Short Communication: The Significance of Rock Glaciers in the Dry Andes – A Discussion of Azócar and Brenning (2010) and Brenning and Azócar (2010). *Permafrost and Periglacial Processes, 21*(3), 282-285.

Arenson, L., Hoelzle, M., & Springman, S. (2002). Borehole deformation measurements and internal structure of some rock glaciers in Switzerland. *Permafrost and Periglacial Processes, 13*(2), 117-135. doi:10.1002/ppp.414

Azócar, G. (2013). *Modelamiento de la distribución del permafrost de montaña a traves de inventario de glaciares rocosos en los Andes semiáridos, cuenca superior del río Huasco, Chile (Submmited).* Tesis profesional, Universidad de Chile, Facultad de Arquitectura y Urbanismo, Escuela de Geografía, Santiago.

Azócar, G. F., Brenning, A., & Bodin, X. (2011). Mapping of rock glaciers in the Andes mountains. Elqui, Limarí and Choapa watersheds. *Annual meeting of the Canadian Association of Geographer-Ontario Division,* (p. 37). Lakehead,Orillia.

Azócar, G., & Brenning, A. (2010). Hydrological and geomorphological significance of rock glaciers in the dry Andes, Chile (27°-33°S). *Permafrost and Periglacial Processes, 21*(1), 42-53.

Azócar, G., Brenning, A., & Bodin, X. (2012). Spatial modeling of permafrost distribution using rock glacier inventories, topographic attributes and temperature data in the semiarid Andes, Chile. *American Geophysical Union 2012 Fall Meeting.* San Francisco,USA.

Bahre, C. J. (1979). *Destruction of the natural vegetation of North-Central Chile.* Berkeley, USA: University of California Press.

Barnsley, M. (2007). *Environmental modeling.* Boca Raton, Florida,USA: CRC Press.

Barry, R. G. (1992). *Mountain weather and climate.* New York, USA: Routledge.

Barry, R., & Yew Gan, T. (2011). *The global cryosphere.* New York USA: Cambridge University Press.

Barsch, D. (1978). Active rock glaciers as indicators for discontinuous alpine permafrost. An example from the Swiss Alps. *Third International Conference on Permafrost, 1*, pp. 349-353. Ottawa.

Barsch, D. (1996). *Rockglaciers: Indicators for the present and former geoecology in high mountain environments.* Berlin, Germany: Springer.

Beniston, M., & Douglas, G. (1996). Chapter 5: Impacts of climate change on mountain regions. In R. Watson, M. Zinyowera, & R. Moss (Eds.), *Climate change 1995 impacts, adaptations and mitigation of climate change: Scientific-technical analyses. Part II—Assessment of impacts and adaptation options.* Cambridge, UK: Cambridge University Press.

Berthling, I. (2011). Beyond confusion: rock glaciers as cryo-conditioned landforms. *Geomorphology, 131*, 98-106.

Birkeland, P. W. (1973). Use of relative age-dating methods in a stratigraphic study of rock glacier deposits, Mt. Sopris, Colorado. *Arctic and Alpine Research, 5*(4), 401-416.

Bodin, X., Krysiecki, J.-M., & Iribarren, P. (2012). Recent collapse of rock glaciers: two study cases in the Alps and in the Andes. *12th Congress interpraevent.* Grenoble, France.

Bodin, X., Rojas, F., & Brenning, A. (2010). Status and evolution of the cryosphere in the Andes of Santiago (Chile, 33.5°S.). *Geomorphology, 118*, 453-464.

Boeckli, A., Brenning, A., Noetzli, J., & Gruber, S. (2012a). A statistical approach to modelling permafrost distribution in the European Alps or similar mountain ranges. *The Cryosphere, 6*(1), 125-140. doi:10.5194/tc-6-125-2012

Boeckli, L., Brenning, A., Gruber, S., & Noetzli, J. (2012b). Permafrost distribution in the European Alps: Calculation and evaluation of an index map and summary statistics. *The Cryosphere, 6*(4), 807-820.

Bolch, T., & Marchenko, S. (2006). Significance of glaciers, rockglaciers, and ice-rich permafrost in the Northern Tien Shan as water towers under climate change conditions. *Selected paper from the Workshop " Assessment of Snow, Glacier and Water Resources in the Asia"*, (pp. 199-211). Almaty, Kasajistán.

Bonnaventure, P. P., Lewkowicz, A. G., Kremer, M., & Sawada, M. C. (2012). A permafrost probability model for the Southern Yukon and Northern British Columbia, Canada. *Permafrost and Periglacial Processes, 23*(1), 52-68. doi:10.1002/ppp.1733

Borde, J. (1966). *Les Andes de Santiago et leur avant-pays: étude de géomorphologie.* Bordeux: Union Francaise d'Impression.

Brenning, A. (2003). La importancia de los glaciares de escombros en los sistemas geomorfológico e hidrológico de la cordillera de Santiago: Fundamentos y primeros resultados. *Revista de Geografía Norte Grande, 30*, 7-22.

Brenning, A. (2005a). *Climatic and geomorphological controls of rock glacier in the Andes of central of Chile.* Doctoral thesis, Humboldt-Universität, Mathematisch-Naturwissenschaftliche Fakultät II, Berlin, Germany.

Brenning, A. (2005b). Geomorphological, hydrological and climatic significance of rock glaciers in the Andes of central Chile (33-35°S). *Permafrost and Periglacial Processes, 16*(3), 231-240. doi:10.1002/ppp.528

Brenning, A. (2005c). Spatial prediction models for landslide hazards:review, comparison and evaluation. *Natural Hazards and Earth System Sciences, 5*(853), 853-862.

Brenning, A. (2008). The impact of mining on rock glaciers and glaciers. In B. Orlove, E. Wiegandt, B. Luckman, B. Orlove, E. Wiegandt, & B. Luckman (Eds.), *Darkening peaks: glacier retreat, science, and society* (Vol. 14, pp. 196-205). Berkeley: University of California Press.

Brenning, A. (2010). Short Communication: The significance of rock glaciers in the dry Andes – Reply to L. Arenson and M. Jakob. *Permafrost and Periglacial Processes, 21*(3), 286-288.

Brenning, A. (2011). RSAGA: SAGA geoprocessing and terrain analysis in R. R package version 0.93-1. Retrieved from http://CRAN.R-project.org/package=RSAGA: http://CRAN.R-project.org /package=RSAGA

Brenning, A. (2012). Spatial cross-validation and bootstrap for the assessment of prediction rules in remote sensing: The R package SPERROREST. *IEEE International Symposium on Geoscience and Remote Sensing IGARSS*, (pp. 5372-5375). Munich, Germany.

Brenning, A., & Azócar , G. F. (2010a). Statistical analysis of topographic and climatic controls and multispectral signatures of rock glaciers in the dry Andes, Chile (27°–33°S). *Permafrost and Periglacial Processes, 21*(1), 54-66. doi:10.1002/ppp.670

Brenning, A., & Azócar, G. (2010b). Minería y glaciares rocosos: impactos ambientales, antecedentes políticos y legales, y perspectivas futuras. *Revista de Geografía Norte Grande, 47*, 143-158.

Brenning, A., & Trombotto, D. (2006). Logistic regression modeling of rock glacier and glacier distribution: Topographic and climatic controls in the semi-arid Andes. *Geomorphology, 81*, 141-154.

Brenning, A., Azócar, G. F., & Bodin, X. (2013). Monitoring rock glacier dynamics and ground temperatures in the semiarid Andes (Chile, 30°S). *European Geosciences Union, General Assembly 2013.* Vienna, Austria: European Geosciences Union.

Brenning, A., Azócar, G., & Bodin, X. (2010). Mapping and monitoring rock glaciers in the Chilean Andes. *Third European Conference on Permafrost.* Svalbard, Norway.

Brenning, A., Grasser, A., & Friend, D. (2007). Statistical estimation and generalized additive modeling of rock glacier distribution in the San Juan Mountains, Colorado, USA. *Journal of Geophysical Research, 112*. doi:10.1029/2006JF000528

Brenning, A., Gruber, S., & Hoelzle, M. (2005). Sampling and statistical analyses of BTS measurements. *Permafrost and Periglacial Processes, 16*(4), 383-393.

Burger, K., Degenhardt, J., & Giardino, J. (1999). Engineering geomorphology of rock glaciers. *Geomorphology, 31*, 93-132.

Caine, N. (2010). Recent hydrologic change in a Colorado alpine basin: an indicator of permafrost thaw? *Annals of Glaciology, 51*(56), 130-134.

Capps Jr, S. (1910). Rock glacier in Alaska. *The journal of Geology, 18*(4), 359-375.

Caviedes, C. N., & Paskoff, R. (1975). Quaternary glaciations in the Andes of North-Central Chile. *Journal of Glaciology, 14*, 155-170.

Clark, D., Eric, S., Noel, P., & Alan, G. (1998). Genetic variability of rock glaciers. *Geografiska Annaler, 80*(3-4), 175-182.

Comisión Nacional del Medio Ambiente [CONAMA]. (2006). *Estudio de la variabilidad climática en Chile para el siglo XXI.* Santiago: Gobierno de Chile.

Contreras, A. (2005). Meteorological data compañía minera Disputada de Las Condes.

Corte, A. E. (1978). Glaciers and glaciolithic systems of the Central Andes. *Actes de l' Atelier de Riederalp, 126*, pp. 11-24.

Curtaz, M., Vagliasindi, M., Letey, S., Di Cella, M., & Pogliotti, P. (2010). New rock glaciers inventory of Aosta valley, Italy. *Poster session presented at the Third European Conference on Permafrost.* Longyearbyen, Svaalbard, Norway.

Davis, N. (2000). *Permafrost: a guide to frozen ground in transition.* Alaska, USA: University of Alaska Press.

Delaloye, R., & Lambiel, C. (2005). Evidence of winter ascending air circulation throughout latus slopes and rock glaciers siuated in the lower belt of alpine disconitnous permafrost (Swiss Alps). *Norsk Geografisk Tidsskrift, 59*, 194-203.

Delaloye, R., Perruchoud, E., Avian, M., Viktor , K., Bodin, X., Hausmann, H., . . . Thibert, E. (2008). Recent interannual variations of rock glacier creep in the European Alps. *Ninth International Conference on Permafrost. I,* pp. 343-348. Fairbanks, Alaska: University of Alaska.

Deluigi, N., & Lambiel, C. (2012). PERMAL: a machine learning approach for alpine permafrost distribution modeling. *Actes du colloque de la Société Suisse de Géomorphologie 29 juin - 1er juillet 2011*, (pp. 47-62). St-Niklaus.

Devenish, C., & Gianella, C. (Eds.). (2012). *20 years of sustainable mountain development in the Andes-from Rio 1992 to 2012 and beyond-.* Lima: CONDESAN-Consorcio para el desarrollo Sostenibla de la Ecorregión Andina.

Dirección General de Aguas [DGA]. (2009). *Inventario de glaciares descubiertos de las cuencas de los ríos Elqui, Limarí y Choapa.* Santiago: Ministerio de Obras Públicas, Chile.

Duguay, C. R. (1993). Radiation modeling in mountainous terrain review and status. *Mountain Research and Development*, 13(4), 339-357.

Duguay, C. R., Zhang, T., Leverington, D. W., & Romanovsky, V. E. (2005). Satellite remote sensing of permafrost and seasonally frozen ground: Measuring environmental change, geophysical monograh series. In R. Duguay, & A. Pietroniro (Eds.), *Remote Sensing of Northern Hydrology* (Vol. 163, pp. 91-118).

Ebohon, H., & Schrott, L. (2008). Modelling mountain permafrost distribution. A new permafrost map of Austria. In D. L. Kane, & K. M. Hinkel (Ed.), *9th International Conference on Permafrost* (pp. 397-402). Fairbanks, Alaska: Institute of Northern Engineering University of Alaska Fairbanks.

Ebdon, D. (1985). *Statistics in Geography.* Worcester, UK: Basil Blackwell Inc.

Embleton, C., & King, C. A. (1975). *Periglacial geomorphology.* London: Edward Arnold Ltd.

Escobar, F., & Aceituno, P. (1998). Influencia del fenónemo ENSO sobre la precipitación nival en el sector Andino de Chile Central durante el invierno. *Institut français d'études andines, 27*(3), 753-759.

Esper, M. (2009). A preliminary inventory of rock glaciers at 30°S latitude, Cordillera Frontal of San Juan, Argentina. *Quaternary International, 195*, 151-157.

Esper, M. (2010). Application of frequency ratio and logistic regression to active rock glacier occurrence in the Andes of San Juan, Argentina. *Geomorphology, 114*, 396-405.

Etzelmüller, B. (2013). Recent advances in mountain permafrost research. *Permafrost and Periglacial Processes, 24*(2), 99-107.

Etzelmüller, B., Heggem, E., Sharkhuu, N., Frauenfelder, R., Kääb, A., & Goulden, C. (2006). Mountain permafrost distribution modelling using a multi-criteria approach in the Hövsgöl area, Northern Mongolia. *Permafrost and Periglacial Processes, 17*(2), 91-104.

Etzelmüller, B., Hoelzle, M., Heggem, E., Isaksen, K., Mittaz, C., Vonder Mühll, D., . . . Sollid, J. (2001). Mapping and modelling the ocurrence and distribution of mountain permafrost. *Norwegian Journal of Geography, 55*, 186-194.

Etzelmüller, B., Farbrot, H., Guðmundsson, Á., & Humlum, O. (2007). The regional distribution of mountain permafrost in Iceland. *Permafrost and Periglacial Processes, 18*(2), 185-199.

Favier, V., Falvey, M., Rabatel, A., Praderio, E., & López, D. (2009). Interpreting discrepancies between discharge and precipitation in high-altitude area of Chile's Norte Chico region (26-32°). *Water Resource Research, 45*, 1-20.

Ferrando, F. (1996). Glaciares relictuales en el marco andino del semiárido de Chile, IV Región. *I Taller Internacional de Geoecología de Montaña de Los Andes del Sur: Manejo de Recrusos y Desarrollo Sustentable* (pages. 287-298). Santiago, Chile: Universidad de Chile.

Ferrando, F. (2003a). Aspectos conceptuales y genético-evolutivos de los glaciares rocosos: Análisis de caso en los Andes semiáridos de Chile. *Revista Geográfica de Chile Terra Australis*, 48, 43-74.

Ferrando, F. (2003b). Cuenca del río Limarí. Chile semiárido. Aspectos de la oferta y la demanda de agua. *Revista de Geografía Norte Grande, 30*, 23-44.

Fiebig-Wittmaack, M., Astudillo, O., Wheaton, E., Wittrock, V., Perez, C., & Ibacache, A. (2012). Climate trend and impact of climate change on agriculture in an arid Andean valley. *Climate Change, 111*(3-4), 819-833.

Field, A., Miles, J., & Field, Z. (2012). *Discovering statistic using R.* London, England: Sage Publication Ltd.

Fitzharris, B. (1996). Chapter 7: The cryosphere-changes and their impacts. In R. Watson, M. Zinyowera, & R. Moss (Eds.), *Climate change 1995 impacts, adaptations and mitigation of climate change: Scientific-technical analyses.Part II—Assessment of impacts and adaptation options.* Cambridge, UK: Cambridge University Press.

Francou, B., Fabre, D., Pouyaud, B., Jomelli, V., & Arnaud, Y. (1999). Symptoms of degradation in a tropical rock glacier, Bolivian Andes. *Permafrost and Periglacial Processes, 10*(1), 91-100.

Frauenfelder, R., Allgöwer, B., Haeberli, W., & Hoelzle, M. (1998). Permafrost investigations with GIS- A case study in the Fletschhorn area, Wallis, Swiss Alps. *Permafrost-Seventh International Conference*, (pp. 291-295). Yellowknife, Canada.

French, H. M. (2007). *The Periglacial environment.* West Sussex, England: John Wiley & Sons Ltd.

Fridley, J. D. (2009). Downscaling climate over complex terrain: high finescale (<1000 m) spatial variation of near-ground temperature in a montane forested landscape (Great Smoky Mountains). *Journal of Applied Meteorology and Climatology, 48*, 1033-1049.

Garreaud, R., & Rutllant, J. (1997). Precipitación estival en los Andes de Chile central: aspectos climatológicos. *Atmósfera, 10*, 191-211.

Garreaud, R. D., & Aceituno, P. (2007). Chapter 3: Atmospheric circulation and climatic variability. In T. T. Veblen, K. R. Young, & A. R. Orme (Eds.), *The Physical Geography of South America* (pp. 45-58). New York: Oxford University Press.

Gascoin, S., Kinnard, C., Ponce, R., Lhermitte, S., MacDonell, S., & Rabatel, A. (2011). Glacier contribution to streamflow in two headwaters of the Huasco River, Dry Andes of Chile. *The Cryosphere, 5*(4), 1099-1113.

Gates, D. M. (1980). *Biophysical ecology.* Mineola, NY, USA: Dover Publications Inc.

Gelman, A., & Hill, J. (2007). *Data analysis using regression and multilevel/hierarchical models.* New York, USA: Cambridge University Press.

Geoestudios Ltda. (2008). *Identificación de glaciares de roca.* Santiago, Chile: Dirección General de Aguas.

Gilleland, E. (2012). Verification package. R package version 2.15.1.0. Retrieved from http://CRAN.R-project.org/package=epicalc

Goetz, J. N., Guthrie, R. H., & Brenning, A. (2011). Integrating physical empirical landslide susceptibility models using generalized additive models. *Geomorphology, 129*, 376-386.

Gorbunov, A. P., Marchenko, S. S., & Seversky, E. V. (2004). Short communication: The thermal environment of blocky materials in the Mountains of central Asia. *Permafrost and Periglacial Processes, 15*(1), 95-98.

Gruber, S. (2012). Derivation and analysis of a high-resolution estimate of global permafrost zonation. *The Cryosphere, 6*(1), 221-223. doi:10.5194/tc-6-221-2012

Gruber, S., & Haeberli, W. (2007). Permafrost in steep bedrock slopes and its temperature-realted destabilization following climate change. *Journal of Geophysical Research, 112*. doi:10.1029/2006JF000547

Gruber, S., & Haeberli, W. (2009). Mountain permafrost. In R. Margesin (Ed.), *Permafrost Soils* (pp. 33-44). Berlin: Springer-Verlag.

Gruber, S., & Hoelzle, M. (2001). Statistical modelling of mountain permafrost distribution: Local calibration and incorporation of remotely sensed data. *Permafrost and Periglacial Processes, 12*(1), 69-77. doi:10.1002/ppp 374

Gruber, S., & Hoezle, M. (2008). The cooling effect of coarse blocks revisited: A modeling study of purely conductive mechanism. *9th International Conference on Permafrost.* Fairbanks, Alaska.

Gruber, S., Hoelzle, M., & Haeberli, W. (2004). Rock-wall temperatures in the Alps: Modelling their topographic distribution and regional differences. *Permafrost and Periglacial Processes, 15*(3), 299-307.

Gubler, S., Fiddes, J., Keller, M., & Gruber, S. (2011). Scale-dependent measurement and analysis of ground surface temperature variability in alpine terrain. *The Cryosphere, 5*(2), 431-443.

Guisan, A., & Zimmermann, N. E. (2000). Predictive habitat distribution models in ecology. *Ecological modelling, 135*, 147-186.

Guisan, A., Edwards, T. C., & Hastie, T. (2002). Generalized linear and generalized additive models in studies of species distribution: setting the scene. *Ecological Modelling, 157*, 89-100.

Guzzetti, F., Reichenbach, P., Ardizzone, F., Cardinali, M., & Galli, M. (2006). Estimating the quality of landslide susceptibility models. *Geomorphology, 81*, 166-184. doi:10.1016/j.geomorph .2006.04.007

Herrera, F., Azócar, G., Brenning , A., & Bodin, X. (Mayo 2011). Inventario de glaciares rocosos en los Andes semiáridos de Chile: Cuenca del Río Elqui. *XVIII Congreso geológico argentino.* Neuquén, Argentina .

Haeberli, W. (1973). Die Basis-temperatur der winterlichen Schneedicke. *Z. Gletsch.Kd. Glazialgeol, 9*, 221-227.

Haeberli, W. (1975). Untersuchungen zur Verbreitung von Permafrost zwischen Flüelapass und Piz Grialetsch (Graubünden)., *17*, p. 221. Zürich.

Haeberli, W. (1985). Creep of mountain permafrost: Internal structure and flow of alpine rock glaciers. *Mitteilungen der Versuchsanstalt für Wasserbau, Hydrologie und Glaziologie, 77*, 142.

Haeberli, W. (1992). Possible effects of climatic change on the evolution of Alpine permafrost. In M. Boer , & E. Koster (Eds.), *Greenhouse-Impact on Cold Climate Ecosystems and Landscapes* (pp. 23-35). Cremlingen-Destedt, Germany.

Haeberli, W. (2000). Modern research perspectives relating to permafrost creep and rock glaciers: A discussion. *Permafrost and Periglacial Processes, 11*(4), 290-293.

Haeberli, W. (2013). Mountain permafrost-research frontiers and a special long-term challenge. *Cold Regions Science and Technology*.

Haeberli, W., & Burn, C. (2002). Natural hazards in forests: glacier and permafrost effects as related to climate change. In R. Sidle, *Environmental Change and Geomorphic Hazards in Forests* (pp. 167-202). New York: CABI Wallingford.

Haeberli, W., & Gruber, S. (2009). Global warming and mountain permafrost. In R. Margesin (Ed.), *Permofrost Soil, Soil Biology 16* (pp. 205-218). Berlin: Springer-Verlag.

Haeberli, W., & Hohmann, R. (2008). Climate, glaciers, and permafrost in the Swiss Alps 2050: scenarios, consequences and recommendations. *9th International Conference on Permafrost*, (pp. 607-612). Fairbanks, Alaska.

Haeberli, W., Brandova, D., Castelli, S., Egli, M., Frauenfelder, R., Kääb, A., . . . Dickau, R. (2003). Absolute and relative age dating of rock-glacier surfaces in alpine permafrost: concept, first results and possible applications. *EGS - AGU - EUG Joint Assembly*, (pp. 343-348). Nice, France.

Haeberli, W., Hallet, B., Arenson, L., Elconin, R., Humlum, O., Kääb, A., . . . Vonder Mühll, D. (2006). Permafrost creep and rock glacier dynamics. *Permafrost and Periglacial Processes, 17*(3), 189-214. doi:10.1002/ppp.561

Hardisty, J., Taylor, D. M., & Metcalfe, S. E. (1995). *Computerised environmental modelling A practical introduction using excel.* West Sussex, England: John Wiley & Sons Ltd.

Harris, C., Arenson, L. U., Christiansen, H. H., Etzelmüller, B., Frauenfelder, R., Gruber, S., & . . . (2009). Permafrost and climate in Europe: Monitoring and modelling thermal, geomorphological and geotechnical responses. *Earth-Science Reviews, 92*, 117-171.

Harris, C., Haeberli, W., Vonder Mühll, D., & King, L. (2001a). Permafrost monitoring in the high mountains of Europe: the PACE project in its global context. *Permafrost and Periglacial Processes, 12*(1), 3-11. doi:10.1002/ppp 377

Harris, C., Michael, D., & Etzelmüller, B. (2001b). The assessment of potential geotechnical hazards associated with mountain permafrost in a warming global climate. *Permafrost and Periglacial Processes, 12*(1), 145-156.

Harris, S. A., & Pedersen, D. E. (1998). Thermal regimes beneath coarse blocky materials. *Permafrost Periglacial Processes, 9*(2), 107-120.

Harris, S., & Corte, A. E. (1992). Interactions and relations between mountain permafrost,glacier, snow and water. *Permafrost and Periglacial Processes, 3*(2), 103-110.

Hastie, T. (2013). Generalized additive models. R package version 1.08. Retrieved from http://CRAN .R-project.org/package=gam

Hastie, T. J., & Tibshirani, R. J. (1990). *Generalized additive models.* Great Britain : Chapman and Hall.

Hauck, C., & Kneisel, C. (Eds.). (2008). *Applied geophysics in periglacial environments.* Cambridge, UK: Cambridge University Press.

Heggem, E., Juliussen, H., & Etzelmüller. (2005). Mountain permafrost in central-Eastern Norway. *Norwegian Journal of Geography, 59*, 94-108.

Herrera, F., Azócar, G., Brenning , A., & Bodin, X. (May 2011). Inventario de glaciares rocosos en los Andes semiáridos de Chile: cuenca del río Elqui. *XVIII Congreso geológico argentino.* Neuquén, Argentina.

Hiebl, J., Auer, I., Böhm, R., Schöner, W., Maugeri, M., Lentini, G., . . . Müller-Westermeier. (2009). A high-resolution 1961–1990 monthly temperature climatology for the greater Alpine region. *Meteorologische Zeitschrift, 18*(5), 507-530.

Hoelzle, M., & Haeberli, W. (1995). Simulating the effects of mean annual air temperature changes on permafrost distribution and glacier size: An example from the Upper Engadin, Swiss Alps. *Annals of Glaciology, 21*, 399-405.

Hoelzle, M., Wagner, S., Kääb, A., & Vonder Mühll, D. (1998). Surface movement and internal deformation of ice-rock mixtures within rock glaciers at Pontresina-Shafberg upper engadin, Switzerland. *Seventh International Conference on Permafrost* (pp. 465-471). Yellowknife: University of Ottawa.

Hoelzle, M., Haeberli, W., & Stocker-Mittaz, C. (2003). Miniature ground temperature data logger measurements 2000-2002 in Murtèl-Corvatsch area, Eastern Swiss Alps. *8th International Conference on Permafrost* (pp. 419-424). Zurich, Switzerland: International Permafrost Association.

Hoelzle, M., Mittaz, C., Etzelmüller, B., & Haeberli, W. (2001). Surface energy fluxes and distribution models of permafrost in European mountain areas: An overview of current developments. *Permafrost and Periglacial Processes, 12*(1), 53-68. doi:DOI: 10.1002/ppp 385

Hoelzle, M., Wegmann, M., & Krummmenacher, B. (1999). Miniature temperature dataloggers for mapping and monitoring of permafrost in high mountain areas: First experience from the Swiss Alps. *Permafrost and Periglacial Processes, 10*(2), 113-124.

Hosmer, D. W., & Lemeshow, S. (2000). *Applied logistic regression.* USA: John Wiley & Sons. Inc.

Humlum, O. (1982). Rock glacier types on Disko, central west, Greenland. *Danish Journal of Geography, 82*, 59-65.

Humlum, O. (1996). Origin of rock glaciers: Observations from Mellemfjord, Disko Island, Central West Greenland. *Permafrost and Periglacial Processes, 7*(4), 361-380.

Humlum, O. (1997). Active layer thermal regime at three rock glaciers in Greenland. *Permafrost and Periglacial Processes, 8*(4), 383-408.

Humlum, O. (2000). The geomorphic significance of rock glaciers: Estimates of rock glacier debris volumes and headwall recession rates in West Greenland. *Geomorphology, 35*, 41-67.

IANIGLA-CONICET. (2010). *Inventario nacional de glaciares y ambiente periglacial: fundamentos y cronograma de ejecución.* Mendoza: Universidad Nacional de Cuyo.

Ikeda, A., & Matsuoka, N. (2002). Degradation of talus-derived rock glacier in the upper Engadin. *Permafrost and Periglacial Processes, 13*, 145-161.

Imhof, M. (1996). Modelling and verification of the permafrost distribution in the Bernese Alps (Western Switzerland). *Permafrost and Periglacial Processes, 7*(3), 267-280.

Iribarren, P. (2008). *Glaciares rocosos en el semiárido chileno. Su significado climático y geomorfológico. Análisis de caso. Cuenca superior del río La Laguna.* Tesis profesional, Universidad de Chile, Facultad de Arquitectura y Urbanismo, Escuela de Geografía, Santiago.

Isaksen, K., Hauck, C., Gudevang, E., Odegard, R., & Ludvig Sollid, J. (2002). Mountain permafrost distribution in Dovrefjell and Jotunheimen, southern Norway, based on BTS and DC resistivity tomography data. *Norwegian Journal of Geography, 56*, 122-136.

Ishikawa, M. (2003a). Spatial mountain permafrost modelling in the Daisetsu mountains, northern Japan. *8th International Conference on Permafrost* (pp. 473-478). Zurich, Switzerland: International Permafrost Association.

Ishikawa, M. (2003b). Thermal regimes at the snow–ground interface and their implications for permafrost investigation. *Geomorphology, 52*, 105-120.

Jaccard, J. (2001). *Interaction effects in logistic regression.* Thousand Oaks,CA, USA: Sage Publication Inc.

Janet, F. (1998). Predicting the distribution of shrub species in southern California from climate and terrain-derived variables. *Journal of Vegetation Science, 9*, 733-748.

Janke, J. (2005a). Modeling past and future alpine permafrost. *Earth Surface Processes and Landforms, 30*, 1495-1580.

Janke, J. (2005b). The occurence of alpine permafrost in the Front Range of Colorado. *Geomorphology, 30*, 375-389.

Janke, J., Regmi, N., Giardino, J., & Vitek, J. (2013). Rock Glaciers. In J. Schroder (Ed.), *Treatise on Geomorphology* (Vol. 8, pp. 238-273).

Jensen, J. R. (2013). *Remote Sensing of the Environment.* Delhi, India: Pearson Education.

Johnson, P. (1984). Rock glacier formation by high-magnitude low-frequency slope processes in the Southwest Yukon. *Annals of the association of American Geographers, 74*(3), 408-419.

Juliussen, H., & Humlum, O. (2008). Thermal Regime of Openwork Block Field on the Mountains Elgahogna and Solen, Central-eastern Norway. *Permafrost and Periglacial Processes, 19*(1), 1-18.

Kammer, K. (1998). Rock glaciers, Western Andes, Chile. Boulder, Colorado, USA. Retrieved from http://nsidc.org/data/ggd282.html

Keller, F. (1992). Automated mapping of mountain permafrost using the program PERMAKART within the geographical information system ARC/INFO. *Permafrost and Periglacial Processes, 3*(2), 133-138.

Keller, F., Frauenfelder, R., Gardaz, J.-M., Hoelzle, M., Kneisel, C., Lugon, R., . . . Wenker, L. (1998). Permafrost map of Switzerland. *7th International Conference on Permafrost* (pp. 557-562). Yellowknife: Internationl Permafrost Association .

Kellerer-Pirklbauer, A., & Kaufmann, V. (2012). About the relationship between rock glacier velocity and climate parameters in central Austria. *Austrian Journal of Earth Sciences, 105*(2), 94-112.

Kellerer-Pirklbauer, A., Lieb, G. K., Schoeneich , P., Deline, P., & Pogliotti, P. (2011). *Thermal and geomorphic permafrost response to present and future climate change in the European Alps.* Permanet project.

Krainer, K., & Ribis, M. (2012). A rock glacier inventory of the Tyrolean Alps (Austria). *Austrian Journal of Earth Sciences, 105*(2), 32-47.

Kull, C., Grosjean, M., & Veit, H. (2002). Modeling modern and late pleistocene glacio-climatological conditions in the North Chilean Andes. *Climatic Change*(52), 359-381.

Lautensach, H., & Bögel, R. (1956). Der Jahrsgang des mittleren geographischen Hohengradienten der Luftemperatur in den verschiedenen Klimagebieten der Erde. *Erdkunde, 10*, 270-282.

Leverington, D. W., & Duguay, C. R. (1996). Evaluation of three supervised classifiers in mapping "depth to late-summer frozen ground" Central Yukon territory. *Canadian Journal of Remote Sensing, 22*(2), 163-174.

Leverington, D. W., & Duguay, C. R. (1997). A Neural Network Method to Determine the Presence or Absence of Permafrost near Mayo, Yukon Territory, Canada. *Permafrost and Periglacial Processes, 8*(2), 205-215.

Lewkowicz, A., & Ednie, M. (2004). Probability mapping of mountain permafrost using the BTS method, Wolf Creek, Yukon Territory, Canada. *Permafrost and Periglacial Processes, 15*(1), 67-80. doi:10.1002/ppp.480

Lliboutry, L. (1953). Internal moraines and rock glaciers. *Journal of Glaciology, 2*(14), 296.

Luke, D. A. (2004). *Multilevel modeling.* Thousan Oaks, USA: Sage Publications Inc.

Mahaney, W., Miyamoto, H., Dohm, J., Baker, V., Cabrol, N., Grin, E., & Berman, D. (2007). Rock glaciers on Mars: Earth-based clues to Mars' recent paleoclimatic history. *Planetary and Space Science, 55*, 181-192.

Maksaev, V., Townley, B., Palacios, C., & Camus, F. (2007). Metallic ore deposits. In T. Moreno, & W. Gibbons (Eds.), *The geology of Chile* (pp. 179-199). Brassmill Lane: The Geological Society of London.

Marangunic, C. (1976). El glaciar de roca Pedregoso, río Colorado, V Región. *Primero Congreso Geologico Chileno*, *Tomo I, Sección D*, pp. 71-80. Santiago, Chile.

Marangunic, C. (1979). *Inventario de glaciares. Hoya del río Maipo.* Santiago: Dirección General de Aguas.

Marshall, S. (2012). *The Cryosphere.* New Jersey: Princeton University Press.

Meyer, R. A. (Ed.). (2009). *Encyclopedia of complexity and systems science* (Vol. 1). Springer.

Milana, J. P., & Güell, A. (2008). Diferencias mecánicas e hídricas del permafrost en glaciares de rocas glacigénicos y criogénicos, obtenidas de datos sísmicos en el Tapado, Chile. *Revista de la Asociación Geológica Argentina, 63*(3), 310-325.

Millar, C. I., & Westfall, R. D. (2008). Rock glaciers and related periglacial landforms in the Sierra Nevada, CA, USA, inventory, distribution and climatic relationships. *Quaternary International, 188*, 90-104.

Monnier, S., & Kinnard, C. (2012). From 'true' glaciers to rock glaciers? The case of the Llanos la Liebre rock glacier, dry Andes of Chile. *European Geophysical Union General Assembly 2012.*

Monnier, S., & Kinnard, C. (2013). Internal structure and composition of a rock glacier in the Andes (upper Choapa valley, Chile) using borehole information and ground-penetrating radar. *Annals of Glaciology, 54*(64), 61-72.

Nakagawa, S., & Schielzeth, H. (2013). A general and simple method for obtaining R Square from generalized linear mixed-effects models. *Methods in Ecology and Evolution, 4*, 133-142.

Nicholson, L., Marín, J., López, D., Rabatel, A., Bown, F., & Rivera, A. (2009). Glacier inventary of the upper Huasco valley, Norte Chico, Chile: Glacier characteristics, glacier change and comparison with central Chile. *Annals of Glaciology, 50*(53), 111-118.

Nyenhuis, M., & Hoelzle, M. (2005). Rock glacier mapping and permafrost distribution modelling in the Turtmanntal, Valais, Switzerland. *Zeitschrift für Geomorphologie, 3*, 275-292.

Ødegard, R., Isaksen, K., Mastervik, M., Billdal, L., & Engler, M. (1999). Comparison of BTS and Landsat TM data from Jotunheimen, southern Norway. *Norsk Geografisk Tidsskrift, 53*, 226-233.

Orme, A. R. (2007). The tectonic framework of South America. In T. T. Veblen, K. R. Young, & A. R. Orme (Eds.), *The Physical geography of South America* (pp. 3-22). New York, USA: Oxford University Press.

Owen, L., & England, J. (1998). Observations on rock glacier in the Himalayas and Karakoram mountains of Northern Pakistan and India. *Geomorphology, 26*, 199-213.

Panda, S. K., Prakash, A., Solie, D. N., Romanovsky, V. E., & Torre Jorgenson, M. (2010). Remote sensing and field-based mapping of permafrost distribution along the Alaska highway corridor, interior Alaska. *Permafrost and Periglacial Processes, 21*(3), 271-281.

Pankhusrt, R. J., & Hervé, F. (2007). Chapter 1: Introduction and overview. In T. Moreno, & W. Gibbons (Eds.), *The Geology of Chile* (pp. 1-4). Brassmill Lane: The Geological Society of London.

Paskoff, R. (1967). Notes de morphologie glaciaire dans la haute vallée du Rio Elqui (Provence de Coquimbo, Chili). *350/351*, 44-55.

Permanet. (2013). *Guide lines for monitoring BTS, Bottom temperature of snow cover.* Retrieved June 16, 2013, from permanet-alpinespace: http://www.permanet-alpinespace.eu/archive/pdf/BTS.pdf

Perucca, L., & Esper, M. (2011). Glacier and rock glaciers' distribution at 28° SL,Dry Andes of Argentina, and some considerations about their hydrological significance. *Environmental Earth Sciences, 64*, 2079-2089.

Pinheiro, J., & Bates, M. (2000). *Mixed-effects models in S and S-Plus.* New York: Springer-Verlag.

Pinheiro, J., Bates, D., DebRoy, S., Sarkar, D., & R Development Core Team. (2013). nlme: Linear and nonlinear mixed effects models-R package version 3.1-108. Vienna.

Pogliotti, P., Cremonese, E., Morra di Cella, U., Gruber, S., & Giardino, M. (2008). Thermal diffusivity variability in Alpine permafrost rock walls. *Ninth International Conference on Permafrost* (pp. 1427-1432). Fairbanks: University of Alaska.

Potter, N. J. (1972). Ice-cored rock glacier, Galena creek Northern Absaroka mountains. Wyoming. *Geological Society of America Bulletin, 83*(10), 3025-3028.

Putnam, A., & David, P. (2009). Inactive and relict rock glaciers of the Deboullie lakes ecological reserve, Northern Maine, Usa. *Journal of Quaternary Science, 24*, 773-784. doi:10.1002/jqs.1252

R Core Team . (2012). R: A language and environment for statistical computing. R Foundation for Statistical Computing. Vienna, Austria. Retrieved from http://www.R-project.org/

Rabatel, A., Castebrunet, H., Favier, V., Nicholson, L., & Kinnard, C. (2011). Glacier change in the Pascua-Lama region, Chilean Andes (29°S): recent mass balance and 50 yr surface area variations. *The Cryosphere, 5*(4), 1029-2011.

Raudenbush, S. W., & Bryk, A. S. (2002). *Hierarchical linear models.* Thousand Oaks, California: Sage.

Riseborough, D., Shiklomanov, N., Etzelmüller, B., Gruber, S., & Marchenko, S. (2008). Recent advances in permafrost modelling. *Permafrost and Periglacial Processes, 19*(2), 137-156. doi:10.1002/ppp.615

Roer, I., & Nyenhuis, M. (2007). Rockglacier activity studies on a regional scale:comparison of geomorphological mapping and photogrammetric monitoring. *Earth Surface Processes and Landforms, 32*(12), 1747-1758. doi:10.1002/esp.1496

Roer, I., Kääb, A., & Dikau, R. (2005a). Rockglacier acceleration in the Turtmann valley (Swiss Alps):Probable controls. *Norwegian Journal of Geography, 59*, 157-163.

Roer, I., Kääb, A., & Dikau, R. (2005b). Rockglacier kinematics derived from small-scale aerial photography and digital airborne pushbroom imagery. *Zeitschrift für Geomorphologie, 49*, 73-87.

Rookes Serrano Ingeniería. (2011). *Monitoreo de la dinámica de los glaciares rocosos, cuenca superior del río Huasco.*

Rundel, P., Villagran, P., Dillon, M., Roig-Juñent, S., & Debandi, G. (2007). Arid and Semi-Arid Ecosystems. In T. T. Veblen, Y. R. Kenneth, & A. R. Orme (Eds.), *The Physical Geography of South America* (pp. 158-183). New York, USA: Oxford University Press.

Schrott, L. (1991). Global Solar Radiation, Soil Temperature and Permafrost in the Central Andes, Argentina: a Progress Report. *Permafrost and Periglacial Processes, 2*(1), 59-66.

Schrott, L. (1996). Some geomorphological-hydrological aspects of rock glaciers in the Andes (San Juan, Argentina). *Annals of Geomorphology, 104*, 161-173.

Schrott, L. (1998). *Mountain Permafrost Hydrology and iths relation to solar radiation. A case study in the Agua Negra Catchment, high Andes of San Juan, Argentina.* IANIGLA.

Schrott, L., Otto, J.-C., & Keller, F. (2012). Modelling Alpine permafrost distribution in the Hohe Taurn region, Austria. *Austrian Journal of Earth Sciences, 105*(2), 169-183.

Scotti, R., Brardinoni, F., Alberti, S., Frattini, P., & Crosta, G. B. (2013). A regional inventory of rock glaciers and protalus ramparts in the central Italian Alps. *Geomorphology, 186*, 136-149.

Squeo, F., Veit, H., Arancio, G., Gutierrez, J. R., Arroyo, M. T., & Olivares, N. (1993). Spatial heterogeneity of high mountain vegetation in the Andean desert zone of Chile. *Mountain Research and Development, 13*(2), 203-209.

Stocker-Mittaz, C., Hoelzle, M., & Haeberli, W. (2002). Modelling alpine permafrost distribution based on energy-balance data: A first step. *Permafrost and Periglacial Processes, 13*(4), 271-282.

Tachikawa, T., Kaku, M., & Iwasaki, A. (2011). Aster GDEM version 2 validation report.

Trombotto, D. (2000). Survey of cryogenic processes, periglacial forms and permafrost conditions in South America. *Revista do Instituto Geológico, 1*(2), 33-55.

Trombotto, D., & Borzotta, E. (2009). Indicators of present global warming through changes in active layer-thickness, estimation of thermal diffusivity and geomorphological observations in the Morenas Coloradas rockglacier, Central Andes of Mendoza, Argentina. *Cold Regions Science and Technology, 55*, 321-330.

Trombotto, D., Buk, E., & Hernández, J. (1997). Short Communication: Monitoring of mountain permafrost in the central Andes, Cordon del Plata, Mendoza, Argentina. *Permafrost and Periglacial Processes, 8*(1), 123-129.

Twisk, J. (2006). *Applied multilevel analysis: A practical guide .* Cambridge: Cambridge University Press.

Ubukawa, T. (2013). *An evaluation of the horizontal positional accuracy of Google and Bing satellite imagery and three roads data sets based on high resolution satellite imagery.* New York: Center for International Earth Science Information Network, Columbia University.

Unidad de Gestión de Proyectos del Instituto de Geografía de la Pontificia Universidad Católica de Chile [UGP UC]. (2010). *Dinámica de glaciares rocosos.* Dirección General de Aguas, Unidad de Glaciología y Nieves. Santiago: Ministerio de Obras Públicas.

Vitek, J., & Giardino, J. (1987). Rock glacier: a review of the knowledge base. In J. Giardino , J. J. Schroder, & J. Vitek (Eds.), *Rock glaciers* (pp. 1-26). Winchester, USA: Allen & Unwin Inc.

Viviroli, D., Dürr, H. H., Messerli, B., & Meybeck, M. (2007). Mountains of the world, water towers for humanity:Typology,mapping and global significance. *Water Resources Research, 43*, 1-13.

Wahrhaftig, C., & Cox, A. (1959). Rock glacier in the Alaska range. *Geological society of America Bulletin, 70*(4), 383-436.

Wainwright, J., & Mulligan, M. (2004). *Environmental modelling finding simplicity in complexity.* West Sussex, England: John Wiley & Sons Ltd.

West, B. T., Welch, K. B., & Galecki, A. T. (2007). *Linear mixed models: A practical guide using statistical software.* Boca Raton, Florida: Chapman & Hall/CRC.

Westriecher, C. A., Merega, J. L., & Palmili, G. (2006). *Review of the literature on pastola economics and marketing .* Argentina : The World Conservation Union .

Whalley, B., & Martin, E. (1992). Rock glaciers: II models and mechanisms. *Progress in Physical Geography, 16*(2), 121-186.

Whiteman, D. C. (2000). *Mountain meteorology fundamental and applications.* New York, USA: Oxford University Press.

Wilson, J. P., & Gallant, J. C. (2000). Chapter 4: Secondary topographic atributes. In J. P. Wilson, & J. G. Gallant, *Terrain analysis: Principles and applications* (pp. 87-131). New York, USA: John Wiley & Sons Inc.

Wood, S. N. (2006). *Generalized additive models - An introduction with R.* Boca Raton, Florida, USA: Chapman & Hall/CRC.

World Glacier Monitoring Service. (2009). *Global glacier changes: Facts and figures.* United Nations.

World Meteorological Organization . (2000). *Guía de Prácticas de Servicios Meteorológicos para el Público.* Ginebra, Switzerland : WMO.

World Meteorological Organization (WMO). (2013, August 12). *Climate data and data related products*. Retrieved from http://www.wmo.int/pages/themes/climate/climate_data_and_products.php

Zevenbergen, L., & Thorne, C. (1987). Quantitative analyses of land surface topography. Earth Surface Processes and Landforms, 12, 47-56.

Zimmermann, M., & Haeberli, W. (1992). Climatic change and debris flow activity in high-mountain areas- A case study in the Swiss Alps. In M. Boer, & E. Koster (Eds.). Cremlingen-Destedt, Germany: Catena.

Zhang, X., Tong Nan, Z., Wu, J., Du, E., Wang, T., & You, Y. (2012). Mountain permafrost distribution modeling using multivariate adaptive regression spline (MARS) in the Wenquan area over the Qinghai-Tibet Plateau. *Sciences in Cold and Arid Regions, 4*(5), 361-370. doi:10.3724/SP.J.1226.2012.00361

Zuur, A. F., Ieno, E. N., Walker, N. J., Saveliev, A. A., & Smith, G. M. (2009). *Mixed effects models and extensions in ecology with R.* New York, USA: Springer.